Für Gerburg

Acknowledgements

Mechanisms of Eph/ephrin mediated cell-cell communication

Dissertation

Der Fakultät für Biologie der

Ludwig-Maximilians-Universität München

Eingereicht am 6. Oktober 2003 von

Manuel Zimmer

aus Osnabrück

1. Gutachter: Dr. Rüdiger Klein

2. Gutachter: Dr. Magdalena Götz

Tag der mündlichen Prüfung: 02. Dezember 2003

6

Erklärung

Ich versichere, daβ ich die Dissertation "Mechanisms of Eph/ephrin mediated cell-cell communication" selbstständig, ohne unerlaubte Hilfe angefertigt, und mich dabei keiner anderen als der von mir ausdrücklich bezeichneten Hilfen und Quellen bedient habe.

Die Dissertation wurde in der jetzigen oder ähnlichen Form bei keiner anderen Hochschule eingereicht und hat noch keinen sonstigen Prüfungszwecken gedient.

_____   _____

(Ort, Datum)   (Manuel Zimmer)

1. Table of Contents

2. Publications from the work presented in this dissertation

Palmer A*, <u>Zimmer M*</u>, Erdmann KS, Eulenburg V, Porthin A, Heumann R, Deutsch U, Klein R.

EphrinB phosphorylation and reverse signaling: regulation by Src kinases and PTP-BL phosphatase.

Molecular Cell 2002 Apr; 9(4):725-37

<u>Zimmer M</u>, Palmer A, Köhler J, Klein R

EphB-EphrinB bi-directional endocytosis terminates adhesion allowing contact mediated repulsion.

Nature Cell Biology 2003 Oct; 5(10):869-878

*Authors with equal contribution.

3. Abbreviations

α	Anti
Abi-1	Abl interacting protein-1
Abl	Abelson kinase
ACE	Adrenal cortex derived endothelial cells
ACp	Anterior Commissure, posterior
ADF	actin-depolymerizing factor
AMP	Adenosin-5'-monophosphate
AMPA	D-2-amino-3-hydroxy-5-methyl-4-isoxazole-propionic acid
AP	Adaptor protein
APS	Ammonium-persulfate
Arg	Abelson related gene
ARP2/3	Actin related protein 2/3
ATP	Adenosin-5'-triphosphate
BDNF	Brain-derived neurotrophic factor
bFGF	Basic fibroblast growth factor
BSA	Bovine serum albumine
CAM	Cell adhesion molecule
CamKII	Ca^{2+}/Calmodulin-dependent kinase II
cAMP	Cyclic AMP
CAP	Cbl associated protein
Cbp	Csk binding protein
CCP	Clathrin coated pit
CCV	Clathrin coated vesicle
Cdc42	Cell division cycle 42
cDNA	Complementary DNA
CHC	Clathrin heavy chain
CLC	Clathrin low chain
CNS	Central nervous system
CREB	Ca^{2+}/cAMP-response element binding protein
Csk	C-terminal Src kinase
CST	Cortical spinal tract
CXCR	CXC motif receptor
DCC	Deleted in colorectal cancer
DIV	Days *in vitro*
DL	Discs large
DMEM	Dulbecco's modified Eagles medium
DNA	Deoxyribonucleic acid
DOCK	Dreadlock
D-PBS	Dulbecco's phosphate buffered saline
DPP	Decapentaplegic
DRG	Dorsal root ganglion
E	Embryonic day
EDTA	Ethylenediamine-tetra acetic acid

Ena	Enabled
Eph	Erythropoietin-producing hepatocellular
Ephexin	Eph-interacting exchange protein
Ephrin	Eph family receptor interacting protein
ERK	Extracellular regulated kinase
FAK	Focal adhesion kinase
FERM	Four point one, Ezrin, Radixin, Moesin
FNIII	Fibronectin type III
Fyn	Fgr/Yes-related Novel gene
GAP	GTPase activating protein
GEF	Guanine nucleotide exchange factor
Glob	Globular (domain)
GluR	Glutamate receptor subunit
GPI	Glycosylphosphatidylinositol
GRIP	Glutamate receptor interacting protein
HBSS	Hank's balanced salt solution
Hepes	(Hydroxyethyl)-piperanzine-ethane sulfonic acid
HGF	Hepatocyte growth factor
HUAEC	Human umbilical cord arterious endothelial cell
HUVEC	Human umbilical cord venous endothelial cell
IF	Immunofluorescence
Ig	Immunoglobulin
IH	Immunohistochemistry
IP	Immunoprecipitation
IRR	Immuno response receptor
ITAM	Immuno response receptor tyrosine activation motif
KD	Kinase dead
lacZ	Gene encoding βgal
LB	Luria-Bertani
LTD	Long-term depression
LTP	Long-term potentiation
MAGUK	Membrane-associated guanylate kinase
MAPK	Mitogen-activated protein kinase
MC	Microcarrier
Mtl	*Mig-two*-like
Nck	Noncatalytic region of tyrosine kinase
Nik	Nck interacting kinase
NMDA	N-methyl-D-aspartate
N-WASP	Neural Wiskott-Aldrich syndrome protein
OTK	Off-track
PAGE	Polyacrylamid gel electrophoresis
PAK	P21-activated kinase
PARG	PTPL1-associated RhoGAP
PCR	Polymerase chain reaction
PDB	PDZ binding (domain)
PDGF	Platelet-derived growth factor

PDZ	PSD95/Discs large/ZO-1
PFA	Paraformaldehyde
PHIP	Ephrin-interacting protein
PI3K	Phosphatidylinositol 3-kinase
PICK	Protein interacting with C kinase
PKA	Protein kinase A
PKC	Protein kinase C
PRK2	PKC related kinase 2
PSD	Postsynaptic density
PSD-95	Postsynaptic density protein 95
Ptc-1	Patched-1
PTP-BAS	Phosphotyrosine phosphatase-basophile
PTP-BL	Phosphotyrosine phosphatase-basophile like
PY	Phospho-tyrosine
R	Receptor
Rac	Ras-related C3 botulinum toxin substrate
Rap	Ras related protein
Ras	Rat sarcoma
RGC	Retinal ganglion cell
RGS	Regulator of G-protein signaling
Rho	Ras homologous member
RNA	Ribonucleic acid
Rnd1	Round 1
Robo	Roundabout
ROCK	Rho-associated, coiled-coil containing protein kinase
rpm	Round per minute
RT	Room temperature
RTK	Receptor tyrosine kinase
SAM	Sterile-α-motif
SC	Superior colliculus
SDF-1	Stromal cell-derived factor 1
SDS	Sodium dodecyl sulfate
SFK	Src family kinase
SH	Src homology
Shh	Sonic hedgehog
Src	Sarcoma virus transforming gene product
srGAP	Slit Robo GAP
TEMED	N,N,N',N'-Tetra-methylethylenediamine
TRIO	Triple functional domain
VASP	Vasodilator-stimulated phosphoprotein
VEGF	Vascular and endothelial growth factor
WB	Western blot
Wnt	Wingless-type mmtv integration site family
Yes	Yamaguchi sarcoma viral
ZO1	Zona-occludens

4. Summary

Eph receptors and their membrane associated ephrin ligands mediate cell-cell repulsion to guide migrating cells and axons. A peculiarity of this signaling system is that both receptors and ligands can transduce signals into the cell resulting in a bidirectional signaling mode. An important step of ephrinB ligand 'reverse signaling' is the regulated tyrosine phosphorylation of the cytoplasmic domain, initiating docking sites for downstream signaling adaptors. Moreover, ephrinB ligands can signal by interactions with various PDZ-domain containing proteins.

Using a broad range of *in vitro* assays the presented work demonstrates that upon binding to their cognate receptor, ephrinB ligands rapidly activate Src family kinases (SFKs) which subsequently phosphorylate ephrinB. Tyrosine phosphorylation appears to be a transient event that is downregulated by the tyrosine phosphatase PTP-BL, which interacts with ephrinB via one of its PDZ-domains. Studies on PTP-BL and another multiple PDZ domain containing protein GRIP (Glutamate Receptor Interacting Protein) revealed that PDZ interactions with ephrinB are also regulated by EphB receptor binding but, unlike tyrosine phosphorylation, these interactions are long lasting. These findings led to postulate a 'switch model' for ephrinB reverse signaling: Tyrosine dependent signaling appears to be a rapid and transient event which is later replaced by stable PDZ-dependent signaling.

EphB 'forward' signaling as well as ephrinB 'reverse' signaling are important for axonal pathfinding and cell migration during development. Prior to their repellent effect on migrating cells and growth cones, Eph receptors form a high affinity complex with their ligands at sites of cell-cell contact. Therefore, mechanisms have to be in place that allow cells to detach from each other permitting retraction and withdrawal. To overcome this adhesive barrier, the ectodomain of ephrinA ligands is cleaved by metalloproteinases and shed upon receptor binding. Intrigued by the previous findings that activated ephrins cluster in cells, we hypothesized that these Eph/ephrin clusters undergo endocytosis. We developed immunofluorescence internalization and co-culture assays to study clustering and endocytosis at cell-cell contact sites. We established an experimental setup to perform fast time lapse imaging studies of cells expressing different fluorescently tagged

proteins. Cell contact-induced ephrinB-EphB complexes are rapidly endocytosed during the retraction of cells and neuronal growth cones. Endocytosis occurs in a bidirectional manner, leading to internalized complexes of full length receptor and ligand, a yet rarely observed phenomenon. Signaling inactive mutants of EphB receptors and ephrinB ligands lead to a strong adhesion between cells. Endocytosis is sufficient to convert this adhesion into the detachment of cells. Bidirectional endocytosis is necessary to efficiently promote axon detachment during growth cone collapse mediated by ephrinB ligands. On the cell biological level, bidirectional endocytosis of two full length transmembrane (TM) proteins is a new phenomenon. Moreover, these studies reveal a novel mechanism of signal termination, de-adhesion and promotion of cell repulsion after intercellular (trans) interaction between two TM proteins.

5. Introduction

During the development of multicellular organisms cells divide, migrate, differentiate and die in a spatially and temporally coordinated manner. One impressive example of morphogenesis is the development of the brain. Billions of neuronal cells begin to form a precise network of nerves and synaptic connections. Such complex processes require that cells communicate with other cells and with their environment. Extracellular information is received by cells via surface receptors that recognize specific stimuli and transduce signals into the interior of the cell in order to evoke the proper responses. Intracellular signal transduction is not just a simple linear transmission of information but rather involves complex networks of molecular interactions that require specific mechanisms for their regulation.

5.1. Molecular mechanisms of axon guidance

5.1.1. Axon guidance molecules and their receptors

A differentiated neuron has four morphologically defined regions: the cell body, dendrites, axons and presynaptic terminals. Inputs are received by postsynaptic sites on dendrites, which are arborized processes that originate from the cell body. The cell body integrates these signals which are propagated in an all-or-none way to presynaptic terminals by the axon via an electrical signal called action potential. The correct wiring of the nervous system relies on the ability of neurons to find and to recognize their appropriate synaptic partners during development. When neurons are born, their cell bodies are placed at locations far away from their postsynaptic targets. How does a developing axon find its way to reach the correct destination? Axon guidance is a special case of cell migration, where only a part of the cell is motile: Each growing neuronal process is provided with a growth cone at its tip. A growth cone resembles the leading edge of a migrating cell. It is a fan like structure composed out of a shaft region equipped with dynamic filopodia and lamellipodia. A neuronal growth cone expresses cell

adhesion molecules (CAMs) that enable it to move by modulating its adhesion to the extracellular matrix (ECM) and to other cells. Moreover, growth cones are guided by attractive and repulsive cues on intermediate targets within their environment. On their journey to their final destination, growth cones can pass several such intermediate targets. Each growth cone expresses a set of axon guidance receptors that recognize the cues and elicit the appropriate responses. Axon guidance molecules can act from a distance by chemoattraction or chemorepulsion. Others can act due to direct cell-matrix or cell-cell contact by contact-attraction or contact-repulsion (Chisholm and Tessier-Lavigne, 1999; Yu and Bargmann, 2001; Dickson, 2002; Grunwald and Klein, 2002) (**Figure 1**).
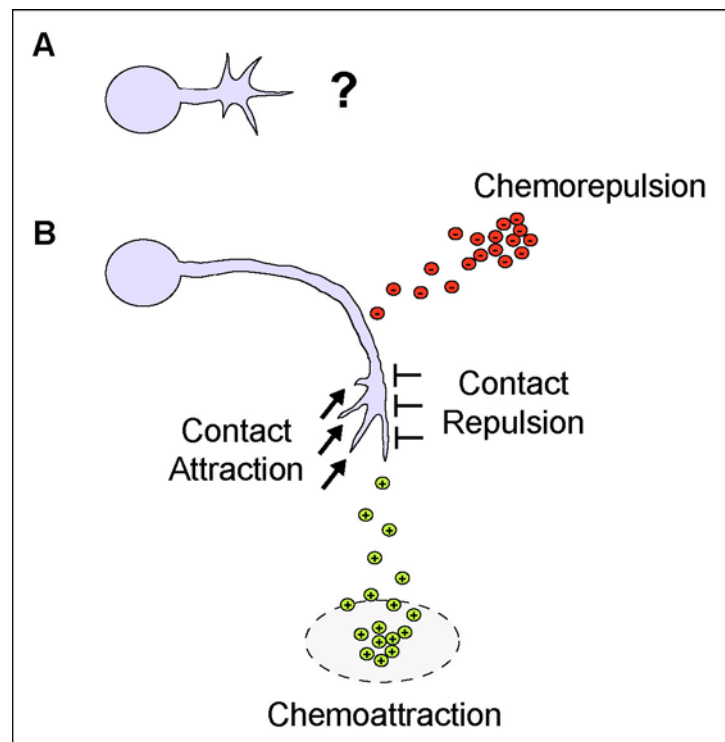
Figure 1. Principles of axon guidance. (**A**) Growth cones on developing axons explore the environment. (**B**) They are guided towards or away from intermediate targets. On their journey they sense various axon guidance molecules that can act from a distance by chemorepulsion or chemoattraction or by direct cell-cell or cell-matrix contact by contact repulsion or contact attraction.

Netrins are extracellular, probably diffusible, molecules that can attract commissural axons towards the ventral midline of the nervous system of several different species from nematodes to vertebrates (Hedgecock et al., 1990; Kennedy et al., 1994). In some cases

netrins can also be repulsive. Two netrin receptors are known: <u>Unc-40/DCC</u> and <u>unc-5</u>. DCC alone mediates attraction. Unc-5, in combination with DCC or alone, mediates repulsion (Hong et al., 1999).

For proper guidance the midline also has to provide repellents, e.g. to prevent ipsilateral axons from crossing and commissural axons from recrossing. At the midline of the *drosophila* or vertebrate central nervous system (CNS) large secreted <u>Slit</u> molecules fulfill these functions. Slits are recognized by <u>roundabout</u> (Robo) receptors (Kidd et al., 1999).

<u>Semaphorins</u> constitute a large family of cell surface molecules that have in common a Sema domain at their N-termini. They are subdivided into eight classes. Class 1-2 semaphorins are found in invertebrates and those of class 3-7 in vertebrates. Semaphorins act as chemo- and contact repellents. They signal through multimeric receptor complexes. The exact composition of all of these complexes is not known yet. It is anticipated that maybe all complexes contain at least one plexin molecule. <u>Plexins</u> are a large family of transmembrane molecules subdivided into 4 classes (A-D). The receptor complex for vertebrate class 3 semaphorins contains other co-receptors of the <u>neuropilin</u> family. The function of neuropilins may be determining the ligand specificity of the complex (Raper, 2000). Other known co-receptors for semaphorins are the CAM L1 (Castellani et al., 2000), the RTK Met (Giordano et al., 2002) and the catalytically inactive RTK OTK (Winberg et al., 2001). Recently integrins have been shown to be important co-receptors for Semaphorin 7A during the guidance of vertebrate lateral olfactory tract axons (Pasterkamp et al., 2003).

<u>Morphogens</u> like Sonic hedgehog (Shh) and Wnt family members have been shown to act 'respectively' as chemo- attractants and repellents in ventral guidance of vertebrate spinal cord neurons (Charron et al., 2003; Yoshikawa et al., 2003).

Finally, the <u>ephrins</u> and their <u>Eph</u> receptors constitute a large family of axon guidance factors which are discussed in greater detail below.

Axon guidance molecules and their receptors are summarized in **Figure 2**.
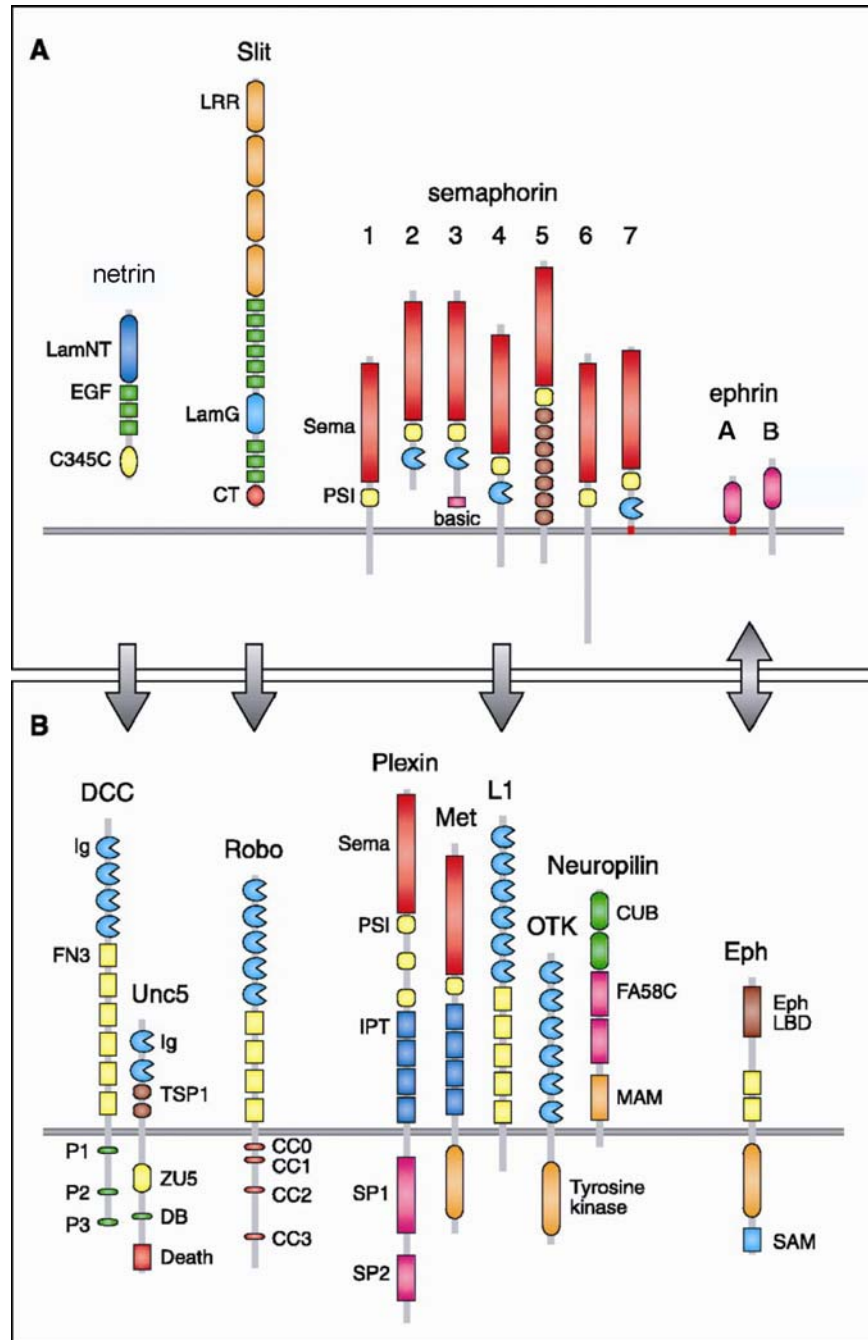
Figure 2. Axon guidance molecules and their receptors. (**A**) Axon guidance cues are either secreted molecules acting as chemorepellents or chemoattractants or are membrane attached to act as contact attractants or contact repellents. (**B**) Receptors for axon guidance cues. Netrins signal via DCC and/or Unc5 and slits via Robo receptors. Semaphorins are recognized by multimeric receptor complexes that contain at least one Plexin molecule and in vertebrates one Neuropilin molecule. Other components can be RTKs like Met or OTK, the CAM L1 or integrins (not shown). The Eph receptors and their ephrin ligands are described in greater detail below. For abbreviations see chapter 3 (scheme taken from Dickson, 2002).

5.1.2. Signaling mechanisms of axon guidance receptors

A vast number of *in vitro* studies have shed light on how axon guidance molecules control the behavior of growth cones. They cause the growth cone to turn away from a repellent and/or towards an attractant (Dickson, 2002). Repellents have the capability to induce the collapse of an entire growth cone, even *in vivo* (Knobel et al., 1999). This may be achieved by regulating the dynamics of the microtubule- and actin cytoskeletons within the growth cone. Axonal growth is mediated by the extension of relatively stable microtubule bundles at the distal ends of each neurite (Bamburg et al., 1986). Some dynamic microtubules extend into the growth cone and explore its peripheral region (Tanaka and Sabry, 1995). Growth cones are rich of filamentous actin, organized into two distinct populations: Parallel filaments that radiate outward into the filopodia and intervening networks of loosely interwoven filaments in lamellipodia (Lewis and Bridgman, 1992). Dynamic microtubules extend out of the neurite along filamentous actin into the filopodia (Schaefer et al., 2002) (**Figure 3A**). They may pioneer the stable microtubule bundles at the neuritic shaft and their capture and stabilization in specific filopodia might be regulated by axon guidance molecules. Thus, axon guidance molecules steer growth cones positively or negatively by influencing the growth of specific filopodia. This is achieved by regulating the balance between actin polymerization and depolymerization within filopodia (O'Connor et al., 1990) (**Figure 3B**). Finally, growth is directed towards the source of attraction or away from a source of repulsion (**Figure 3C**).
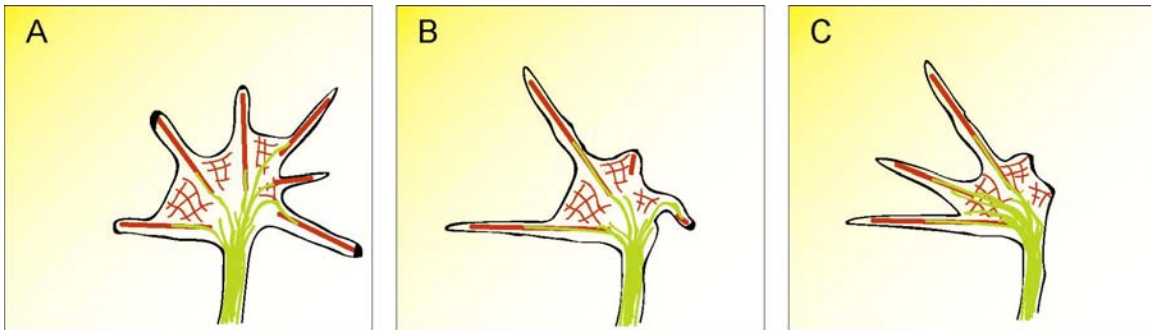
Figure 3. Model for growth cone steering by cytoskeletal dynamics. (**A**) Microtubules (green) extend at the distal end of a neurite and into the growth cone. The growth cone contains two forms of F-actin (red): thick bundles extending into filopodia and thin interwoven filaments in lamellipodia. Dynamic microtubules extend along actin bundles. (**B**) A gradient of an attractant (yellow) promotes actin assembly and capture of microtubules in filopodia that extend towards relative high concentrations. Other filopodia are dilated. (**C**) Neurite growth by microtubule extension toward the attractive gradient.

The assembly and disassembly of actin filaments is highly dynamic. Two key regulators of actin dynamics are the Arp2/3 complex which mediates the initiation and elongation of juvenile filaments and ADF/cofilin which severs and depolymerizes aging filaments. The motor protein myosin II regulates cell contraction behavior. Signaling pathways regulating actin dynamics in cell and growth cone motility converge on these three components (Brown and Bridgman, 2003; Pollard and Borisy, 2003). Rho family GTPases are strong candidates for a link between guidance receptors and the actin cytoskeleton. Rho family GTPases act as molecular switches. In their inactive form they bind GDP. Activation occurs via guanine nucleotide exchange factors (GEFs) that mediated the exchange of GDP with GTP. In the GTP bound form they can activate their effector molecules. Then they turn back into the inactive GDP bound state by the action of GTPase activating proteins (GAPs), which promote the hydrolysis of GTP to GDP (Luo, 2000). The GTPase switch cycle is summarized in **Figure 4**.
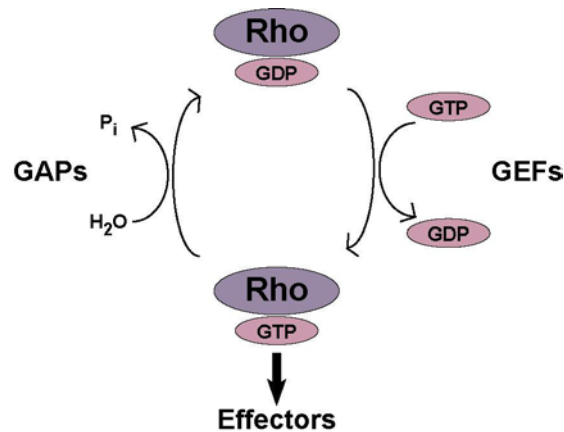
Figure 4. Molecular switch of Rho family GTPases. Inactive Rho bound to GDP is transformed into its active GTP bound state by a guanosine nucleotide exchange factor (GEF). Rho bound to GTP activates effector molecules. GTPase activity is promoted by a GTPase activating protein (GAP) that turns back Rho into its inactive GDP bound state. Axon guidance receptors signal to GEFs and GAPs.

The Rho family GTPases Cdc42 and Rac promote actin driven cell protrusion whereas Rho controls acto-myosin based cell contraction. Consistent with this model, Cdc42 and Rac have been implicated in neurite extension and Rho with neurite retrieval (Luo, 2000). Cdc42 activates N-WASP, an important positive regulator of the Arp2/3 complex (Rohatgi et al., 1999). Genetic studies in flies and nematodes revealed that Rho family GTPases of the Rac type are specifically involved in guidance (Lundquist et al., 2001; Hakeda-Suzuki et al., 2002). During the guidance of *drosophila* photoreceptor axons, Rac is regulated by the GEF Trio and signals via the p21 activated kinase (PAK) (Newsome et al., 2000). Yet unidentified guidance receptors signal to Trio and PAK via the SH2-SH3 adaptor molecule DOCK which recruits these molecules to the plasma membrane (Hing et al., 1999; Newsome et al., 2000). PAK is an activator of LIM kinase which directly inhibits ADF/cofilin (Edwards and Gill, 1999; Edwards et al., 1999). Robo negatively regulates Cdc42 by activation of the GAP srGAP (Wong et al., 2001). Plexins can bind directly to Rho family GTPases and GEFs and may even have intrinsic GAP activity (Rohm et al., 2000; Vikis et al., 2000). Plexins signal to Rac and RhoA (Hu, 2001). Also Eph receptors have been shown to regulate GEFs (see below). The Rho signaling pathway converges on myosin II via the Rho activated kinase ROCK (Riento and Ridley, 2003). Signaling pathways of molecules acting in axon guidance downstream of Rho family GTPases are summarized in **Figure 5**.
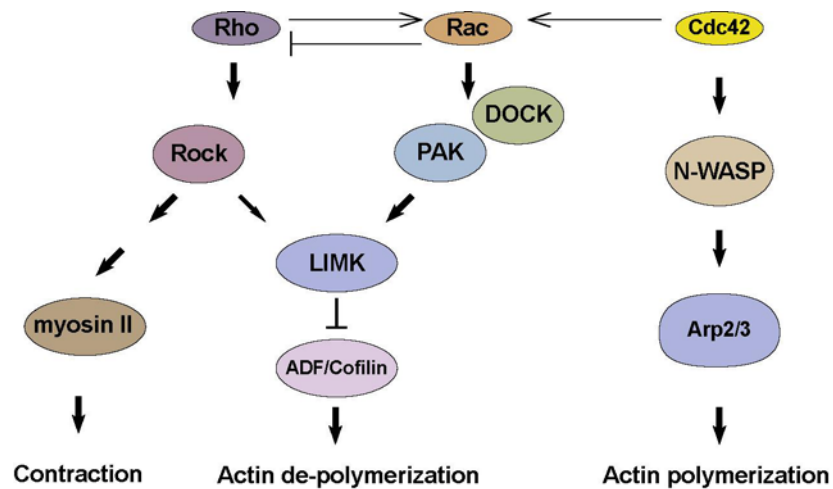
Figure 5. Simplified scheme of how Rho family GTPases signal to the actin cytoskeleton.
Signals from Rho family GTPases target myosin II, Arp2/3 and ADF/Cofilin. Rho signals via
ROCK to myosin II to mediate acto myosin based cell-contraction. Rac signals via DOCK/PAK
to LIMK which in turn inhibits ADF/cofilin. Cdc42 can signal via N-WASP to Arp2/3. Cell
behavior is a result of the relative activity of these GTPases. When activity shifts towards Rho
cell behavior turns towards contraction, whereas enhanced Rac and Cdc42 activity promotes
formation of lamellipodia and filopodia, respectively. All proteins shown in this scheme have
been implicated in axon guidance.

Ena/VASP proteins are known regulators of actin assembly. They antagonize actin
capping proteins thereby promoting filament elongation. In fibroblasts, depending on
their site of action, they can enhance or decrease the motility of the cells. In neurons,
Ena/Vasp proteins are expressed at the tips of filopodia where they may promote their
elongation (Lanier et al., 1999; Koleske, 2003). Ena/Vasp proteins have been implicated
in netrin and slit mediated axon repulsion (Colavita and Culotti, 1998; Bashaw et al.,
2000).

Calcium signaling may play an important role in axon guidance. Growth cones produce
spontaneous calcium transients. The frequency of these transients can be correlated to
reduced growth (Gomez and Spitzer, 1999; Gomez et al., 2001). It has been shown that
netrin can induce a concentration gradient of calcium ions in the growth cone.
Interestingly, the artificial establishment of a Ca^{2+} gradient is sufficient to induce turning
of the growth cone in the absence of netrin (Hong et al., 2000; Zheng, 2000). A recent
study implicated the protease calpain in Ca^{2+} mediated growth cone turning. Calpain
negatively regulates tyrosine kinase activities in filopodia preventing their extension on
integrin substrates (Robles et al., 2003).

5.1.3. Regulation of axon guidance receptors

Specifying the trajectory of axons is not just a simple matter of providing it with a constant set of guidance receptors. Obviously, on its journey through several intermediate targets axons must change their responsiveness to various guidance cues *en route*.

For example mechanisms have to be in place that prevent commissural axons from recrossing the CNS midline. In *Drosophila* Robo receptors are downregulated on such axons when they reach the midline, making them insensitive to the repellent slit, thereby permitting them to cross. Once they have crossed, Robo becomes upregulated again, recovering slit responsiveness, thereby prohibiting them to recross. The protein commissureless regulates membrane trafficking of Robo, removing it from the cell surface while axons cross the midline (Keleman et al., 2002).

Axons can modulate their response to the same guidance molecule by regulating the intracellular levels of the cyclic nucleotides cAMP or cGMP. *In vitro*, lowering cAMP or cGMP levels can convert an attractive response into a repulsive one. Conversely elevating cAMP or cGMP levels converts repulsive responses to attractive ones. The same effects can be obtained by pharmacologically inhibiting or activating cAMP dependent protein kinase (PKA) or cGMP dependent protein kinase (PKG) (Ming et al., 1997; Song et al., 1997; Song et al., 1998). For example, *Xenopus* retinal axons are attracted by netrin out of the eye at the optic nerve head. They become indifferent to netrin as they approach and finally are repelled as they reach the tectum. These changes correlate with a gradual decline of cAMP levels and they can be converted experimentally by raising cAMP levels (Shewan et al., 2002).

Recently it has been shown, that growth cones are capable to locally translate transmembrane guidance receptors like EphA2. Moreover, EphA2 translation is regulated by an intermediate target (Brittis et al., 2002).

The discovery of these mechanisms indicates that the complex wiring of the nervous system may be established by a rather small set of guidance molecules that are themselves subject of dynamic regulation. An axon changes its responsiveness to intermediate targets *en route* by regulating its cAMP or cGMP levels and/or changing its composition of guidance receptors within the growth cone.

5.2. Receptor mediated endocytosis

5.2.1. Mechanisms of endocytosis

Once activated by ligand binding many cell surface receptors undergo a process of regulated endocytosis. This process is crucial for proper regulation of signal transduction (see below). Macromolecules and large particles cannot easily pass the cell membrane such as ions, amino acids or sugars which enter via pores formed by integral membrane proteins. Instead, they enter via invaginations at the plasma membrane, which subsequently pinch off and form intracellular vesicles. This process defines the term endocytosis. There are different mechanisms how endocytosis can occur (**Figure 6**).
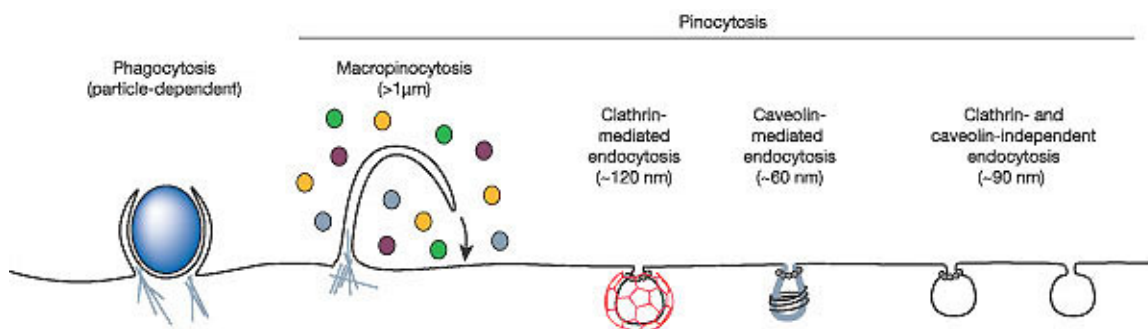
Figure 6. Portals of entry into the cell. Different mechanisms that are described in the text mediate the regulated uptake of extracellular material into the cell by endocytosis. Phagocytosis and macropinocytosis can lead to invagination of large particles. Material of up to 120nm in diameter can be invaginated by clathrin- caveolin- or other clathrin- and caveolin independent mechanisms (scheme taken from Conner and Schmid, 2003).

In a process called phagocytosis, specialized cells can uptake large particles like pathogens, debris, cell remnants etc. For example, Fc receptors on macrophages are activated by immunoglobulin-γ molecules bound to bacterial pathogens. Signaling cascades downstream of the Fc receptor activate small GTPases of the Rho family, which mediate the formation of actin rich protrusions. The protrusions zipper up around the bacterium to finally engulf it (Chimini and Chavrier, 2000). The process of phagocytosis is illustrated in **Figure 7**. Once the bacteria are taken up into membrane surrounded phagosomes they are getting destroyed by infusion of several bactericides (Aderem and Underhill, 1999).

Another process called pinocytosis mediates the uptake of smaller particles, molecules, solutes and extracellular fluids. Pinocytosis can occur via several different molecular mechanisms:

Macropinocytosis accompanies membrane ruffling induced by growth factors and other signals. Similar like in phagocytosis the involved signaling mechanisms activate Rho-family GTPases in order to form actin rich protrusions. These protrusions collapse onto and fuse with the plasma membrane. Particles of up to 1μm can be engulfed to generate large endocytic vesicles called macropinosomes (Nichols and Lippincott-Schwartz, 2001). Macropinocytosis plays a role in immune surveillance by dendritic cells (Mellman and Steinman, 2001). Interestingly, macropinocytosis induced by Platelet Derived Growth Factor (PDGF) might plays a role in directed cell migration (Ridley, 2001).
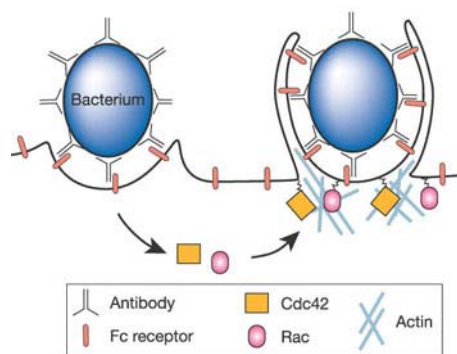
Figure 7. Mechanism of phagocytosis. Large particles (for example bacteria) are recognized by cell surface receptors which activate Cdc42 and Rac. Cdc42 and Rac promote the formation of actin rich membrane protrusions that engulf the particles leading to their uptake. Macropinocytosis follows the same principle (scheme taken from Conner and Schmid, 2003).

Caveolin mediated endocytosis. Caveolae are small sphingolipid and cholesterol rich invaginations abundant on the plasma membrane of many cell types (e.g. endothelial cells). Their shape results from the action of caveolin a dimeric cholesterol binding protein that inserts at the inner loop of the plasma membrane. It self-associates to form a striated coat around the invagination. Caveolae are static structures. However, their endocytosis can be triggered by tyrosine phosphorylation of its constituents, mediated by activated signaling receptors within the caveolae (**Figure 8**). Caveolin mediated endocytosis involves actin and the GTPase dynamin (see below). Endocytosed vesicles

fuse to the caveosome for further sorting to the endoplasmic reticulum (ER) or the Golgi complex (Pelkmans and Helenius, 2002).
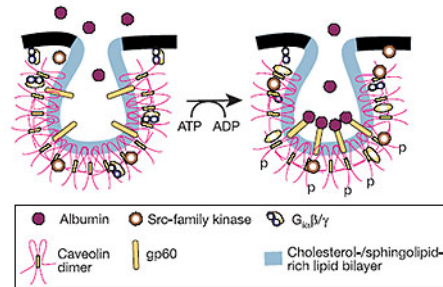
Figure 8. Caveolae. Caveolin forms a dimer at the inner leaflet in cholesterol and sphingolipid rich sub domains (Rafts) of the plasma membrane. Caveolin assembles into a striated coat leading to membrane invagination. Activated receptors (here gp60 activated by albumin) can lead to tyrosine phosphorylation in caveolae, promoting their fission into the cell (scheme taken from Conner and Schmid, 2003).

The so far best characterized way of endocytosis is *clathrin mediated endocytosis (CME)*. Clathrin is a three legged structure in form of a triskelion. One triskelion consists out of three clathrin heavy chains (CHC) each tightly associated with one clathrin light chain (CLC). The triskelions have the ability to self-assemble into polygonal cages. *In vivo*, however, cage formation only occurs at 'hot spots' at the plasma membrane. Receptors dedicated for endocytosis recruit assembly proteins (APs) like AP180 or the heterotetrameric adaptor complex AP2 to these 'hot spots'. The assembly proteins promote the caging process leading to invagination of the plasma membrane into clathrin coated pits (CCP). Therefore the APs represent the link between regulated cargo uptake and the endocytic machinery. The GTPase dynamin forms a collar at the edge of deeply invaginated pits. Dynamin is thought to act as a 'poppase' and/or as a 'pinchase' propelling the nearly completed vesicle towards the cytosol and finally mediating its fission to form a clathrin coated vesicle (CCV). This process requires GTP hydrolysis by dynamin. Entering the cytosol CCVs loose their clathrin coat and the liberated vesicles are subsequently targeted to early endosomes (Kirchhausen, 2000; Conner and Schmid, 2003). CME is involved in a variety of processes like transferrin uptake, synaptic vesicle recycling or growth factor receptor signaling (see below). The process of CME is illustrated in **Figure 9**.
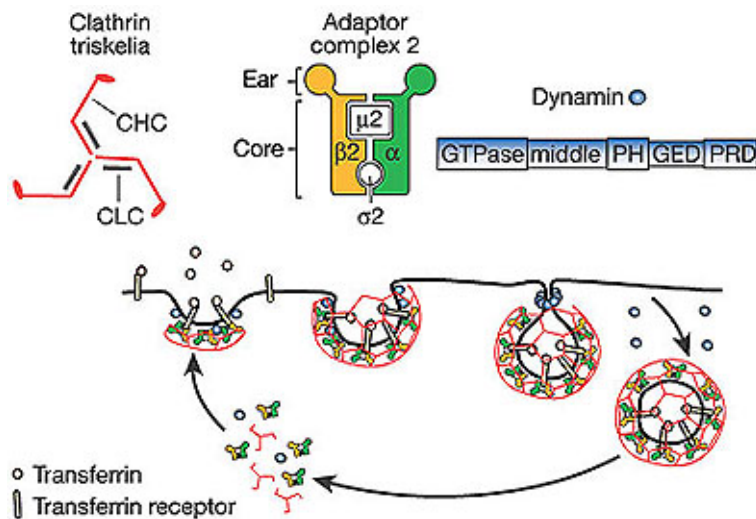
Figure 9. Clathrin mediated endocytosis. Activated receptors (here transferrin receptor activated by transferrin) recruit heterotetrameric assembly proteins like AP2 to initiate hot spots at the plasma membrane. AP2 promotes the assembly of clathrin triskelions that form a clathrin coated pits (CCPs) at the plasma membrane. The GTPase dynamin forms a collar at the end of each CCP and drives its fission into the cell (scheme taken from Conner and Schmid, 2003).

5.2.2. Endocytosis and signaling

Endocytosis provides a mechanism for attenuation of signaling over an extended time period (Sorkin and Von Zastrow, 2002). For example, upon activation, ligand bound epidermal growth factor receptor (EGFR) is rapidly downregulated by endocytosis into endosomes and subsequent lysosomal degradation. In an alternative route, EGFR can be dissociated from its ligand in endosomal compartments. Via different pathways it can be recycled back to the cell surface. Interfering with EGFRs capability to endocytose led to enhanced signaling with the result of increased mitogenic responses in cells (Wells et al., 1990). Similar processes are relevant for a vast number of cell surface receptors (Sorkin and Von Zastrow, 2002).

An alternative more rapid mechanism for signal attenuation is the desensitization of activated receptors. Not less important for proper function is their resensitization afterwards. For example G-protein coupled receptors are rapidly desensitized by phosphorylation of their intracellular C-terminal tails. This process occurs while the receptors are still located at the plasma membrane. After endocytosis and targeting to

endosomes, in addition to ligand removal, these receptors become dephosphorylated, before traveling back to the cell surface. Thus, endocytosis plays a central role in the resensitization of these receptors (Sorkin and Von Zastrow, 2002).

Endocytosis may play a crucial role in the spatial distribution of morphogens. A morphogen is a molecule that usually forms a gradient over the tissue, endowing cells with positional information in a concentration dependent manner. The transforming growth factor (TGF)-β homologue decapentaplegic (DPP) forms a morphogen gradient along the anterior to posterior axis of the *Drosophila melanogaster* wing. The establishment of the gradient depends on dynamin. In a planer transcytosis model DPP spreads over the tissue from cell to cell by sequential endocytosis and exocytosis. Other morphogens like sonic hedgehog (Shh) are membrane anchored molecules. It was proposed that Shh is transferred from the donor cells via membranous vehicles to the receiving cells, where the vehicles are uptaken by endocytosis (Gonzalez-Gaitan, 2003).

Before mechanisms of downregulation take place, activated receptors can signal from intracellular compartments. This leads to a compartmentalization of different signaling events with functional relevance: For example in PC12 cells the nerve growth factor (NGF) receptor TrkA activates the GTPase Ras1 at the plasma membrane leading to a transient activation of the mitogen activated protein kinases (MAPK) ERK. Transient ERK activation elicits a survival response of the cells. Conversely, endocytosed TrkA activates the GTPase Rap1, leading to sustained ERK activation which is required for the differentiation of the cells. Moreover, signal transduction from endosomes provides a mechanism by which signals from presynaptic terminals of neurons are communicated to the cell bodies. Activated Trk receptors endocytose and form an ERK activation complex on endosomes. These signaling endosomes become retrogradely transported along the neurites to the cell bodies. Here, the ERK activation complex meets its substrate CREB, which becomes phosphorylated and subsequently translocated to the nucleus (Barker et al., 2002). The different effects that endocytosis can have on signaling by cell surface receptors are summarized in **Figure 10**.
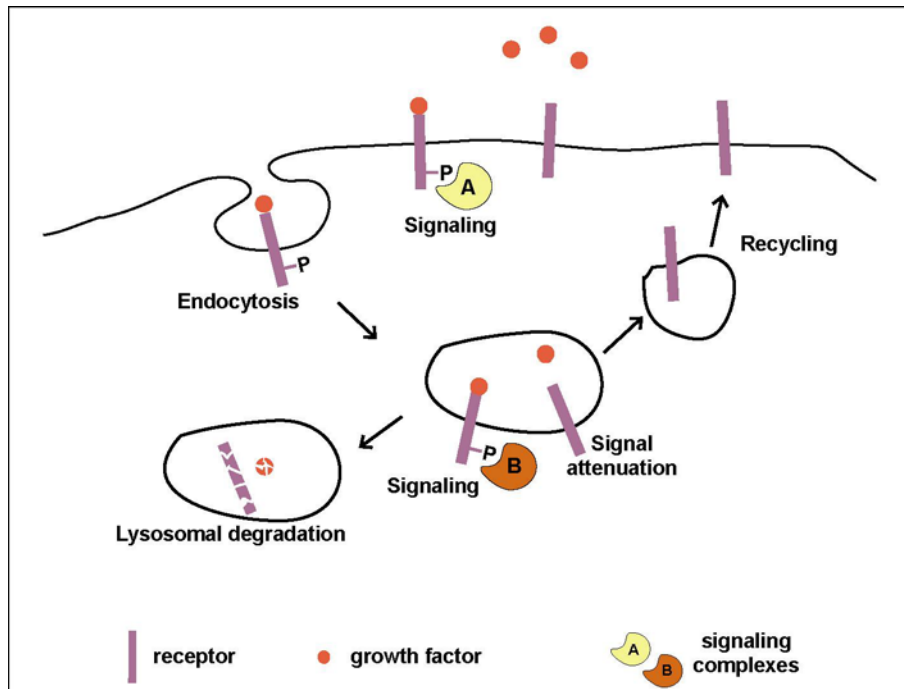
Figure 10. Endocytosis and signaling. Cell surface receptors get activated by binding to their ligands. Rapid intracellular modifications like phosphorylation lead to immediate signaling from the plasma membrane or in some cases provide a mechanism for desensitization. Activated receptors get endocytosed and vesicular traffic sorts them to endosomes. Specific signaling events can occur from endosomes. Subsequent targeting to lysosomal degradation leads to the downregulation of the receptors. Alternatively, resensitized receptors are recycled back to the plasma membrane.

5.2.3. Endocytosis and axon guidance

It is anticipated, that like other cell surface receptors, axon guidance receptors also undergo endocytosis upon their activation. However, only a few axon guidance receptors have been studied in this context. Therefore, little is known about the role of endocytosis in axon guidance. Directed movement of cells is a concerted action involving actin dynamics, cell-substrate adhesion and de-adhesion as well as membrane traffic (de Curtis, 2001).

Endocytosis can regulate substrate adhesion of growth cones as shown for L1, a member of the immunoglobulin superfamily of CAMs. L1 is endocytosed at the central domain of the growth cone followed by centrifugal vesicular transport and reinsertion into the plasma membrane of the leading edge. This way adhesion sites are constantly recycled towards the growth direction of the cell, allowing directed movement (Kamiguchi and

Lemmon, 2000). Interfering with L1 endocytosis decreased L1 dependent growth cone migration (Kamiguchi and Yoshihara, 2001).

Endocytosis occurs during growth cone collapse induced by the semaphorin Sema3A and by ephrinA2-Fc. These effects were different from constitutive endocytosis at growth cones and depended on the Rho family GTPase Rac. Filamentous actin was reorganized in a Rac1 dependent manner to endocytic organelles. Based on these studies it was suggested that growth cone collapse requires both, rearrangements of filamentous actin as well as the rapid reorganization of plasma membrane (Fournier et al., 2000; Jurney et al., 2002).

5.3. Eph receptors and their ephrin ligands

The Eph receptors constitute the largest class of receptor tyrosine kinases in the human genome. They are conserved among vertebrates, insects, nematodes and even sponges. They function in an amazing variety of developmental and adult processes like cell migration, axon pathfinding and topographic mapping, segmental patterning, angiogenesis and tumorigenesis, synapse morphology and synapse plasticity. One peculiarity is that Ephs and ephrins signal in a bidirectional way, i.e. Eph receptors as well as their ligands transduce signals into the cells expressing them. Thus, ephrin ligands also act as receptor like molecules. Signaling downstream of the receptors is called 'forward' and downstream of the ligands is called 'reverse' signaling.

5.3.1. The Eph class of receptor tyrosine kinases

The human genome encodes 13 different Eph receptors. Based on sequence similarity and ligand binding characteristics they are subdivided into 8 EphA receptors (EphA1-EphA8) and 5 EphB receptors (EphB1-EphB4, EphB6). Chickens encode an additional EphB receptor, EphB5 (Wilkinson, 2001). The genomes of the nematode *Caenorhabditis elegans* and the fruitfly *Drosophila melanogaster* encode one Eph receptor each (Vab-1

and Dek respectively) (George et al., 1998; Scully et al., 1999). Thus, the diversity of the family in vertebrates must have arisen by more recent gene duplications. Ephs are transmembrane receptors. Their extracellular domain consists of an N-terminal globular ligand binding domain, followed by a cysteine rich region and two fibronectin type III repeats (FNIII). The single transmembrane spanning region is followed by a juxtamembrane region, a tyrosine kinase domain, a sterile-α-motif (SAM)-domain and a C-terminal PDZ-binding motif (PDB) (**Figure 11**). Ligand binding specificity is encoded within the N-terminal globular domain.

5.3.2. Ephrin ligands

The vertebrate ephrin ligands are also subdivided into two classes. While all ephrins share a homologous N-terminal ephrin-domain, only the ephrinB ligands have a single transmembrane domain, and a cytoplasmic domain containing 5-6 conserved tyrosine residues and a C-terminal PDZ-binding motif. EphrinA ligands are tethered to the membrane by a glycosile-phosophatidyl-inositol (GPI)-anchor (**Figures 11 & 17**). In vertebrates there are 5 ephrinA ligands (ephrinA1-ephrinA5) and 3 ephrinB ligands (ephrinB1-ephrinB3). EphA receptors bind ephrinA ligands, whereas EphB receptors bind ephrinB ligands. Binding across subclasses does not occur with the exception of EphA4 (Wilkinson, 2000). Binding specificity within a subclass is low. All EphA receptors bind to all ephrinA ligands. EphB1, EphB2, and EphB3 receptors bind equally well to both ephrinB1 and ephrinB2. There is some specificity within subclass B: EphB4 appears to only bind ephrinB2 (Wang et al., 1998; Adams et al., 1999; Gerety et al., 1999). In *C. elegans* there are 4 GPI-anchored ephrin ligands (EFN1-EFN4). The sequence of their N-terminal domains shares equal similarities with vertebrate A- and B-type ephrins (Chin-Sang et al., 1999). In *Drosophila*, Dephrin is the only known ligand for Dek. The Dephrin coding sequence predicts 3 TM domains, an extracellular ephrin domain after the first TM domain and a cytoplasmic domain with some sequence similarity to vertebrate B-type ephrins (Bossing and Brand, 2002).
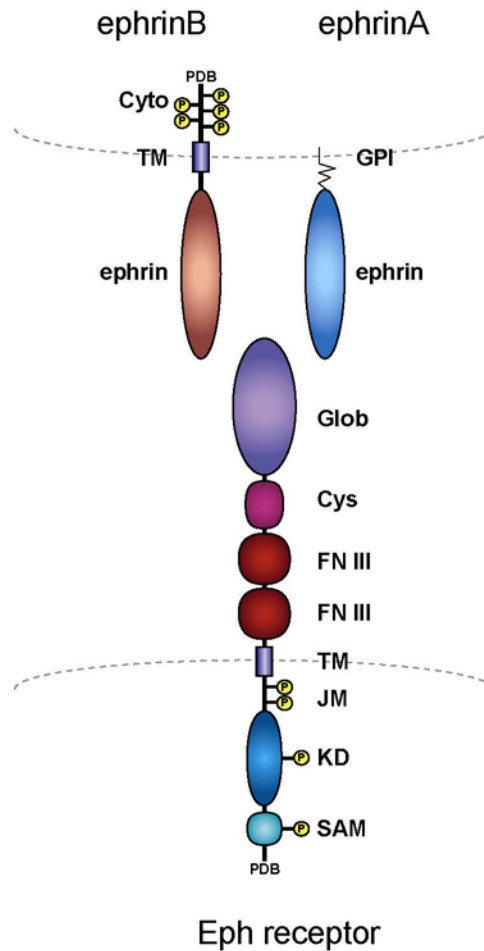
Figure 11. Eph receptors and their ephrin ligands. Eph receptors: N-terminal globular ligand binding domain (Glob), cysteine rich region (Cys), fibronectin type III repeat (FNIII), transmembrane domain (TM), juxtamembrane region (JM), kinase domain (KD), sterile-α-motif (SAM), PDZ-binding motif (PDB), tyrosine phosphorylation sites (P). EphrinA ligands: N-terminal ephrin domain (ephrin), glycosylphosphatidylinositol (GPI) anchor. EphrinB ligands: N-terminal ephrin domain (ephrin), transmembrane domain (TM), cytoplasmic domain (Cyto), PDZ-binding motif (PDB), tyrosine phosphorylation sites (P).

5.3.3. Forward and reverse signaling during axon guidance

Neurons of many sensory organs, like the visual system, project in a topographic manner. For example neighboring neurons within the vertebrate retina (Retinal ganglion cells, RGCs) project to neighboring regions in the mammalian superior colliculus (SC) or the avian tectum. Their relative positions in the retina with respect to the temporal-nasal axis determine their target areas in the tectum/SC with respect to the anterior-posterior axis. Thus, based on axonal projection patterns spatial visual information is transferred from a

sensory organ to higher brain centers. Ephs/ephrins were first described as molecules involved in retinotopic map formation during development (O'Leary and Wilkinson, 1999). EphrinA ligands are expressed in an anterior (low) to posterior (high) gradient in the tectum/SC. EphA receptors are expressed in a nasal (low) to temporal (high) gradient in the retina. EphrinA ligands represent repellents for axons expressing EphA receptors. In a simplified model axons from temporal neurons expressing high EphA receptor, respond already to low levels of ephrinA ligand in the anterior tectum. Conversely, axons from nasal neurons expressing low levels of EphA receptors require high levels of ephrinA ligand to respond, thus they can extend to more posterior positions within the tectum/SC. Retinotopic mapping by Ephs/ephrins is far more complex than described above. (Wilkinson, 2000; McLaughlin et al., 2003). However, this naïve model describes already sufficiently the principle of how Eph/ephrins navigate axons (**Figure 12**).
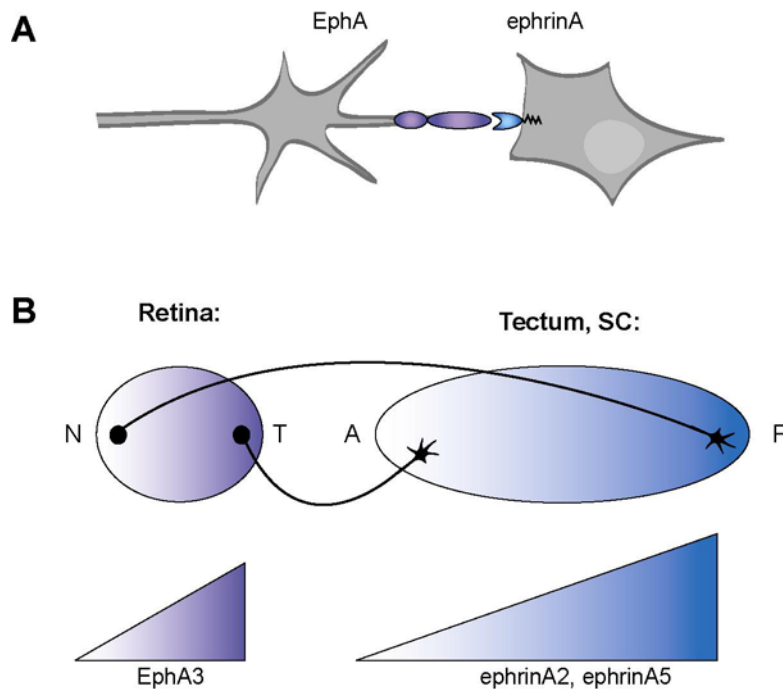
Not only ephrins but also the Eph receptors can represent guidance cues for axons. EphB2$^{-/-}$ mice have a defect in the posterior part of the anterior commissure (ACp) (**Figure 13**). In mammals, axons originating from the temporal sides of the cortex normally fasciculate and cross the midline in the dorsal forebrain to find their targets on the contra-lateral sides of the cortex. In EphB2$^{-/-}$ mice these axons fail in midline crossing and instead misproject into the ventral forebrain. Interestingly this phenotype was rescued in genetically engineered mice expressing a chimeric EphB2 receptor which has its cytoplasmic domain replaced by lacZ (EphB2-lacZ). Thus, the N-terminal domain of EphB2 is sufficient for correct guidance. EphB2 is not expressed by ACp axons but in the tissue of the ventral forebrain. Conversely, ephrinB ligands are expressed on the axons (Henkemeyer et al., 1996; Orioli et al., 1996). These data suggested that ACp axons sense a repellent represented by the ectodomain of EphB2 in the ventral forebrain and ephrinB ligands act as receptor like molecules transducing signals *in reverse* via their cytoplasmic domains. Eph/ephrins are crucial for the formation of many other axonal projections. In some cases reverse signaling, and in other cases classical Eph receptor forward signaling is required (Palmer and Klein, 2003).

Figure 12. Simplified model of retinotopic mapping by EphA receptors and ephrinA ligands. (**A**) EphA receptors are expressed on growth cones of retinal ganglion cell (RGC) axons. EphrinA ligands are expressed on tectal or superior collicular cells. They represent repellents that transmit growth inhibitory signals into the EphA receptor expressing cell. (**B**) EphA3 is expressed in a nasal (N) to temporal (T) gradient in the retina. EphrinA ligands are expressed in an anterior (A) to posterior (P) gradient in the tectum/SC. RGCs located to nasal positions in the retina express relative low levels of EphA3. High levels of ephrinA ligands are required to stop their growth. The result is that their axons project into relative posterior regions in the tectum/SC. Conversely temporally located RGCs expressing high levels of EphA3 receptor stop growing already in response to low levels of ephrinA ligands in the anterior tectum/SC.
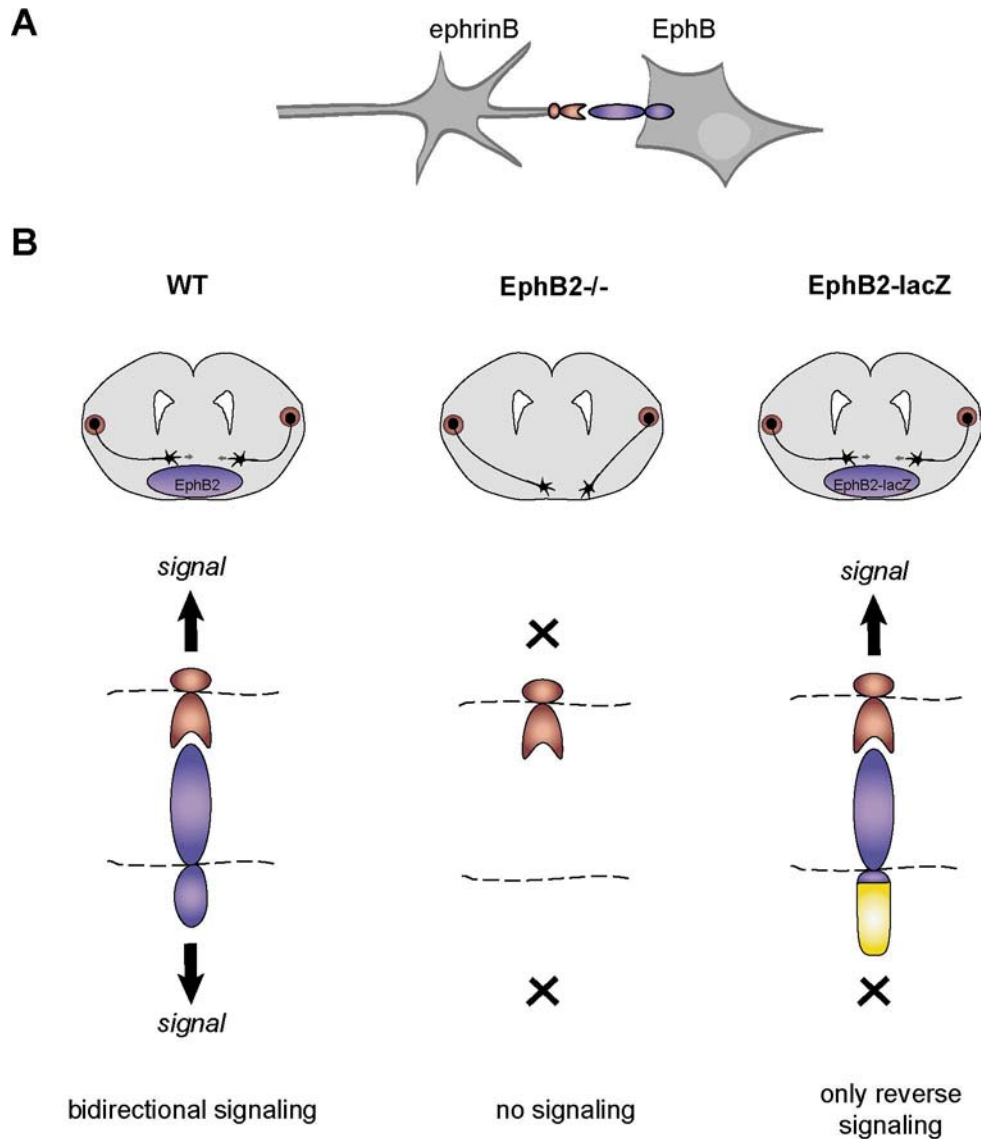
Figure 13. Guidance of commissural axons is independent of Eph receptor forward signaling. (**A**) Commissural neurons in the anterior forebrain express ephrinB ligands on their growth cones that sense EphB2 as a repellent guidance cue. (**B**) Axons of the ACp derive from the temporal cortices, fascicle and cross at the midline to innervate the contra lateral sites. EphB2 is expressed ventral to the commissure in the anterior forebrain and ephrinB ligands are expressed on the axons (left panel). In EphB2 knock out mice (EphB2$^{-/-}$) the axons fail to cross the midline and misproject into the ventral anterior forebrain (middle panel). This phenotype is rescued in mice expressing a chimeric EphB2-lacZ receptor which is incapable of forward signaling. Reverse signaling by ephrinB ligands in the growth cones of ACp axons might be sufficient for repulsive guidance (right panel).

5.3.4. Bidirectional signaling by Eph/ephrins during segmentation

In the previous chapter two examples were discussed, where either forward or reverse signaling is required for the guidance of axons. However, in these cases unidirectional signaling appears to be sufficient and there is no evidence for the requirement of bidirectional signaling. Segmentation occurs during the development of the vertebrate hindbrain. Seven segments or rhombomeres (r1-r7) specify the identity and origin of certain nerves as well as different streams of neural crest cell migration into the branchial arches. Each rhombomere is a restricted compartment of cells and cell intermingling between the segments is prohibited. Ephs and ephrins are expressed in a complementary pattern in alternating rhombomeres (Cooke and Moens, 2002; Tepass et al., 2002). This observation led to the idea that repulsive Eph/ephrin signaling leads to cell sorting at the boundaries between rhombomeres. Ectopic expression studies in the *zebrafish* hindbrain demonstrated the requirement for the cytoplasmic domain of ephrinB ligands for the correct sorting of cells (Xu et al., 1999). In a zebrafish animal cap assay EphA4 expressing cells sort from ephrinB2 expressing cells, resulting in an artificial boundary. Boundary formation required the cytoplasmic domains of both, EphA4 and ephrinB2, indicating the requirement of a bidirectional signaling mode (Mellitzer et al., 1999). Genetic evidence for this model is still missing, perhaps due to functional redundancy of several receptors and ligands.

5.3.5. Eph/ephrins and synaptic plasticity

Chemical neuronal synapses are formed by a presynaptic terminal that releases neurotransmitters to the postsynaptic site. Synaptic strength, hence synaptic plasticity, memory and learning are regulated and achieved by the pre- and postsynaptic machinery. Several Eph receptors and ephrin ligands have been shown to be expressed at neuronal synapses (Gerlai, 2001; Murai and Pasquale, 2002). In many CNS synapses the postsynaptic sites are formed by mushroom like structures called spines. The morphology of spines is thought to be important for synaptic function (Hering and Sheng, 2001;

Bonhoeffer and Yuste, 2002). Eph receptor signaling has been shown to be involved in synaptic spine formation and morphology (see below).

Activity dependent synaptic plasticity often requires N-methyl-D-aspartate (NMDA)-type glutamate receptors. NMDAR dependent Ca^{2+} influx and associated signaling pathways orchestrate synapse formation and plasticity (Helmchen, 2002). In young hippocampal neuron cultures EphB2 receptor activation leads to interaction with and clustering of NMDAR. EphB receptor signaling can enhance NMDAR dependent Ca^{2+} influx leading to increased CREB (cAMP Response Element Binding Protein) dependent transcription, a process important for synapse plasticity, learning and memory. In the same system EphB receptor stimulation finally elicited the formation of new synapses. These findings suggest that ephrinB ligands in presynaptic membranes induce the maturation of glutamatergic synapses by NMDAR aggregation and regulating NMDAR function (Dalva et al., 2000; Takasu et al., 2002). The EphB2-NMDAR interaction has been confirmed to occur in adult mice and targeted inactivation of the mouse EphB2 gene in the hippocampus interfered with spatial learning and long-term potentiation of synapses of the Schaffer collateral pathway. Interestingly, expression patterns and genetic studies suggested that ephrinB ligand reverse signaling is important for these processes (Grunwald et al., 2001). Recent data support a model where ephrinB ligands signal in postsynaptic membranes via the PDZ domain protein GRIP to glutamate receptors of the AMPA type, regulating their surface distribution at synapses (I. C. Grunwald et. al., submitted for publication). NMDAR independent LTP occurs at hippocampal Mossy fiber synapses. Electrophysiological studies suggested that postsynaptic PDZ interactions link EphB receptor forward signaling to non-NMDA type glutamate receptor functions. Presynaptic ephrinB reverse signaling in this case may regulate long lasting presynaptic changes (Contractor et al., 2002).

5.3.6. Eph/ephrin functions in vascular development

During embryonic development blood vessels arise via two distinct processes. In a process called vasculogenesis, endothelial cells form *de novo* by differentiation of mesodermal precursors. This leads to the formation of a primary vascular plexus, an

unorganized meshwork of capillaries. In a process called angiogenesis, mature blood vessels are formed by remodeling the primary plexus or by sprouting form pre-existing vessels. Mice bearing targeted mutations in the ephrinB2 or EphB4 genes halt at the stage of plexus formation leading to embryonic lethality (Wang et al., 1998; Adams et al., 1999). EphrinB2 is expressed on primordial arterial vessels whereas EphB4 is expressed on primordial venous vessels. This suggests a role for ephrinB2 and EphB4 in establishing arterial and venous identities. Other EphB receptors and ephrinB ligands are expressed on both arteries and veins, as well as on mesenchymal cells that surround the blood vessels suggesting more complex mechanisms how Ephs and ephrins organize the vasculature (Adams 2002). Genetically engineered mice expressing a C-terminally truncated form of ephrinB2 have a similar vascular phenotype like the ephrinB2 knock out mice, indicating an important role for ephrinB reverse signaling in angiogenesis (Adams et al., 2001). *In vitro* soluble ephrinB-Fc fusion proteins can induce the sprouting of endothelial cells in two-dimensional matrigels. These findings suggest that the functions of Eph/ephrin signaling in angiogenesis are to regulate the migration of endothelial cells (Adams et al., 1999). Thus, it is likely that growth cone guidance and patterning of the vasculature during development follow similar mechanistic principles.

Eph/ephrin signaling is not only restricted to embryonic angiogenesis. EphrinB2 is also expressed in adult arteries and extends into small diameter microvessels (Gale et al., 2001; Shin et al., 2001). Ephs and ephrins may even play a role in tumorangiogenesis (Palmer and Klein, 2003).

5.3.7. Signaling mechanisms by Eph receptors and ephrin ligands

5.3.7.1. Mechanisms of Eph receptor forward signaling

Most RTKs activate signaling pathways that target transcription in the nucleus leading to proliferative and/or differentiation responses. By contrast, Eph receptors regulate cell migration, repulsion, and attachment to the extracellular matrix. The signaling cascades

that they activate, therefore, ultimately converge on the cytoskeleton and on integrin adhesion sites.

The first step in initiation of Eph signaling is the recognition and binding of receptors with ligands on opposing cell surfaces. Biophysical and crystallographic studies led to a model of a two step mechanism: Initially a high affinity heterodimer is formed between one N-terminal globular domain of the Eph receptor and the N-terminal domain of an ephrin molecule. Recognition proceeds via an induced fit mechanism where a loop of the ligand induces the folding of a hydrophobic binding pocket on the receptor. This heterodimeric 1:1 complex then favors tetramerization to a 2:2 complex. Low affinity binding sites between tetramers may then lead to further oligomerization (Himanen et al., 2001). It has been shown that Eph-receptors require higher order oligomerized ligands for full activation when presented as soluble recombinant Fc-fusion proteins (ephrin-Fc) (Stein et al., 1998). It is thought that this oligomerization mimics the membrane anchorage of the ligand.

There is no evidence that the ligand induced change in the secondary structure of the receptor is translocated outside of the globular domain. Thus, mechanisms of kinase activation are rather similar to those of other RTKs. Ligand binding brings together two catalytically autoinhibited receptors into an orientation that favors trans-autophosphorylation on a tyrosine residue located on the so called activation-loop (A-loop) within the kinase domain. In its unphosphorylated form, the A-loop folds into the catalytic pocket of the kinase domain, thereby inhibiting its activity. Steric forces liberate the phosphorylated loop outside the pocket, leading to kinase activation. Another inhibitory interaction exists between the kinase domain and the juxtamembrane region. Upon phosphorylation of two conserved tyrosines within this region, this interaction folds up permitting the full activation of the receptor (**Figure 14**).
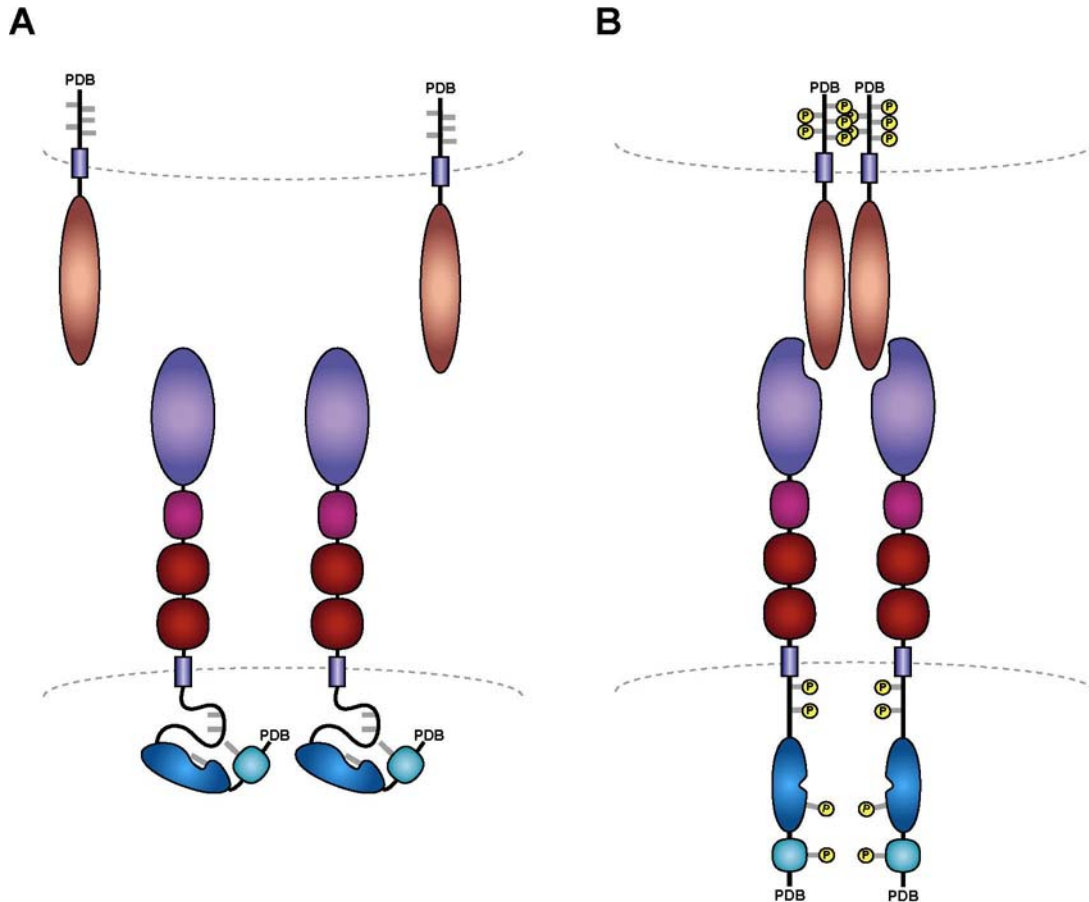
Figure 14. Mechanisms of Eph receptor activation. (**A**) In the unbound state, the cytoplasmic domain of Eph receptors is in a close conformation held by a fold in the juxtamembrane (JM) region. A tyrosine residue in the A-loop of the kinase domain keeps the enzyme inactive. (**B**) Ligand binding occurs by an induced fit mechanism leading to a conformational change in the Glob domain. Ligand receptor interactions promote the formation of a heterotetramer followed by higher order heteromultimers (not shown). Kinase domains come close together and basal activity leads to trans-autophosphorylation. Phosphorylation of the A-loop tyrosine activates the kinase. Phosphorylation at the JM tyrosines opens the close conformation leading to full kinase activity.

The activated receptors then interact with adaptor molecules that transmit signals into the cell. Adaptor molecules contain functional protein-protein interaction domains as the src-homology-2 (SH2) and SH3 domains. SH2 domains bind to phosphorylated tyrosine motifs of the receptor thereby connecting upstream and downstream signaling events. The interaction of a variety of such adaptors with Eph receptors has been shown (**Figure 15**).

The SH2 domains of the non receptor tyrosine kinases Abl and Arg bind to the phosphorylated juxtamembrane tyrosine residues. Abl and Arg are known regulators of

the actin cytoskeleton and activation of EphB1 receptor led to a decrease in Abl activity. Coexpression of EphB1 and Abl in neuronal growth cones, indicates a possible role for their interaction in repulsive growth cone guidance (Yu et al., 2001). Eph receptors also interact with the related non receptor tyrosine kinases of the Src family (SFK) (Ellis et al., 1996; Zisch et al., 1998). SFKs have been implicated in regulation of cytoskeletal dynamics and cell-substrate adhesion via integrins (Thomas and Brugge, 1997).

The GTPases of the Rho family Rho, Rac and Cdc42 are known regulators of actin dynamics. Activated Rho promotes disassembly of actin fibers and growth cone collapse, whereas activated Rac and Cdc42 promote the formation of filopodia and lamellipodia respectively (see above). The Rho guanine nucleotide exchange factor (GEF) Ephexin (Eph interacting exchange protein) provides a link between Eph receptors and Rho family GTPases. Ephexin binds to the kinase domain of EphA4 and has differential effects such that RhoA becomes activated and Rac as well as Cdc42 are inhibited. The net result is a shift of actin dynamics towards contraction and reduced extension. Dominant negative forms of Ephexin abolished Eph receptor dependent growth cone collapse (Wahl et al., 2000; Shamah et al., 2001).

Eph receptors are regulators of substrate adhesion via integrins. Their action can lead to enhanced or reduced adhesion. Activated EphB2 receptor in NIH3T3 fibroblasts led to phosphorylation of the GTPase R-Ras, a known regulator of integrin mediated adhesion. Phosphorylation of R-Ras led to decreased adhesion (Zou et al., 1999). Focal adhesion kinase (FAK) is an important regulator of integrins. EphA2 receptor was shown to dephosphorylate FAK, suppressing the adhesion of prostate carcinoma cells in culture (Miao et al., 2000). Other studies reported that Eph receptor signaling can lead to enhanced adhesion by integrins. In human kidney cells EphB1 can promote integrin adhesion via the SH2-SH3 adaptor Nck (Huynh-Do et al., 2002) activating the Nck interacting kinase (NIK) (Becker et al., 2000). In NIH3T3 and HEK293 cells activation of EphA8 receptor caused the plasma membrane recruitment of the p110γ subunit of phosphatidylinositol 3-kinase (PI3Kγ), promoting integrin mediated adhesion and cell migration (Gu and Park, 2001; Gu and Park, 2003). The signaling events described are summarized in **Figure 15**.
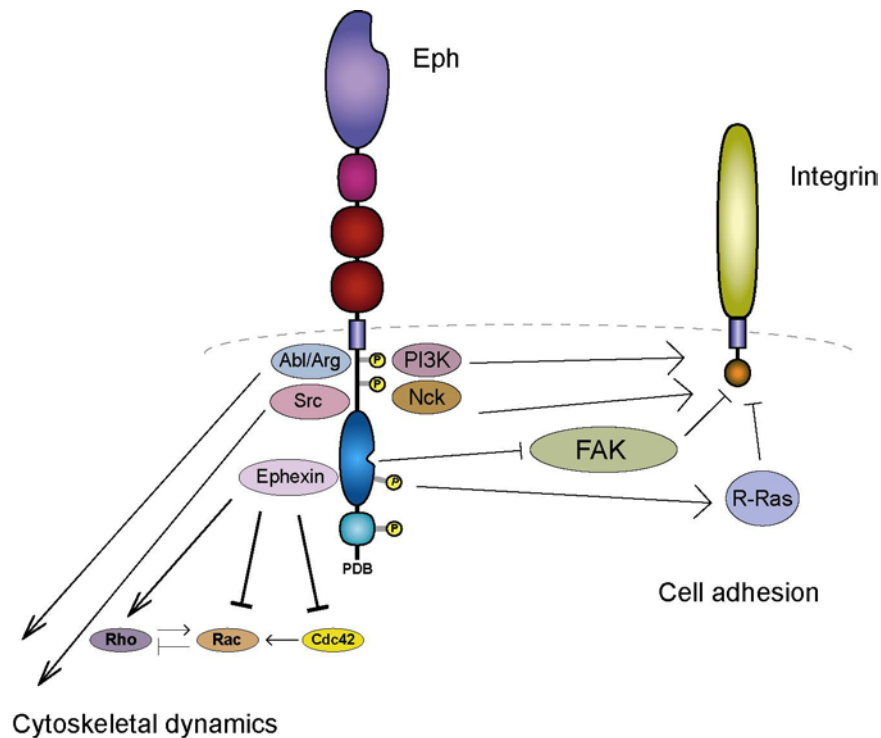
Figure 15. Summary of adaptor interactions described in the text. Cytoplasmic tyrosine kinases like Abl/Arg and Src act downstream of Eph receptors to regulate cytoskeletal dynamics. The GEF Ephexin shifts the balance of Rho family GTPase activity towards Rho leading to growth cone collapse. Signaling via PI3K, Nck, FAK and R-Ras modulates cell adhesion by integrins.

Three recent studies shed light on how Eph receptors regulate synaptic spine morphology. The neuronal cell surface proteoglycan syndecan-2 is an important cell adhesion molecule in the process of spine maturation (Ethell and Yamaguchi, 1999). EphB2 activation led to syndecan-2 clustering in cultured hippocampal neurons resulting in the formation of new spines. This effect was depending on the PDZ-domain protein syntenin, a known interactor of syndecan-2 and EphB2, as well as on tyrosine phosphorylation of syndecan-2 by EphB2 (Ethell et al., 2001). Filamentous actin is an important structural feature of spines. Stimulation of neurons with soluble ephrinB1-Fc activated the RhoGEF kalirin. A pathway involving the Rho family GTPase Rac1 and its downstream effector p21 activated kinase (PAK) links EphB receptors to actin dynamics in spines (Penzes et al., 2003). EphB2 also interacts with the RhoGEF intersectin an activator of Cdc42 providing another link between EphB receptors and actin assembly in spines (Irie and Yamaguchi, 2002). Signaling pathways downstream of Eph receptors that regulate spine morphology are summarized in **Figure 16**. EphB2 receptor can directly

modulate the activity of NMDA receptors. In young immature neurons activated EphB2 caused the co-clustering of NMDARs. EphB2 activates the cytoplasmic tyrosine kinase Src, which can phosphorylate cytoplasmic tyrosine residues in NMDAR. Phosphorylation enhanced the ability of NMDAR to flux calcium ions, an important step in synaptic plasticity (Dalva et al., 2000; Takasu et al., 2002).
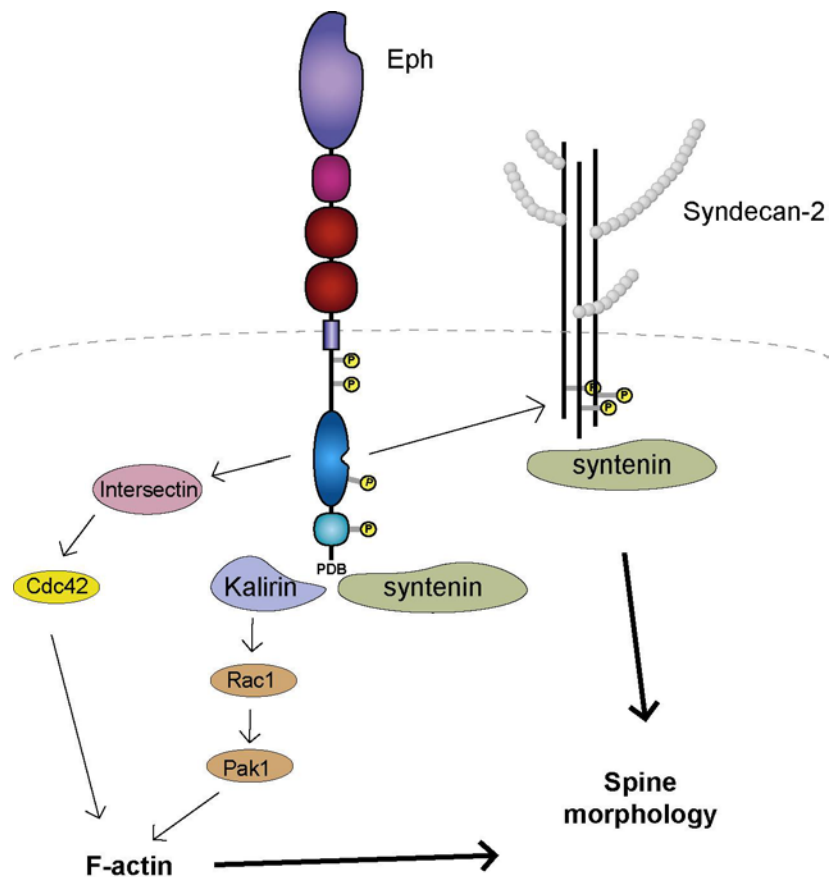
Figure 16. Eph signaling pathways leading to spine formation. The proteoglycan syndecan-2 mediates synaptic spine formation. Eph receptors activate syndecan-2 by phosphorylation. PDZ interactions via syntenin are required in these processes. The PDZ protein kalirin signals via Rac and Pac to mediate F-actin formation, a prerequisite of spine formation. The molecule intersectin connects Eph signaling to Cdc42 promoting F-actin formation.

5.3.7.2. Mechanisms of ephrin ligand reverse signaling

Much less is known about the signaling mechanisms that act downstream of ephrinB ligands. The conservation of the five tyrosine residues in all EphrinBs suggests a role in downstream signaling similar to that of RTKs (**Figure 17**).

```
Ephrin B1    L R K R H R K H T Q Q R A A A L S L S . . . T L A S P K G G S .    292
Ephrin B2    Y R R R H R K H S P Q H T T T L S L S . . . T L A T P K R S G .    279
Ephrin B3    R R R R A K P S E S R H P G P G S F G R G G S L G L G G G G G M    283


Ephrin B1    G T A G T E P S D I I I P L R . . . T T E N N Y C P H Y E K V S    321
Ephrin B2    N N N G S E P S D I I I P L R . . . T A D S V F C P H Y E K V S    308
Ephrin B3    G P R E A E P G E L G I A L R G G G A A D P P F C P H Y E K V S    315
                                                                  *

Ephrin B1    G D Y G H P V Y I V Q E M P P Q S P A N I Y Y K V—COOH            346
Ephrin B2    G D Y G H P V Y I V Q E M P P Q S P A N I Y Y K V—COOH            333
Ephrin B3    G D Y G H P V Y I V Q D G P P Q S P P N I Y Y K V—COOH            340
                   *       *              !         * *
```

Figure 17. Alignment of the cytoplasmic domains of human ephrinB1, –B2, and -B3. As from residue -33 the C-terminal tail is highly conserved among the three ephrinB ligands. The same conservation exists among phylogeny (not shown). 5 conserved tyrosine residues (*) are potential phosphorylation sites. Residues -18, -23, and -4 (C-terminal residue counted as -1) have been identified as major phosphorylation sites *in vivo*. The C-terminal PDZ binding motif is underlined. Note, that one of the tyrosine residues is part of this motif. The possible involvement of a serine residue at position -9 (!) in PDZ binding is discussed in chapters 6.2.2. and 7.1.7.

EphrinB molecules immunoprecipitated from embryonic nervous tissue are indeed tyrosine phosphorylated (Brückner et al., 1997). Phosphorylation occurs mainly at tyrosine residues -23, -18 and -4 (C-terminal residue counted as -1) (Kalo et al., 2001). Stimulation of cells heterologously expressing ephrinB ligands with soluble Fc fusions of EphB receptors (EphB-Fc) resulted in their subsequent phosphorylation on tyrosine (Holland et al., 1996; Brückner et al., 1997). Ephrin phosphorylation was also induced in these cells by contact with EphB expressing cells (Holland et al., 1996). Thus, trans-interactions of EphrinBs with their cognate receptors, activates signaling pathways, involving tyrosine kinases, in the ligand expressing cells. Concomitant overexpression of ephrinB with Src led to ephrinB phosphorylation but the relevance of this finding was, at that time, still unclear (Holland et al., 1996). Tyrosine phosphorylation of EphrinBs can also be achieved in *cis* by activation of platelet derived growth factor (PDGF)- or fibroblast growth factor (FGF)-receptors when they are expressed in the same cells (Brückner et al., 1997; Chong et al., 2000). Therefore it is likely that EphrinBs can serve as components of the signaling pathways downstream of these receptors. However, the

functional relevance of this *cis* phosphorylation has never been tested. So far one adaptor molecule has been identified to bind to ephrinB ligands in a phosphotyrosine dependent way: The SH2- and SH3 domain containing Nck homologue Grb4 (Nckβ). Prolonged stimulation of cells heterologously expressing ephrinB molecules with EphB-Fc resulted in a reduction of F-actin stress fibers and the disassembly of focal adhesions, leading to the detachment of the cells from the substratum. This effect was accompanied by FAK phosphorylation and delivery of the focal adhesion protein paxillin from the plasma membrane, indicating the regulated disassembly of focal adhesion sites. The rearrangements in the actin cytoskeleton were abolished by co-overexpression of a dominant negative form of Grb4. Grb4 binds to a variety of other signaling molecules including Abl interacting protein-1 (Abi-1), axin, a scaffold protein in the Wnt signaling pathway and the c-Cbl associated protein CAP (Cowan and Henkemeyer, 2001).

EphrinB ligands interact with several PDZ domain proteins (Torres et al., 1998; Brückner et al., 1999; Lin et al., 1999; Lu et al., 2001). Some of them like GRIP1, GRIP2 and syntenin are adaptor proteins containing only PDZ-domains. Others are linked to functional domains like the protein interacting with C-kinase (PICK1) or the tyrosine phosphatase PTP-BL. Interestingly the PDZ binding motif in EphrinBs (YKV) contains one tyrosine phosphorylation site. *In vitro* peptide binding studies revealed that phosphorylation might influence PDZ binding (Lin et al., 1999). Only one ephrinB-PDZ interaction so far has been shown to be functional relevant. EphrinB ligands bind constitutively to PDZ-RGS3, a cytoplasmic protein containing one PDZ and one 'regulator of G-protein signaling' (RGS) domain. RGS domains have GTPase activating (GAP) activity on the α subunit of heterotrimeric G-proteins, thereby serving as negative regulators of G-protein signaling. EphrinB reverse signaling via PDZ-RGS interferes with signaling of the chemokine stromal derived factor (SDF)-1 via its G-protein coupled receptor CXCR4. SDF-1 is an attractant for migrating cerebellar granule cells. The inhibitory action of ephrinB reverse signaling was implicated in the correct layering of these cells during cerebellar development (Lu et al., 2001).

Both, B- and A-type ephrins localize to lipid rafts. Rafts are small subdomains in cell membranes rich in cholesterol and sphingolipids. Rafts serve as signaling platforms harboring a variety of membrane anchored signaling molecules (Simons and Toomre,

2000). EphrinB ligands recruit the PDZ domain containing proteins GRIP1 and -2 to lipid rafts (Brückner et al., 1999). The GPI anchor targets ephrinA ligands to rafts. EphrinA molecules engaged with their cognate EphA receptor activate the Src family kinase (SFK) Fyn, which is also targeted to rafts via its myristoyl moiety. Associations via rafts are thought to provide a mechanism how ephrinA ligands are able to transduce signals despite the fact that they lack a cytoplasmic domain. EphrinA reverse signaling regulates integrin mediated adhesion (Davy et al., 1999; Davy and Robbins, 2000; Huai and Drescher, 2001).

Recently it has been shown that ephrinB reverse signaling can also promote integrin mediated adhesion of endothelial cells. It was suggested that this processes involve the C-terminal Jun kinase (JNK). Indeed ephrinB stimulation led to JNK activation. Interestingly this was dependent on the PDZ binding motif in ephrinB1 (Huynh-Do et al., 2002). Signaling pathways downstream of ephrin ligands are summarized in **Figure 18**.
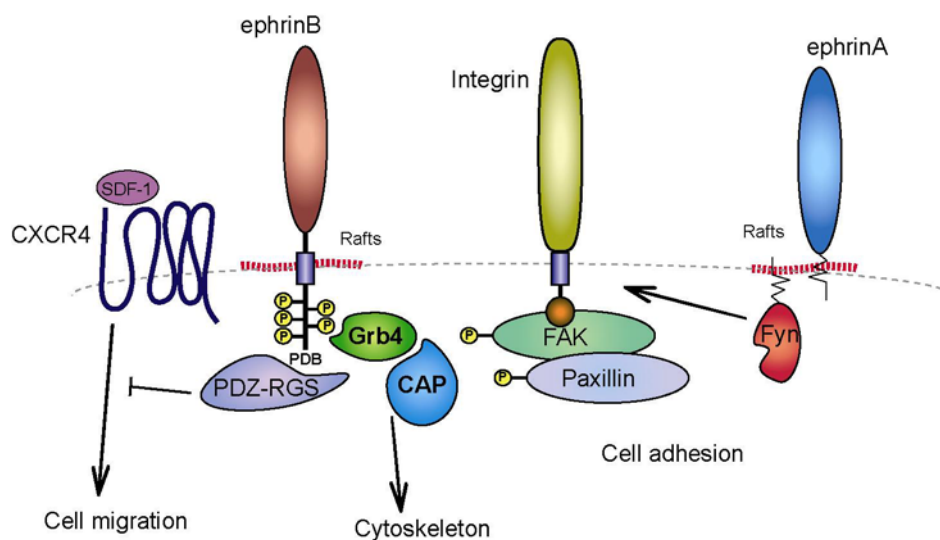
Figure 18. Ephrin reverse signaling. EphrinB ligands signal via PDZ-RGS to inhibit SDF-1/CXCR4 mediated cell migration. Upon receptor binding ephrinB ligands become tyrosine phosphorylated on their cytoplasmic domain. This provides docking sites for the SH2 adaptor Grb4. Grb4 signals via CAP to the cytoskeleton. The focal adhesion proteins FAK and Paxillin become tyrosine phosphorylated downstream of ephrinB ligands. Integrin adhesion can be modulated by both ephrinB and ephrinA reverse signaling. EphA receptor binding to ephrinA ligands leads to activation of Fyn kinase. The mechanism of Fyn activation may rely on interactions within Rafts.

5.4. The thesis project

Previous studies revealed an important role for tyrosine phosphorylation in ephrinB reverse signaling. Tyrosine phosphorylation of the ephrinB cytoplasmic domain initiates signal transduction cascades involving SH2 domain containing proteins. However, the first step in this pathway remained to be elucidated. Since ephrinB ligands lack any intrinsic kinase activity within their cytoplasmic domain the identity of a tyrosine kinase initiating signaling was postulated. The studies presented in this thesis, identified Src family kinases (SFKs) to be the kinases required for ephrinB tyrosine phosphorylation and reverse signaling. In addition this work provides insights of how this signaling is attenuated by the phosphatase PTP-BL leading to a switch from tyrosine dependent to PDZ-dependent signaling. PDZ-dependent signaling involves regulated ephrinB PDZ interactions. This work sheds light on a mechanism of how this regulation might be achieved.

Prior to their repellent effect on migrating cells and growth cones, Eph receptors form a high affinity complex with their ligands at sites of cell-cell contact. Mechanisms have to be in place that remove these complexes, permitting retraction and withdrawal of the cells. A second aim of this thesis project was to identify these mechanisms. This work led to the discovery that Eph/ephrin complexes formed at cell-cell contacts are endocytosed during the retraction of cells and growth cones. Endocytosis occurs bidirectionally and internalizes transmembrane complexes of the full length proteins. Cells expressing signaling inactive mutants of ligand and receptor form strong abnormal adhesion sites. Endocytosis is sufficient to convert this effect into detachment. Bidirectional endocytosis is necessary for efficient axon detachment during growth cone guidance. This work revealed a novel mechanism of signal termination and de-adhesion during cell-cell contact mediated repulsion.

6. Results

6.1. EphrinB Phosphorylation and Reverse Signaling: Regulation by Src Kinases and PTP-BL Phosphatase

The project presented in chapter 6.1. was a collaboration with Dr. Amparo Palmer (Max-Planck-Institute for Neurobiology, Munich, Germany), Dr. Kai Erdmann and Dr. Volker Eulenburg (Both at the department of Dr. Rolf Heumann, Ruhr University Bochum, Germany). For completeness all results are shown. The data presented in **Figure 19**, **20**, **22A**, **23**, **24A** and **25A** were generated by Dr. Amparo Palmer. The data presented in **Figure 24B**, **24D** and **25B** were generated by Dr. Volker Eulenburg. All data shown in chapter 6.1. are published in Palmer, Zimmer et al., 2002. All data shown in chapter 6.3. are published in Zimmer et al., 2003.

6.1.1. A 60kDa kinase phosphorylates the cytoplasmic domain of ephrinB1 in an EphB receptor-dependent manner

To identify the kinase/s responsible for ephrinB phosphorylation, an *in vitro* kinase assay was established using as the substrate the purified ephrinB1 cytoplasmic domain fused to GST (GST-cytoB1). GST-cytoB1 can serve as a general *in vitro* substrate in this kinase assay, since all five tyrosine residues, which are conserved in the three known ephrinB ligands (ephrinB1-B3) are located in a C-terminal stretch of 33 identical amino acids (**Figure 17**). NIH3T3 fibroblasts stably expressing ephrinB1 (NIH3T3-ephrinB1), which were acutely stimulated with the EphB2 receptor ectodomain fused to the Fc portion of human IgG (EphB2-Fc), contained a kinase activity that phosphorylated GST-cytoB1 (**Figure 19A**, left panel). The kinase/s activated by EphB2-Fc bound to GST-cytoB1 as they were also detected in pull-down experiments with GST-cytoB1 (**Figure 19A**, middle panel). No phosphorylation of GST-cytoB1 was observed when the cells were stimulated with unfused Fc, or when GST-cytoB1 was exogenously added to GST control pull-downs (**Figure 19A** and data not shown). A similar kinase activity bound to and phosphorylated full length ephrinB1 immunoprecipitated from cells stimulated with EphB2-Fc (**Figure 19A**, right

panel) showing that kinase/s were able to bind ephrinB1 ligands in intact cells. Phosphoamino acid analysis of GST-cytoB1, which was phosphorylated *in vitro* in a pull-down assay in the presence of $(\gamma\text{-}^{32}P)ATP$, revealed the presence of phosphoserine and phosphotyrosine, but not phosphothreonine residues (**Figure 19B**).

The related ephrinB2 ligand is an essential regulator of early cardiovascular development and an angiogenic factor for endothelial cells *in vitro* (Wang et al., 1998; Adams et al., 1999; Gerety et al., 1999). To test if the putative ephrinB C-terminal kinase is also activated by engagement of ephrinB2 with its receptor EphB4, primary human umbilical aortic endothelial cells (HUAECs) were used in this assay. HUAECs endogenously express ephrinB ligands (**Figure 19C**), including ephrinB2, which is specifically enriched on arteries (Wang et al., 1998; Adams et al., 1999). Acute stimulation of HUAECs with the ephrinB2-specific receptor EphB4 (Gale et al., 1996) activated a kinase that specifically bound and phosphorylated GST-cytoB1 (**Figure 19C**). The kinase was active 10min after stimulation with the EphB4 receptor and became inactivated at later time points. These findings suggested that the observed *in vitro* kinase activity represented that of the physiological 'ephrinB C-terminal kinase', which is activated by EphB/ephrinB interaction.

Next, an in-gel kinase assay was performed to determine the apparent molecular mass of the putative ephrinB C-terminal kinase. Total cell lysates of EphB-Fc activated NIH3T3-ephrinB1 cells and HUAECs were separated using SDS-PAGE polymerized in the presence of the substrate GST-cytoB1. In-gel *in vitro* kinase assays revealed the presence of a kinase that specifically phosphorylated GST-cytoB1 in an EphB-Fc dependent manner and migrated with an apparent molecular mass of 60kDa (**Figure 19D**). Identical results were obtained in both NIH3T3-ephrinB1 cells and HUAECs. When a duplicate of the samples was analyzed in gels polymerized with GST alone, faint signals could be detected which are likely to be autophosphorylated 60kDa kinase (**Figure 19D**). Among the protein tyrosine kinases, Src family kinases (SFKs) have a molecular mass of approx. 60kDa and were previously shown to phosphorylate the C-terminal tail of ephrinB ligands *in vitro* (Holland et al., 1996; Brückner et al., 1997), suggesting that the receptor-stimulated kinase could be a SFK.
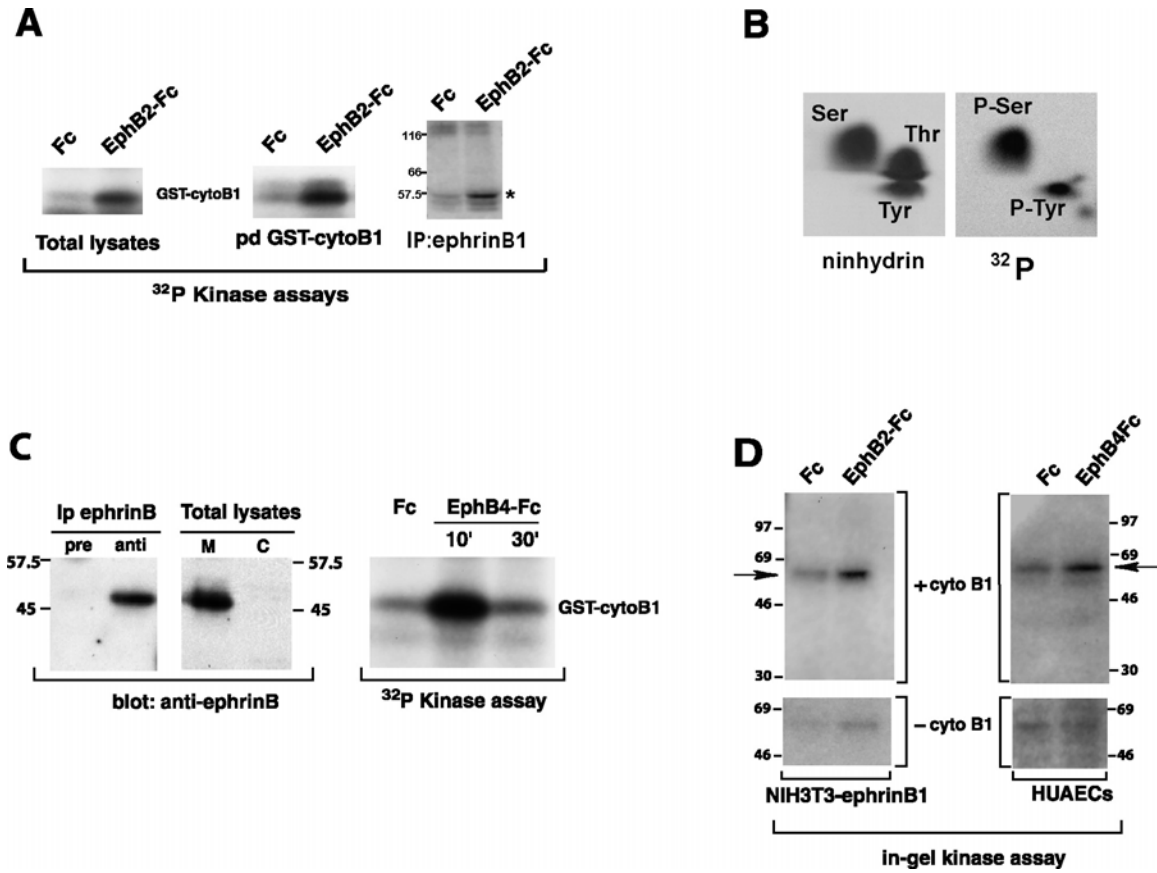
Figure 19. A 60kDa kinase phosphorylates the cytoplasmic domain of ephrinB1 in an EphB receptor-dependent manner. (**A**) NIH3T3 cells ectopically expressing ephrinB1 (NIH3T3-ephrinB1) were serum starved for 16h and then stimulated with either pre-clustered unfused Fc (Fc) or EphB2-Fc receptor bodies for 10min. Total lysates (left panel) were used in an *in vitro* kinase assay using as a substrate the cytoplasmic domain of ephrinB1 fused to GST (GST-cytoB1). Pull-down experiments (pd) to detect binding of kinases to ephrinB1 were performed with GST-cytoB1 (middle panel). Immunoprecipitates of EphrinB1 from lysates of Fc and EphB2-Fc stimulated NIH3T3-ephrinB1 cells were used in an *in vitro* kinase assay to detect phosphorylation of full length ephrinB1 (right panel). The asterisk indicates phosphorylated ephrinB1. (**B**) Phosphoamino acid analysis of *in vitro* phosphorylated GST-cytoB1 in pull-down experiments from NIH3T3-ephrinB1 cells stimulated with pre-clustered EphB2-Fc. Thin layer chromatography on hydrolyzed phosphorylated GST-cytoB1 shows phosphorylation on tyrosine and serine residues. (**C**) Immunoprecipitation with preimmune serum (pre) or anti-ephrinB polyclonal antiserum (anti) to detect endogenous ephrinB ligand levels in extracts from primary human umbilical aortic endothelial cells (HUAECs). The levels of ephrinB in HUAECs were also detected by directly immunoblotting membrane (M) and cytosolic (C) fractions of cell lysates. For stimulation, 16 hour serum-starved cells were incubated for the indicated time points with unfused Fc or EphB4-Fc receptor bodies. Total lysates were used in GST-cytoB1 kinase assays (right panel). (**D**) In-gel kinase assays using as a substrate either GST-cytoB1 (upper panels) or GST-alone (lower panels) were performed with lysates from Fc-stimulated and EphB-Fc-stimulated NIH3T3-ephrinB1 and HUAECs. Arrows in the upper panel indicate the kinase that phosphorylated GST-cytoB1.

54

6.1.2. SFKs are required for phosphorylation of ephrinB ligands.

To investigate the requirement for SFKs in ephrinB phosphorylation, specific SFK inhibitors were used in the *in vitro* ephrinB kinase assay. PP2 inhibitor completely neutralized the ephrinB C-terminal kinase in EphB4-stimulated HUAECs (**Figure 20A**, left panel), whereas the structurally nearly identical control compound PP3 was ineffective. The inhibition was dose dependent with half maximal inhibition at 1μM. Interestingly, ephrinB phosphorylation induced by calf serum was unaffected by PP2, showing the specificity of the inhibitor for the receptor-stimulated kinase and indicating that kinases other than SFKs can mediate the serum response (**Figure 20A**). These data were independently confirmed by using the recently developed SFK inhibitor SU6656 (Blake et al., 2000). SU6656 abolished EphB4-Fc induced phosphorylation of GST-cytoB1 in HUAECs as did the PP2 inhibitor (**Figure 20A**, right panel).

To obtain biochemical evidence for a requirement of SFKs in ephrinB phosphorylation, an anti-SFK specific antibody (anti-cst1) (Kypta et al., 1990) was used to immunodeplete this kinase activity from lysates of EphB4-stimulated HUAECs. Anti-cst1 immunoprecipitation of SFKs depleted the amount of SFK protein in a dose-dependent manner (**Figure 20B**, left panel). Concomitantly, ephrinB C-terminal kinase activity was reduced proportionally to the reduction of SFK from the lysates (**Figure 20B**, left panel). As a control, immunoprecipitation of EphB4-stimulated HUAECs with preimmune serum did not deplete the 'ephrinB kinase' present in these cells (**Figure 20B**, right panel). Thus, two independent methods, i.e. use of specific Src inhibitors and anti-Src immunodepletion, demonstrated a requirement for SFKs in ephrinB phosphorylation *in vitro*.
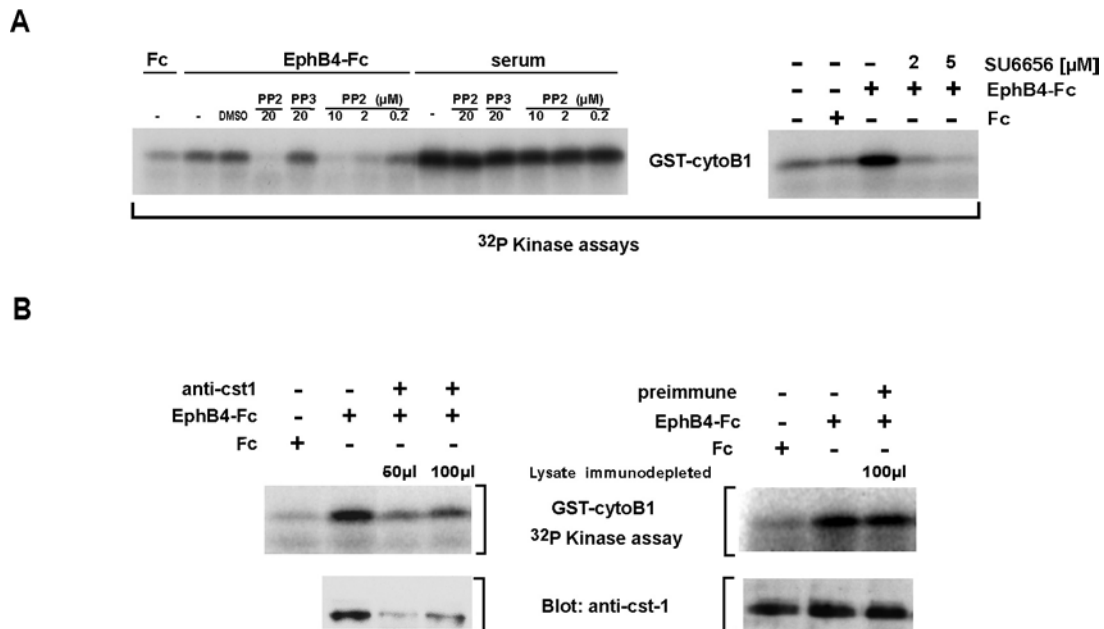
Figure 20. Src family kinases (SFKs) are required for phosphorylation of ephrinB ligands. (A) 16h serum-starved HUAECs were stimulated with either pre-clustered unfused Fc, EphB4-Fc, or serum for 10min in the absence or presence of decreasing concentrations of the SFK inhibitor PP2 (left panel). DMSO and PP3, an inactive analogue of PP2, were used as controls. 16h serum-starved HUAECs were treated with SU6656 (2 and 5μM) for 1h prior to stimulation with Fc or EphB4-Fc. Lysates were used for GST-cytoB1 kinase assays. **(B)** Immunodepletion of Src family kinases from HUAECs. SFKs were immunoprecipitated from lysates of EphB4-Fc stimulated HUAECs using an antibody against all SFK isoforms (anti-cst1) to deplete these lysates from SFKs. GST-cytoB1 kinase assays were performed before and after immunodepletion (upper panel left). Two different amounts (50 and 100μl) of stimulated cell lysate were immunodepleted with the same amount of antibody. The amount of SFKs remaining in the lysates was monitored by immunoblotting of the same extracts with anti-cst1 antibody (lower panel left). Control immunoprecipitation with preimmune serum was done in parallel (right panels).

6.1.3. *In vivo* ephrinB phosphorylation in primary cortical neurons requires SFKs

We next asked if SFKs are required for ephrinB phosphorylation *in vivo* and whether this pathway is active in other cell types as well. EphrinB reverse signaling is also thought to occur in forebrain cortical neurons, in particular during commissural axon tract formation during development (Henkemeyer et al., 1996; Orioli et al., 1996; Kullander et al., 2001). Most of the evidence came from genetic studies, however, Eph receptor-induced ephrinB phosphorylation has never been demonstrated in neurons. As shown in **Figure 21A**, stimulation of primary mouse cortical neurons with preclustered EphB1-Fc led to a marked

increase in phosphorylation of the endogenous ephrinB ligand, compared to the stimulation with preclustered, unfused Fc control protein (**Figure 21A**, upper panel). In the presence of the PP2 inhibitor, but not of the control compound PP3, this increase in phosphorylation was completely abolished. These observations strongly suggest that in living neurons, EphB receptor-induced ephrinB tyrosine phosphorylation required the activity of SFKs. Moreover, short-term stimulation of neurons with EphB1-Fc significantly increased *in vitro* autophosphorylation of both Src and Fyn kinases (**Figure 21B**). Increased Src and Fyn autophosphorylation was used as an indication of kinase activity. The increase was transient and returned to baseline by 30min, thus correlating with the *in vitro* activity of the ephrin C-terminal kinase (see **Figure 21C**). Cortical neurons did not show detectable levels of Yes kinase (data not shown).
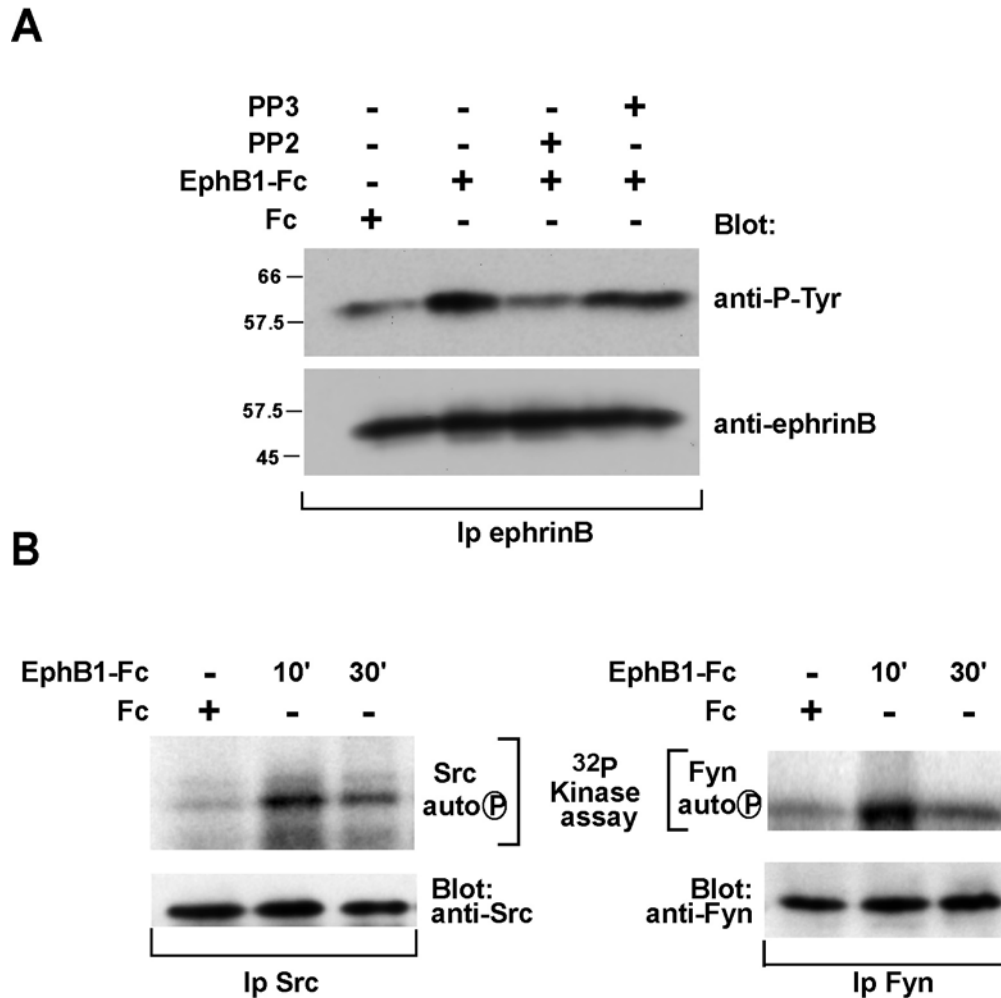
Figure 21. SFK activation is required for endogenous ephrinB ligand phosphorylation in primary cortical neurons. (**A**) EphB1-Fc-induced tyrosine phosphorylation of endogenous ephrinB ligands is inhibited by PP2 but not by PP3. Primary cortical neurons from embryonic day (E) 14.5 mouse embryos were stimulated after two days in culture with either pre-clustered unfused Fc or EphB1-Fc in the presence or absence of PP2 or the control compound PP3. Cell lysates were immunoprecipitated with anti-ephrinB polyclonal antiserum (#23), analyzed by 15% Anderson PAGE and immunoblotted with anti-phosphotyrosine monoclonal antibody (4G10) (upper panel). Blots were stripped and reprobed with anti-ephrinB polyclonal antiserum (#200) (lower panel). (**B**) Neurons were stimulated as above for the indicated time. Cell lysates were precleared with protein G-beads and then immunoprecipitated with either monoclonal antibodies anti-Src (2-17) or anti-Fyn (Fyn-14). Immunoprecipitates were subjected to *in vitro* kinases assays with (γ-^{32}P)ATP and analyzed by 10% Laemmli SDS-PAGE followed by autoradiography (upper panels) or immunoblotting with antibodies anti-Src and anti-Fyn (lower panels). Autophosphorylation (auto P) is used as an indication of Src and Fyn kinase activities.

6.1.4. EphrinB ligands and Src colocalize in membrane rafts and are coclustered by EphB receptors

EphrinB ligands colocalize with PDZ proteins such as glutamate-receptor-interacting-protein (GRIP) in membrane rafts (Brückner et al., 1999), which can serve as platforms for the assembly of signaling molecules (Simons and Toomre, 2000). GPI-anchored ephrinA ligands are also recruited to membrane rafts in cultured cells and in the mouse embryo and the Fyn SFK has been implicated in ephrinA-regulated cell adhesion (Davy and Robbins, 2000; Huai and Drescher, 2001). Membrane raft microdomains are characterized by detergent-insolubility at low temperatures and low buoyant density. In order to investigate if ephrinB ligands and Src colocalize in membrane rafts, Triton X-100 flotation gradients were prepared from E12.5 mouse embryo heads. A large fraction of ephrinB was found in the top fractions of the flotation gradient, indicating raft localization (**Figure 22A**, upper panel). Probing the same fractions with the SFK antibody anti-cst1 revealed the colocalization of SFKs in the rafts fraction. The raft protein caveolin and the non raft membrane protein transferrin receptor segregated into top and bottom fractions, respectively, demonstrating the quality of the raft preparation (**Figure 22A**, lower panels).

EphB2-Fc, but not unfused Fc, stimulation of NIH3T3-ephrinB1 cells induced the formation of large membrane clusters visualized with anti-human Fc antibody conjugated to Texas Red (**Figure 22B** and **22C**, left panels). Immunofluorescence using anti-ephrinB antibodies showed the redistribution of ephrinB1 into these receptor clusters (**Figure 22B**, middle and right panels). Double immunostainings with anti-human Fc and anti-Src monoclonal antibodies revealed a redistribution of endogenous Src protein into clusters that essentially overlapped with EphB/ephrinB complexes (**Figure 22C**, middle and right panels), indicating regulated colocalization of these proteins in the living cell. EphB-induced recruitment of Src into membrane clusters was also confirmed in primary cultures of cortical neurons, expressing endogenous ephrinB ligands and Src kinases (**Figure 22D**).

EphrinB/SFK co-clustering may require membrane raft lipid domains. Cholesterol is the key component in maintaining the integrity of raft microdomains and methyl-β-cyclodextrin (MßCD) is a membrane impermeable oligosaccharide that selectively and rapidly extracts cholesterol from the plasma membrane (Kilsdonk et al., 1995). Surprisingly, cholesterol depletion in NIH3T3-ephrinB1 cells did not prevent the formation of ephrinB/Src co-clusters

when cells were stimulated with EphB2-Fc (**Figure 22C**, lower panels). However, treatment with MßCD dramatically elevated the phosphotyrosine content of ephrinB ligands, even in unstimulated cells (**Figure 22E**). These findings indicate that co-clustering of ephrinB and SFKs occurs independently of rafts, but that raft localization of ephrinB and SFKs is required for proper regulation of ephrinB phosphorylation.
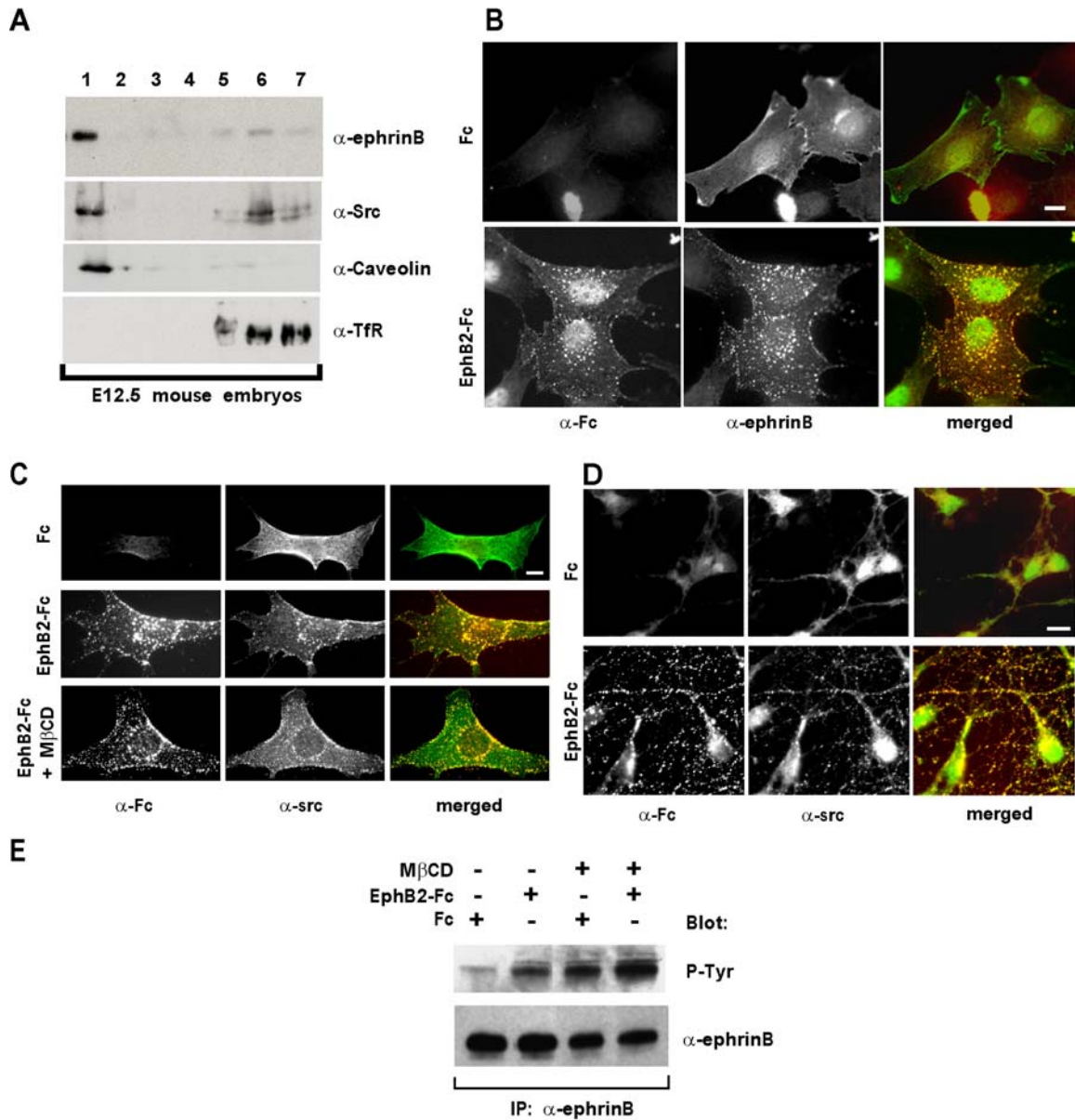
SFKs are required for sprouting angiogenesis mediated by ephrinB ligands

Based on the presented studies it was hypothesized that SFKs are also required for ephrinB reverse signaling. Adrenal-cortex derived microvascular endothelial (ACE) cells co-express ephrinB ligands and EphB receptors and can be induced *in vitro* to form small capillary sprouts (Koblizek et al., 1998; Adams et al., 1999). In the presence of soluble, preclustered ephrinB-Fc, sprouting is induced, presumably via activated EphB receptors (Adams et al., 1999). Interestingly, sprout formation could also be induced in a reverse manner, i.e. by soluble, preclustered EphB4-Fc, suggesting that ephrinB ligands can trigger this response (**Figure 23A**). EphB4-Fc induced a 2-fold until 5-fold increase in the number of sprouts depending on the experiment (compare all four panels in **Figure 23A**). The activity of EphB4-Fc was comparable to potent angiogenic factors such as vascular-endothelial growth factor (VEGF) (Koblizek et al., 1998) (**Figure 23A**, Exp1). It was examined whether in this

Figure 22. Stimulation with EphB receptors induces formation of large membrane clusters containing ephrinB ligands and Src. (**A**) EphrinB ligands and Src colocalize in membrane rafts in the mouse embryo. A membrane preparation of heads from embryonic day (E) 12.5 mouse embryos was subjected to Triton X-100 extraction followed by Optiprep flotation gradients. Seven fractions were collected from the top to the bottom and analyzed by SDS-PAGE and Western-blotting for the presence of ephrinB and Src. EphrinB and Src are both found in the upper fraction of the gradient, indicating raft localization. Caveolin and transferrin receptor (TfR) were used as raft and non raft markers. (**B**) EphB2-Fc stimulation of NIH3T3-ephrinB1 cells causes a redistribution of ephrinB1 into large membrane clusters. Cells were stimulated with Fc (upper panels) or EphB2-Fc (lower panels). Receptor bodies were visualized with an anti-human Fc antibody conjugated to Texas-Red (left panels). EphrinB1 was detected using anti-ephrinB1 antiserum (#200) (middle panel). The merge of the two signals is shown in the right panel. (**C**) Src is recruited into ephrinB- containing clusters induced by EphB-Fc. NIH3T3-ephrinB1 cells were stimulated with Fc (upper panels) or EphB2-Fc (horizontal-middle and lower panels). Receptor bodies were visualized with an anti-human Fc antibody conjugated to Texas-Red (left panels). The vertical-middle panels show distribution of endogenous Src detected with an anti-Src monoclonal antibody (2-17) and panels on the right show the merge of the two signals. Patch formation and recruitment of Src were not affected when rafts were disrupted by cholesterol depletion as described below with 10mM MβCD (lower panels). (**D**) Src is recruited to EphB receptor-induced clusters in cortical neurons. Primary cortical neurons from E14.5 mouse embryos were stimulated with either Fc (upper panels) or EphB2-Fc (lower panels). Immunofluorescence to detect EphB2-Fc clusters and endogenous Src was performed as described above. (**E**) Cholesterol rafts are required for regulation of ephrinB phosphorylation. NIH3T3-ephrinB1 cells were pretreated for 20min with or without 10mM MβCD and subsequently stimulated for 10min with Fc or EphB2-Fc in the presence or absence of MβCD. Immunoprecipitates of ephrinB1 were analyzed by Western-blotting for phosphotyrosine (upper panel) and ephrinB1 (lower panel). MβCD-treatment resulted in increased phosphorylation levels of ephrinB1. Scale bars: 10μm.

assay SFKs are required for the angiogenic response mediated by ephrinB ligands. The SFK kinase inhibitor PP2, when applied at moderate concentrations (0.5µM), completely neutralized EphB4-Fc induced sprouting, but did not reduce basal sprouting activity (**Figure 23A, B**). Basal sprouting activity of ACE cells was only inhibited at higher concentrations of PP2 (data not shown). The control compound PP3 was not inhibitory in this assay, at concentrations up to 40-fold above (0.5µM-20µM) the effective concentrations of PP2 (**Figure 23A**, Exp4). The effect of PP2 in the angiogenic response mediated by ephrinB ligands was specific, since PP2 was unable to block the angiogenic response of the chemokine stromal cell-derived factor-1 (SDF-1) and Angiopoietin-1, the ligand of the Tie-2 receptor tyrosine kinase (Nagasawa et al., 1998; Gale and Yancopoulos, 1999) (**Figure 23A**, Exp2 and Exp3).
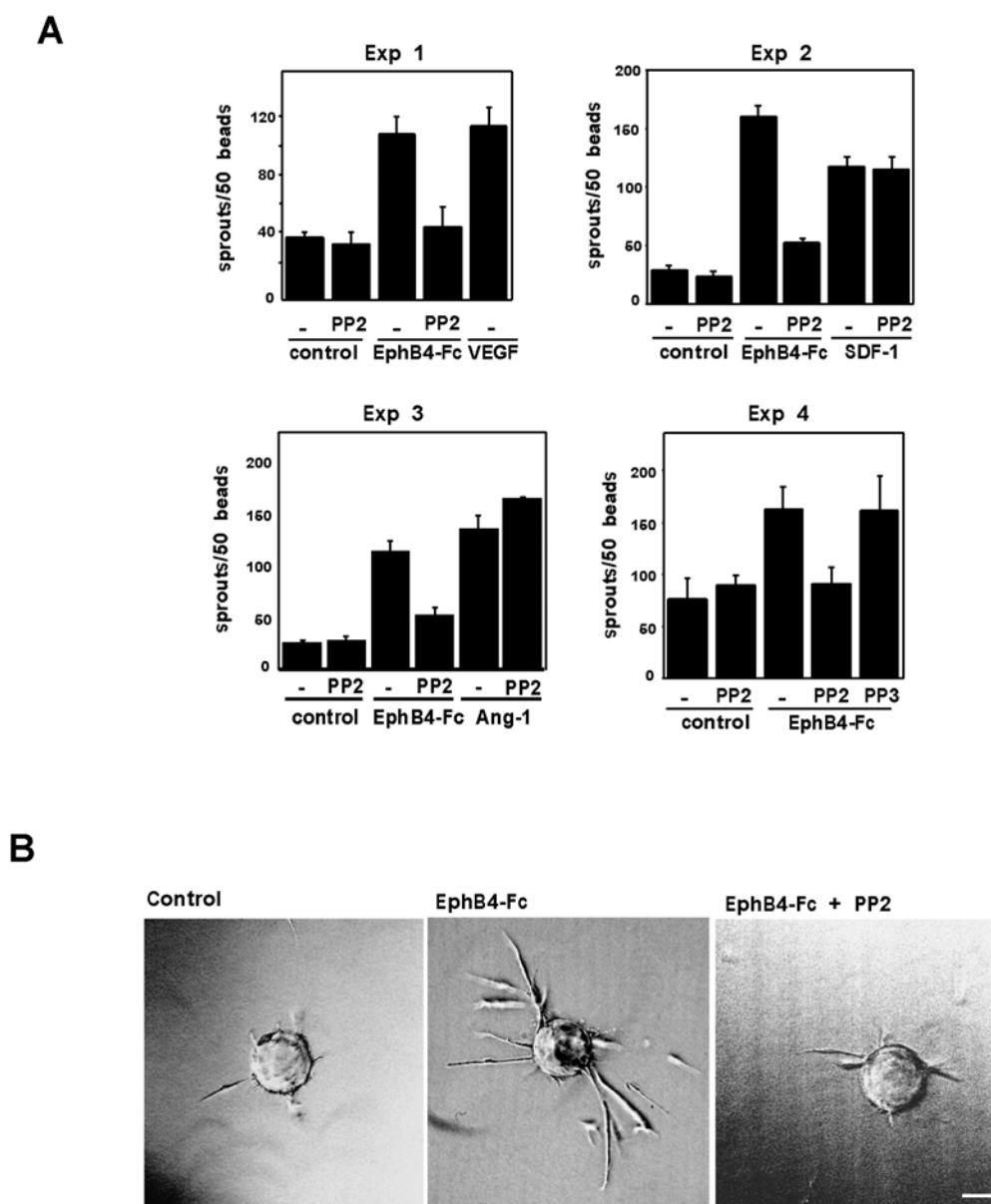
Figure 23. Src family kinases are required for the angiogenic sprouting response mediated by ephrinB ligands. Adrenal-cortex derived microvascular endothelial (ACE) cells were seeded on micro carrier (MC) beads and incubated in three-dimensional fibrin gels with different angiogenic factors in the presence or absence of the Src inhibitor PP2. (**A**) Quantitative analysis of sprout formation expressed as the number of capillary sprouts with lengths exceeding the diameter of the MC bead for every 50 MC beads counted. EphB4-Fc induced sprouting was completely inhibited in the presence of low concentrations of PP2 (0.5µM) (Exp 1, 2, 3 and 4). The control compound PP3 did not affect sprouting activity (Exp 4). Sprouting induced by SDF-1 and Ang-1 was not affected by inhibition of SFKs (Exp 2 and 3). (**B**) Phase contrast photomicrographs of angiogenic sprouts induced by EphB4-Fc in the presence and absence of PP2. Scale bars represent 25µm.

6.1.5. PTP-BL tyrosine phosphatase, a negative regulator of ephrinB phosphorylation

Next we attempted to identify mechanisms that attenuate SFK-mediated ephrinB phosphorylation. One candidate molecule was the murine cytoplasmic tyrosine specific phosphatase PTP-BL (Chida et al., 1995; Hendriks et al., 1995), and its human homologue PTP-BAS (Maekawa et al., 1994; Saras et al., 1994; Sato et al., 1995), which are 250kDa proteins containing an N-terminal FERM domain (Four point one, Ezrin, Radixin, Moesin domain), common to cytoskeleton associated proteins (Chishti et al., 1988; Arpin et al., 1994), five PDZ domains, and a C-terminal PTP domain. PTP-BL is expressed prominently in the developing peripheral nervous system, including the dorsal root ganglia (DRGs) (Thomas et al., 1998), and the PTP-BL PDZ4 domain was shown to bind to ephrinB1 *in vitro* (Lin et al., 1999). Since ephrinB ligands have also been shown to be expressed during development in the DRGs (Brückner et al., 1999), it was hypothesized that PTP-BL could co-localize with ephrinB in the growth cones of DRG neurons and that it could regulate the phosphorylation state of ephrinB and Src.

Up to now the interaction of ephrinB1 and PTP-BL was only demonstrated *in vitro* by pull-down assays from COS-1 cells overexpressing ephrinB1 using a PDZ-domain of PTP-BL fused to GST (Lin et al., 1999). In order to verify the interaction *in vivo* pull-down assays were performed with GST-cytoB1 on lysates prepared from E12.5 mouse embryos. GST-cytoB1, but not GST alone, specifically pulled down endogenous PTP-BL (**Figure 24A**). Moreover, the interaction between ephrinB1 and PTP-BL was confirmed in living cells by co-IP of an expression construct of PTP-BL (PDZ1-5) and full length ephrinB1, but not ephrinB1 lacking the PDZ domain target site (**Figure 24B**). Interestingly, a proportion of PTP-BL phosphatase localized to rafts in membranes prepared from E12.5 mouse embryos and cultured cortical neurons (**Figure 24C**), indicating the presence of PTP-BL in the same subcellular compartment as ephrinB and SFKs. Subcellular colocalization of endogenous ephrinB and PTP-BL was also tested by immunofluorescence in dissociated DRG neurons. Cells were fixed and proteins were visualized using EphB2-Fc and anti-PTP-BL antiserum. Colocalization was detected in clusters along the processes and in the growth cone (**Figure 24D**).
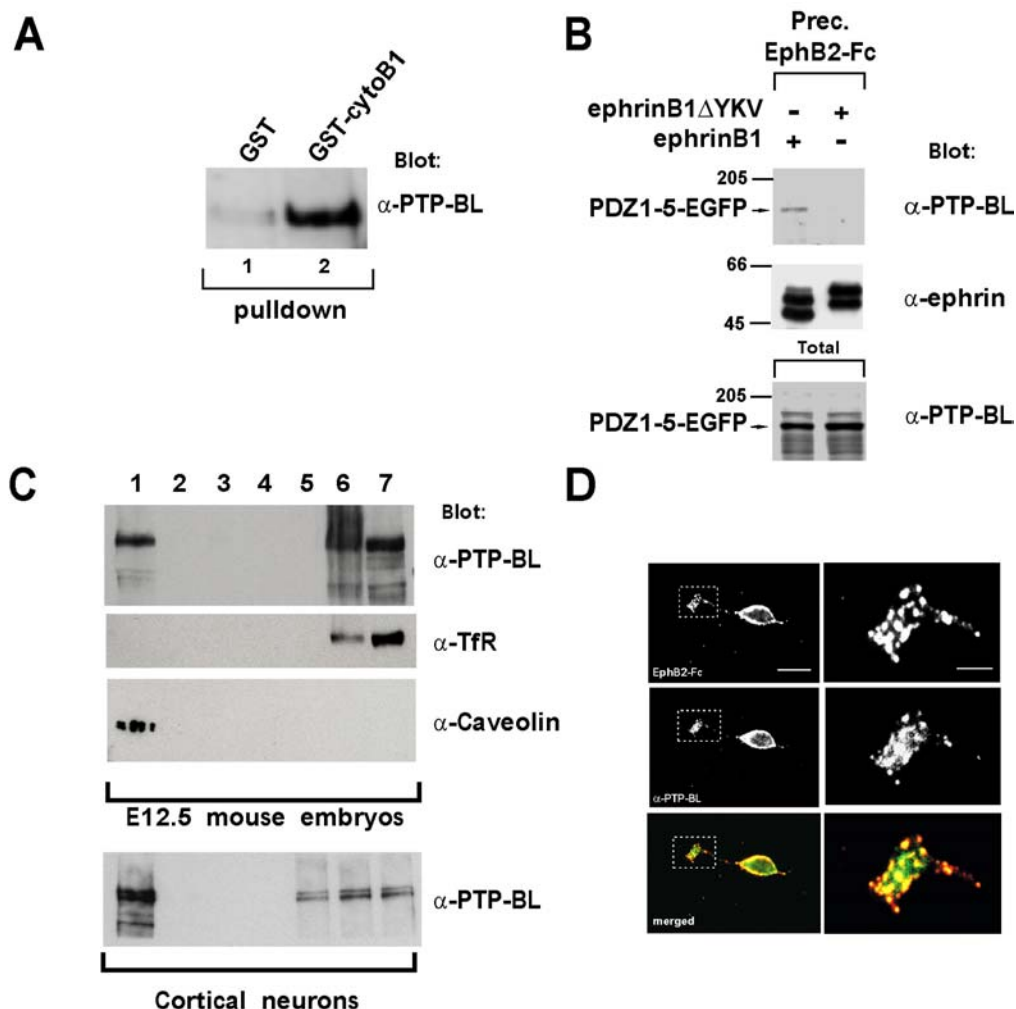
Figure 24. Interaction and colocalization between PTP-BL and ephrinB ligands. (**A**) PTP-BL binds to the C-terminus of ephrinB ligands. GST or GST-cytoB1 pull-downs were prepared from E12.5 head embryo lysates and the presence of PTP-BL in these pull-downs was analyzed by Western-blotting using an anti-PTP-BL polyclonal antibody. (**B**) Interaction of PTP-BL with ephrinB1 in HeLa cells. An expression construct of PTP-BL containing the PDZ domains 1 to 5 fused to GFP was co-expressed in HeLa cells with full length ephrinB1 or ephrinB1 lacking its PDZ-binding motif (ephrinB1ΔYKV). EphrinB1 was precipitated from cell lysates using EphB2-Fc and the samples were analyzed by Western-blotting for PTP-BL (upper panel) and ephrinB1 (middle panel). Levels of PTP-BL PDZ1-5 in total lysates are shown in the lower panel. PTP-BL PDZ1-5 co-precipitated only with full length ephrinB1. (**C**) PTP-BL is located in rafts in the mouse embryo and in cortical neurons. A membrane preparation of heads from embryonic day (E) 12.5 mouse embryos was subjected to Triton X-100 extraction followed by Optiprep flotation gradients. Seven fractions were collected from the top to the bottom and analyzed by Western-blotting for the presence of PTP-BL. Caveolin and transferrin receptor (TfR) were used as raft and non raft markers. Primary cortical neurons were cultured as described and membrane rafts were prepared as above. (**D**) PTP-BL co-localizes with ephrinB-containing clusters in the growth cones of primary dorsal root ganglion neurons. DRG-neurons were dissected from E9 chick embryos and cultured for 4h in low serum. Cells were fixed**,** stained with EphB2-Fc, permeabilized and then stained for PTP-BL. Scale bars represent 10μm and 2μm for the enlargement.

The next step was to investigate whether Src and ephrinB might serve as substrates for PTP-BL. Bacterially expressed wild-type PTP-BL phosphatase domain, but not a catalytically inactive point mutant of PTP-BL (PTP-BL-CS) dephosphorylated Src specifically on Y418, a tyrosine autophosphorylation site required for Src activation (Kmiecik and Shalloway, 1987). In contrast, Y529, whose phosphorylation inhibits Src kinase activity (Thomas and Brugge, 1997) was not dephosphorylated by PTP-BL (**Figure 25A**, left panels), suggesting that dephosphorylation of Src by PTP-BL would lead to inactivation of Src. Moreover, wild-type PTP-BL tyrosine phosphatase domain, but not the Cys→Ser mutant led to the complete dephosphorylation of ephrinB immunoprecipitated from mouse embryo lysates, suggesting its specificity for ephrinBs *in vivo* phosphorylation sites (**Figure 25A**, right panels). It was further investigated, if ephrinB-ligands could also serve as substrates for PTP-BL in intact cells. HeLa cells were transiently transfected with an ephrinB1 expression construct either alone or together with expression constructs encoding PTP-BL or PTP-BL-CS. After stimulation with EphB2-Fc, ephrinB1 was precipitated using the soluble EphB2-Fc receptor bodies and its phosphorylation and protein levels were scored by Western-blotting. EphB2-Fc induced tyrosine phosphorylation on ephrinB1 could be detected in ephrinB1-transfected cells and in double transfections together with the mutant PTPBL-CS (**Figure 25B**, lanes 2 and 6). When cotransfected with wild-type PTP-BL, tyrosine phosphorylation of ephrinB1 was reduced (**Figure 25B**, compare lanes 2 and 4) indicating that ephrinB ligands are *in vivo* substrates of the phosphatase PTP-BL.
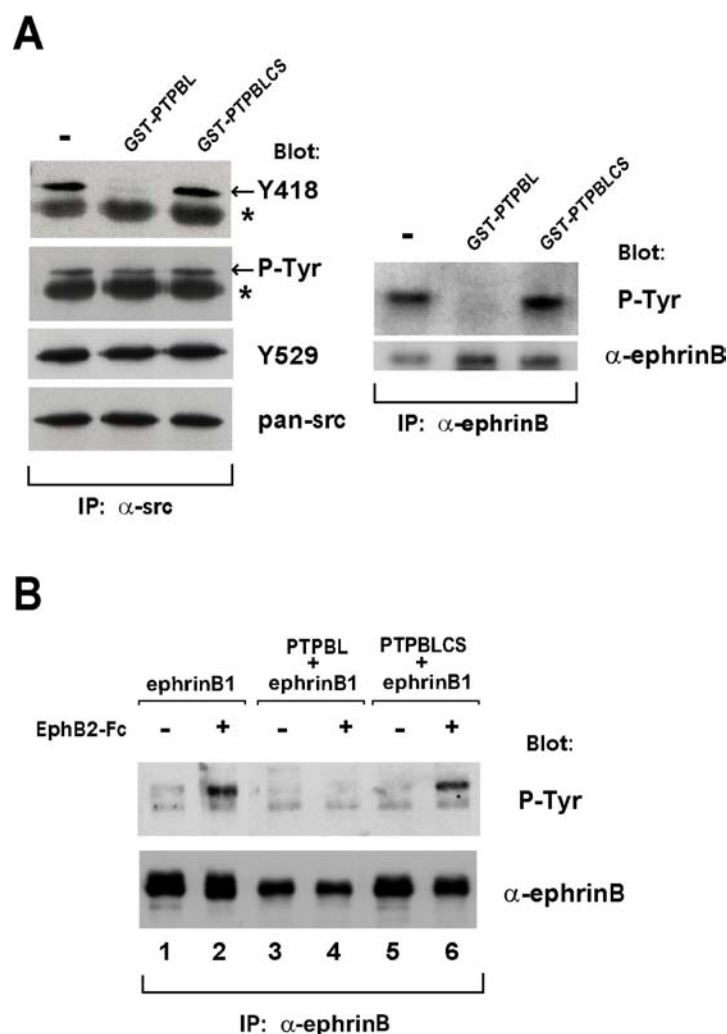
Figure 25. Regulation of ephrinB- and Src phosphorylation by the phosphotyrosine phosphatase PTP-BL. (**A**) EphrinB and Src are dephosphorylated *in vitro* by PTP-BL. Phosphorylated EphrinB and Src proteins were immunoprecipitated from E12.5 mouse embryos and incubated with GST-PTP-BL or the catalytically inactive GST-PTP-BL CS. Phosphorylation and total levels of ephrinB ligands were detected using anti-phosphotyrosine antibodies (4G10) and anti-ephrinB polyclonal antiserum (#23), respectively (right panel). Phosphorylation state of specific tyrosine residues in Src was monitored using anti-Y416 and anti-Y529 polyclonal antibodies. Total level of Src phosphorylation and Src were detected using 4G10 and pan-Src polyclonal antibody, respectively. Asterisks indicate IgG bands (left panel). (**B**) EphrinB ligands are *in vivo* substrates of PTP-BL phosphatase. HeLa cells were transiently transfected with expression constructs encoding ephrinB1 alone (lanes 1 and 2) or cotransfected with PTP-BL (lanes 4 and 5) or the corresponding inactive mutant PTP-BL CS (lanes 5 and 6). After 30min stimulation with EphB2-Fc, ephrinB was precipitated using the EphB2-Fc receptor bodies and phosphorylation was monitored using 4G10 antibody (upper panel). Total levels of ephrinB1 in the precipitates were detected by Western-blotting with antibodies anti-ephrinB (lower panels).

6.1.6. Kinetics of Src-activation and its recruitment to Eph/ephrin complexes

The data so far indicated that SFK activation was required for ephrinB phosphorylation and that PTP-BL turned this pathway off. Such a model would require that SFKs are recruited to ephrin clusters and activated more rapidly than PTP-BL. Moreover, because PTP-BL carries multiple PDZ domains and was shown to interact with other cytoplasmic effectors (Saras et al., 1997; Erdmann et al., 2000), prolonged association of PTP-BL with ephrins would indicate a signaling role of PTP-BL in addition to its function as a phosphatase.

Therefore the kinetics of Src-ephrinB co-clustering and ephrinB phosphorylation/de phosphorylation were examined. The stimulation protocol was modified such that after a 10min pulse of EphB2-Fc, this stimulus was removed from the medium and cells were left untreated for an extended period of time. Src recruitment into ephrinB/EphB-containing clusters was observed already at 2-5min after EphB2-Fc addition and was maintained until 30min to 1h past removal of EphB2-Fc from the cell medium (**Figure 26A**). SFK activity was highest at 10min (see also **Figures 19C** and **21B**) and decreased at later time points, even when EphB2-Fc continued to be present in the cell medium (**Figure 26B**).

Figure 26. Src kinase is recruited rapidly to ephrin-containing clusters and activated transiently after stimulation with EphB-Fc. (**A**) Rapid and prolonged Src-recruitment to EphB2-Fc induced clusters. NIH3T3-B1 cells were stimulated and fixed at the indicated time points (upper four panels). After 10min of stimulation cells were washed and left in medium without EphB2-Fc for 15, 30 and 60min prior fixation (lower three panels). Immunostaining was performed as described above. (**B**) Rapid and transient SFK activation after stimulation with EphB-Fc. NIH3T3-ephrinB1 cells were stimulated with EphB2-Fc for the indicated time points and *in vitro* kinase assays were performed as described above. SFK-activity peaks at 10min of stimulation.

A

Fc

EphB2-Fc

2'

5'

10'

10'+ 15'

10' + 30'

10' + 1h

α-Fc   α-src   merged

B

EphB2-Fc   —   10'   30'   1h
Fc   +   —   —   —

GST-cytoB1

^{32}P kinase assay
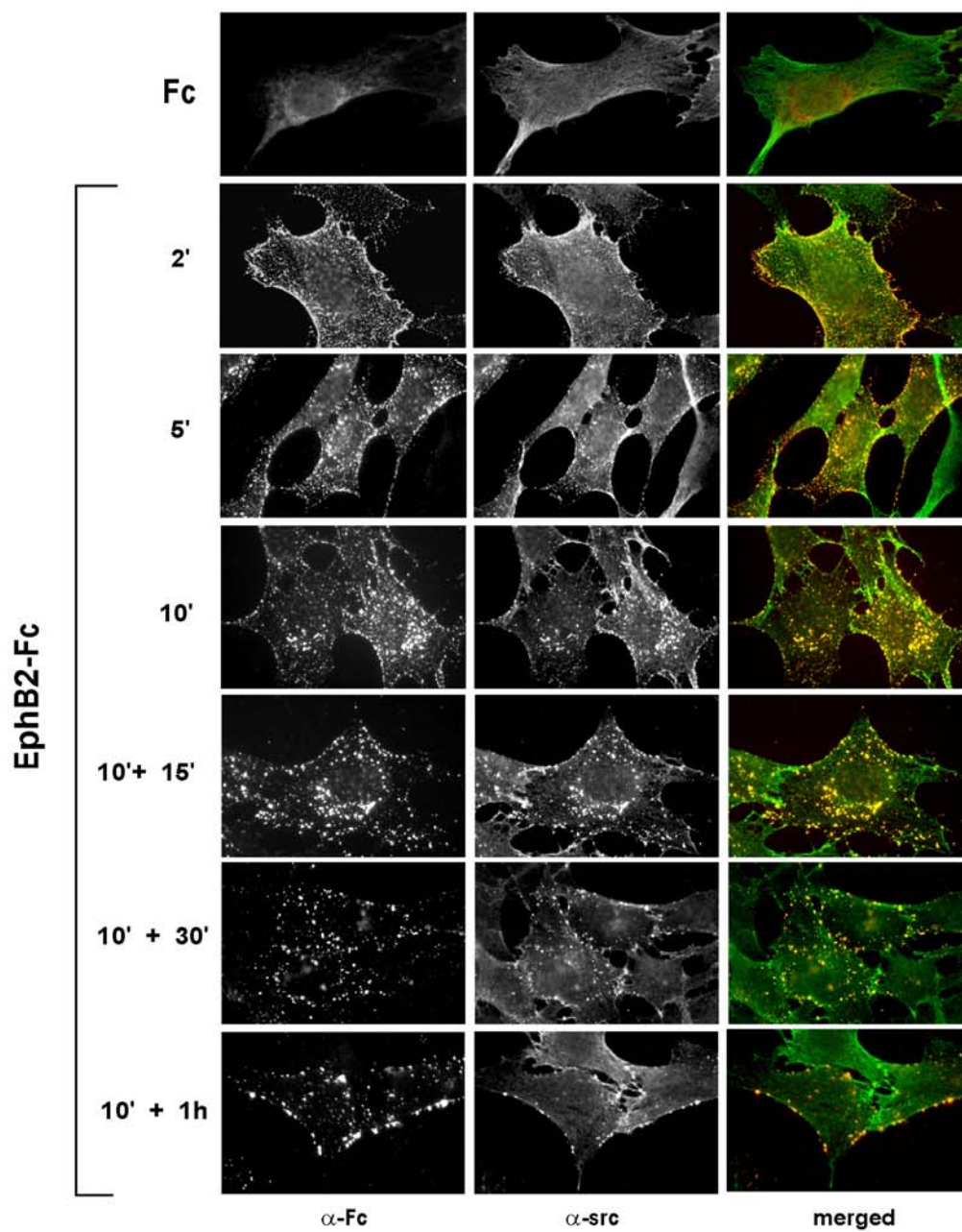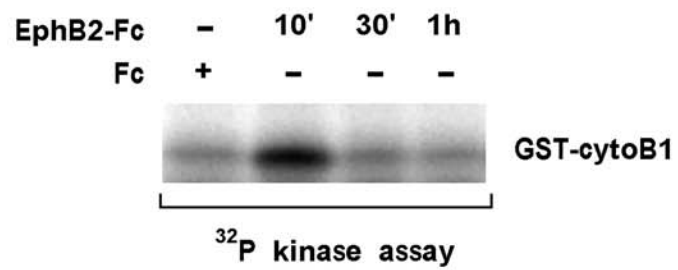
6.1.7. PTP-BL recruitment to Eph/ephrin clusters is coincident with ephrinB dephosphorylation

The kinetics of ephrinB phosphorylation correlated very well with SFK activity and was first detected after 10min stimulation, and decreased progressively after removal of EphB2-Fc (**Figure 27B**). PTP-BL recruitment to receptor bound ephrins was not observed until 30min past EphB2-Fc removal and was maintained for at least another period of 30min (**Figure 27A**). These findings therefore support a model in which EphB2 stimulation causes rapid recruitment and activation of SFKs, which will phosphorylate ephrinB on tyrosine and allow reverse signaling via SH2-containing effectors. This signaling is then terminated by delayed recruitment of PTP-BL and subsequent silencing of SFKs and ephrinB dephosphorylation.

_____

Figure 27. Downregulation of ephrinB phosphorylation coincides with delayed kinetics of PTP-BL recruitment. (**A**) PTP-BL is recruited to EphB2-Fc induced clusters with delayed kinetics. NIH3T3-B1 cells were stimulated for the indicated time points (upper two panels). After 10min of stimulation cells were washed and left in medium without EphB2-Fc for the indicated time points (lower three panels). Cells were fixed and stained using EphB2-Fc and PTP-BL antiserum. Panels *a* show the merge of the two signals with anti-Fc staining in red and anti-PTP-BL staining in green. Panels *b-d* show the zoom of the dashed box in panel *a* (*b*: merge, *c*: anti-Fc, *d*: anti-PTP-BL). Colocalization of PTP-BL with EphB-Fc labeled membrane clusters was observed at late points (30min and 1 h) after pulse-stimulation. Arrows indicate places of accumulation and colocalization of PTP-BL with EphB2-Fc-induced clusters. (Scale of dashed box: 28·19µm). (**B**) Downregulation of ephrinB phosphorylation. NIH3T3-ephrinB1 cells were stimulated as described above. Immunoprecipitates of ephrinB1 (left panel) and total cell lysates (right panel) were subjected to SDS-PAGE and Western-blotting using phosphospecific antibodies for ephrinB ligands that were generated using a peptide epitope corresponding to ephrinB phosphorylated at tyrosines –18 and –23.

A

| | *a* | *b* | *c* | *d* |

merge   EphB2-Fc   α-PTP-BL

B
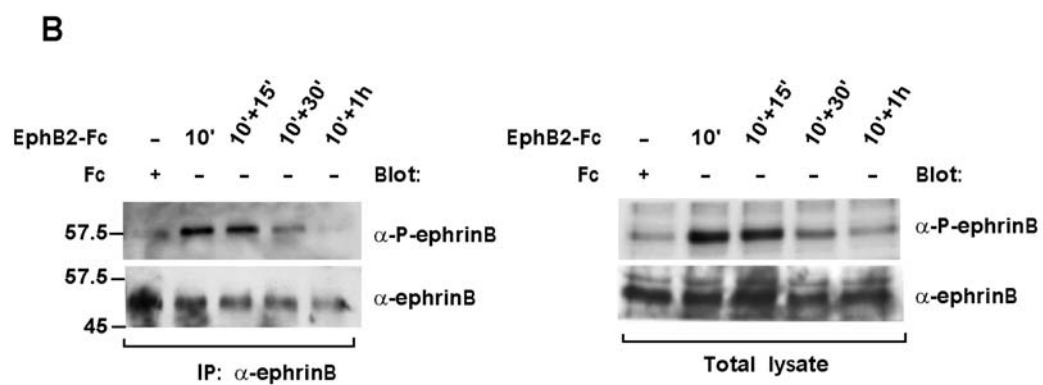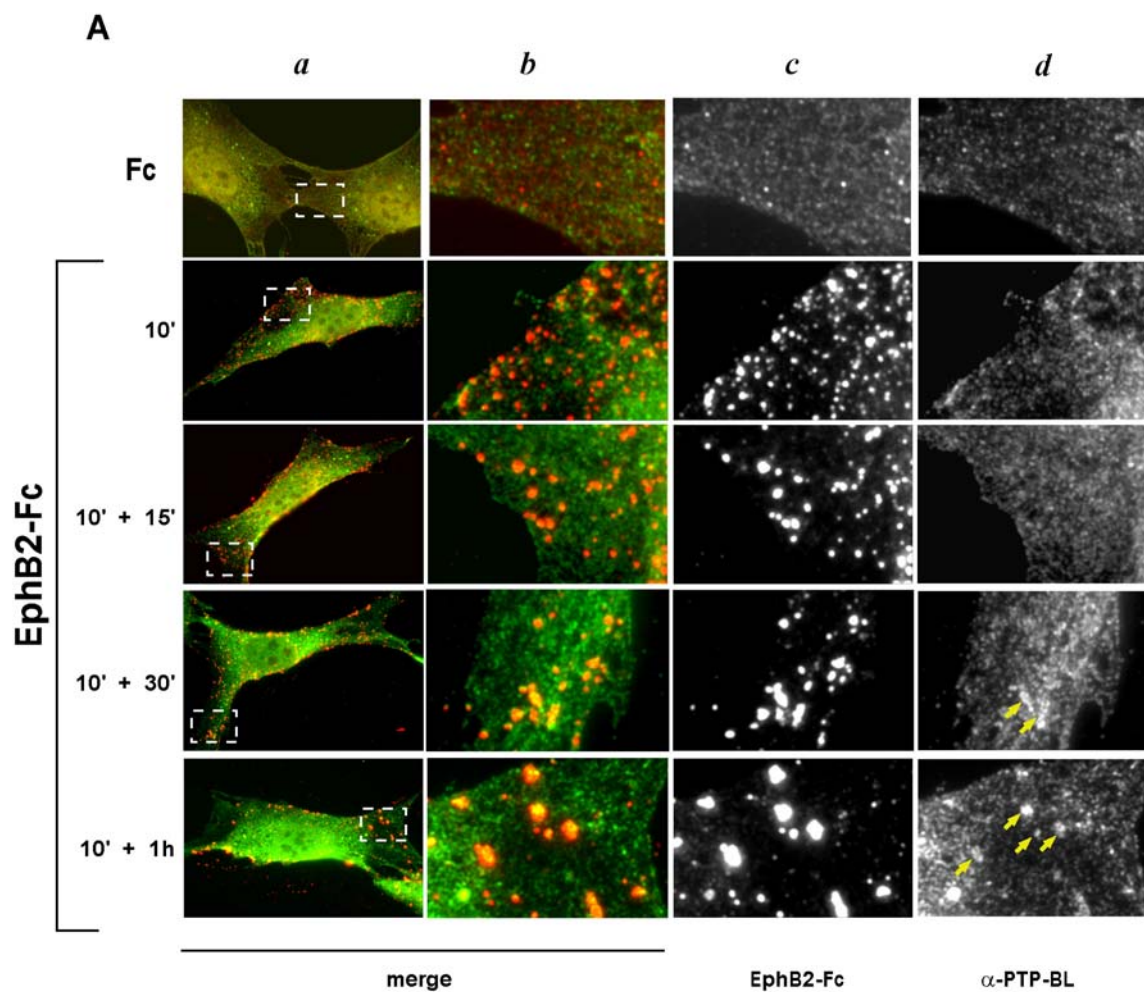
6.2. PDZ-dependent signaling by ephrinB ligands

In the studies presented in the previous section it was discovered that colocalization of PTP-BL with ephrinB occurred after engagement with its EphB receptor. PDZ interactions usually are reported to be constitutive. A few studies demonstrated that phosphorylation on serine residues within the PDZ-binding motif of several proteins can affect the affinities to their interaction partners (Cao et al., 1999; Chung et al., 2000). Thus, some PDZ interactions have the potential to be regulated by signaling cascades involving serine/threonine kinases. We therefore investigated the interactions of ephrinB molecules with other PDZ-domain containing proteins and the underlying mechanism of regulation.

6.2.1. EphrinB1 interaction with GRIP2 is regulated by EphB2 receptor binding

EphrinB molecules were shown to interact with the multiple PDZ domain containing protein GRIP. When both binding partners were heterologously expressed in HEK293 cells the interaction appeared to be constitutive (Brückner et al., 1999). In these experiments a putative regulation of this interaction may have been obscured by the strong overexpression in these transiently transfected cells. Stable protein expression in NIH3T3 cells appears to be moderate and therefore, these cell lines provide a better tool to study regulated interactions between proteins. Therefore, stable cell lines co-expressing a myc-tagged version of GRIP2 (myc-GRIP2) and an HA-tagged version of wild-type (clone MZ4-6) or C-terminally truncated HA-ephrinB1-ΔC (clone MZ5-23) were generated from NIH3T3 cells. As shown in **Figure 28A** HA-immunoprecipitates from these cells efficiently pulled down ephrinB1. Myc-GRIP2 could hardly be detected in HA-immunoprecipitates from unstimulated (Fc control) cells (**Figure 28A**). Only a weak myc-epitope positive band could be detected in immunoprecipitates using an anti-ephrinB antibody (#23) (**Figure 28B**). After 10min stimulation with pre-clustered EphB2-Fc myc-GRIP2 co-immunoprecipitated with ephrinB1 using either one of the two antibodies (**Figure 28A-B**). No myc-GRIP2 was detected in HA-immunoprecipitates from MZ5-23 control cells, expressing HA-ephrinB1-ΔC and myc-GRIP2 (**Figure 28A**).

The Fc-tag of Fc-fusion proteins has high affinity to ProteinG and can be used for precipitation in pull down experiments. ProteinG pull downs from lysates of cells expressing wild-type HA-ephrinB1 together with myc-GRIP2 that were stimulated with EphB2-Fc precipitated efficiently EphB2-Fc, myc-GRIP2 and HA-ephrinB1, indicating that these molecules form a stable ternary complex in stimulated cells (**Figure 28C**). Next, it was attempted to co-localize myc-GRIP2 to clusters of stimulated ephrinB1 by immunofluorescence. Interestingly myc-GRIP2 could be detected in a punctuated pattern in unstimulated (Fc control) cells. Consistent with results above ephrinB1 was homogenously distributed in unstimulated cells. After stimulation with EphB2-Fc all myc-GRIP2 clusters colocalized to ephrinB1 clusters (**Figure 28D**).

6.2.2. EphrinB1 interaction with GRIP2 depends on serine but not tyrosine based motifs

The C-terminal PDZ-binding motif YKV conserved in all EphrinBs contains a putative tyrosine phosphorylation site at position -3. The tyrosine residue just adjacent at -4 position has been shown to be a major phosphorylation site *in vitro* as well as *in vivo* (Kalo et al., 2001). A PDZ domain of the protein syntenin bound with less affinity to a peptide based on the sequence of the ephrinB carboxyl terminus with a phosphorylated tyrosine at position -3 than to an unphosphorylated peptide (Lin et al., 1999). Based on these findings we hypothesized that tyrosine phosphorylation at at least one of these residues could positively or negatively influence GRIP binding. A cell line co-expressing myc-GRIP2 and HA-ephrinB1 with all its tyrosine residues converted to phenylalanine (HA-ephrinB1-6F) was generated (cell clone MZ8-7). As shown in **Figure 29A** myc-GRIP2 co-immunoprecipitated with HA-ephrinB1-6F to a lesser extend than the wild-type protein. The interaction was still regulated by EphB2-Fc binding. The lack of the negatively charged hydroxyl group in phenylalanine may slightly decrease the affinity of HA-ephrinB1-6F to myc-GRIP2. Based on these findings, ephrinB tyrosine phosphorylation can be excluded as a major regulator of ephrinB-GRIP interaction. No interaction between HA-ephrinB1 and myc-GRIP2 could be detected when the serine residue at position -9 in ephrinB1 was changed to alanine (HA-ephrinB1_S-9A) (cell

clone MZ8-7). This finding demonstrates the requirement of this residue in ephrinB-GRIP binding. Together with the finding that ephrinB molecules are phosphorylated on serine residues (**Figure 19B**) the results suggest that serine phosphorylation could regulate ephrinB-GRIP binding.

Figure 28. Regulated interaction between ephrinB1 and GRIP2. (**A**) NIH3T3 cells stably expressing N-terminally HA-tagged full length ephrinB1 (HA-ephrinB1) or C-terminally truncated HA-ephrinB1-ΔC together with N-terminally myc-tagged GRIP2 (Clones MZ4-6 and MZ5-23 respectively) were stimulated either with Fc or EphB2-Fc. HA-immunoprecipitates from cell lysates were analyzed by SDS-PAGE following western blotting with anti-HA (upper panel) and anti-myc antibodies (middle panel). For control myc immunoprecipitates were analyzed with anti-myc antibodies (lower panel). Myc-GRIP2 specifically co-immunoprecipitates with full length HA-ephrinB1 after EphB2-Fc stimulation. (**B**) Similar experiment as in (**A**), but an anti-ephrinB (#23) antibody was used for ephrinB1 immunoprecipitation. A small amount of myc-GRIP1 co-immunoprecipitates in Fc control stimulated cells, indicating weak constitutive interaction. The interaction increases greatly after EphB2-Fc stimulation. (**C**) Cells were stimulated with Fc, EphB2-Fc or multimerized EphB2-Fc (EphB2-Fc+anti-Fc). Cell lysates were used for ProteinG affinity purification and analyzed as above. In addition EphB2-Fc was detected by western-blotting. EphB2-Fc, GRIP2 and ephrinB1 interact in a ternary complex. (**D**) MZ4-6 cells were stimulated with Fc (control, upper panels) or EphB2-Fc (lower panels). HA- ephrinB1 and myc-GRIP2 were visualized by immunocytochemistry. Myc-GRIP2 is expressed in a punctuated pattern in Fc stimulated cells. Stimulation with EphB2-Fc leads to co-clustering with HA-ephrinB1. Some co-clusters are indicated by arrowheads. The nuclear staining detected by the anti-ephrinB antibody is unspecific.
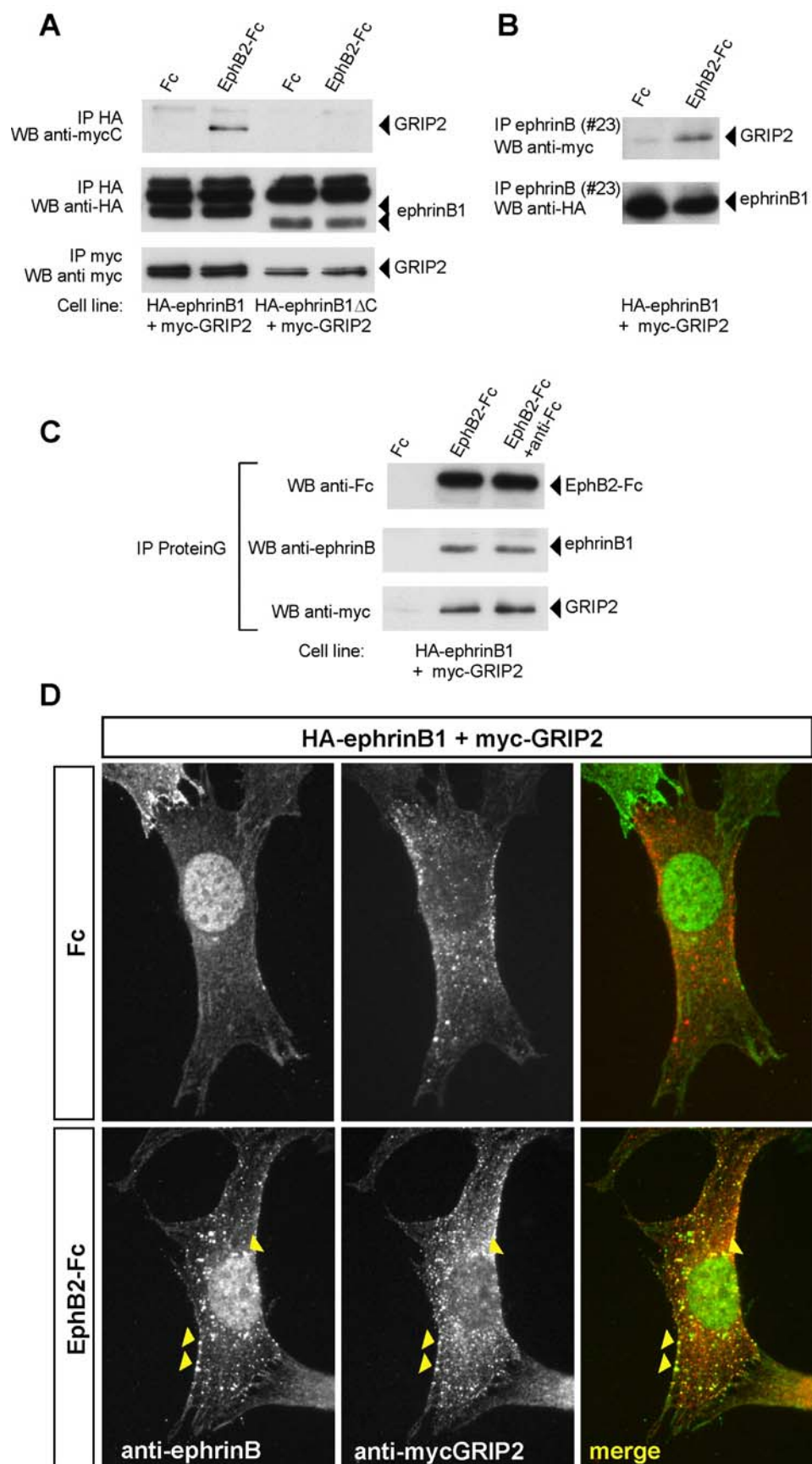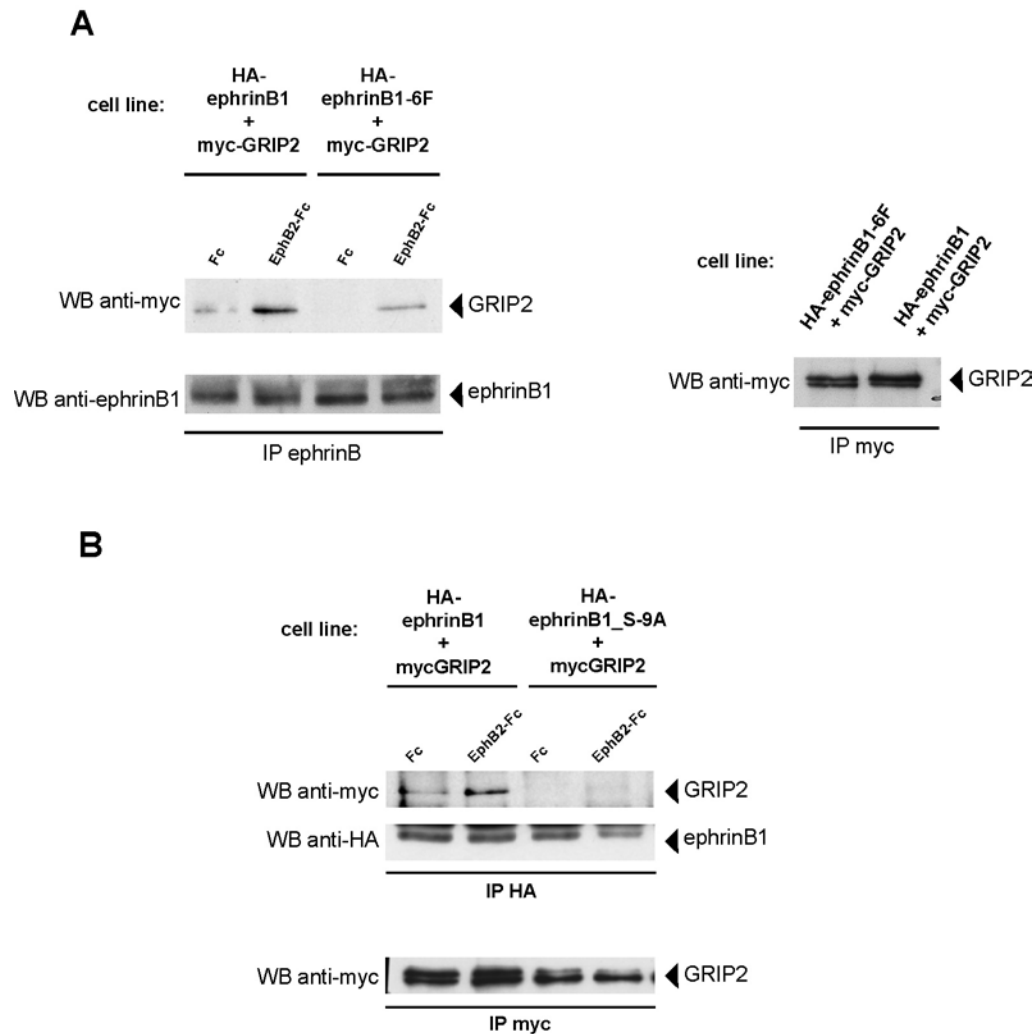
Figure 29. Regulated interaction between ephrinB1 and GRIP2 depends on serine but not tyrosine based motifs. (**A**) NIH3T3 cells stably expressing HA-ephrinB1 and HA-ephrinB1-6F together with myc-GRIP2 (clones MZ-4-6 and MZ7-8 respectively) were stimulated with Fc (control) or EphB2-Fc and analyzed as above. Left panel: Less binding is observed between HA-ephrinB1-6F and myc-GRIP2 but the interaction is still inducible by EphB2-Fc stimulation. Right panel: Levels of myc-GRIP2 in MZ4-6 and MZ8-7 cells. (**B**) NIH3T3 cells stably expressing HA-ephrinB1 and HA-ephrinB1_S-9A together with myc-GRIP2 (clones MZ-4-6 and MZ13-8 respectively) were stimulated with Fc (control) or EphB2-Fc and analyzed as above. Exchange of a serine residue at position -9 to alanine in HA-ephrinB1 abolishes interaction with myc-GRIP2.

6.2.3. Kinetics of ephrinB1-GRIP2 binding

The data presented in the previous chapters demonstrated that the ephrinB interaction with PTP-BL occurs with delayed kinetics. To further test the switch model the binding kinetics of ephrinB1 with GRIP2 were examined. As shown in **Figure 30A** myc-GRIP2 binds with rapid kinetics to HA-ephrinB1, already after 10min stimulation with EphB2-Fc. After EphB2-Fc removal from the cell culture medium the cells were left untreated for the indicated times before lysis. HA-ephrinB1 myc-GRIP2 complexes were stable for an extended time period of up to 1h. After 2h slightly reduced amounts of myc-GRIP2 co-immunoprecipitated with HA-ephrinB1. Stable complexes of myc-GRIP2 and HA-ephrinB1 were still detected at this time by immunocytochemistry (**Figure 30B**). These results suggest that the ephrinB GRIP interaction occurs with rapid kinetics and is maintained for a prolonged period of time. The kinetics of the ephrinB-GRIP interaction in primary cells remains to be confirmed.

A

Fc (min):	10	0	0	0	0	0
EphB2-Fc (min) pulse > chase:	0	10	10 >15	10 >30	10 >60	10 >120

IP ephrinB
WB anti-MYC

Cell line: HA-ephrinB1 + myc-GRIP2

B

Fc 10'

EphB2-Fc
10' > 120'

α-ephrinB1   α-myc   merge
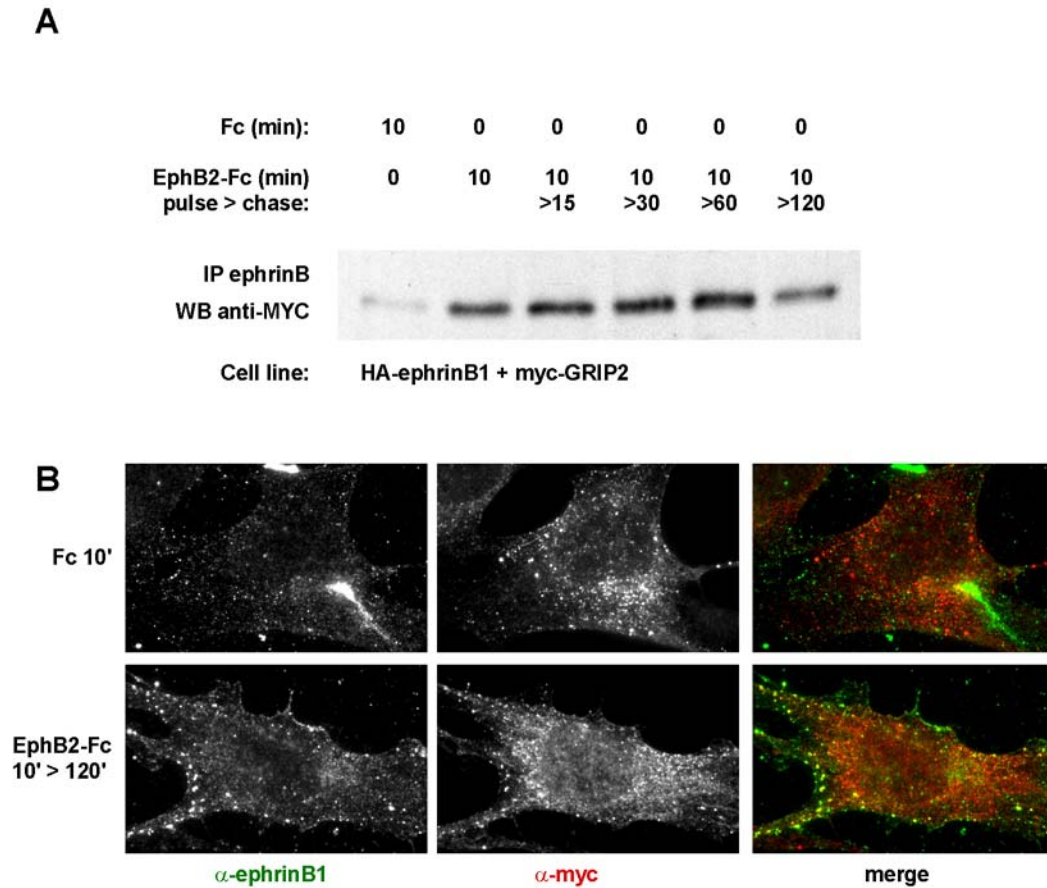
Figure 30. Kinetics of myc-GRIP2 binding to HA-ephrinB1. MZ4-6 cells were stimulated with Fc (control) or EphB2-Fc for 10min. EphB2-Fc was removed from the medium and the cells were left untreated for the indicated times. (**A**) Kinetics of ephrinB-GRIP interaction analyzed by co-immunoprecipitation following western blotting. (**B**) Immunohistochemistry of Fc control (upper panel) and 10min EphB2-Fc stimulated cells, 2h after removal of Ephb2-Fc (lower panel).

6.3. EphB/ephrinB bidirectional endocytosis terminates adhesion allowing contact mediated repulsion

In the studies presented above it was observed that stimulation of ephrinB1-expressing fibroblasts with soluble EphB ectodomains fused to the Fc portion of IgG (EphB2-Fc) caused the rapid clustering of ephrinB1. A significant portion of clustered ephrinB1 was observed in a punctuated, vesicular pattern throughout the cytoplasm and in the perinuclear region, suggestive of internalization. The aim of the following studies was to investigate if Ephs and ephrins undergo regulated endocytosis and to implicate endocytosis in a possible function.

6.3.1. Regulated endocytosis of ephrinB and EphB proteins in NIH3T3-cells

To establish whether surface ephrinB1 can be internalized, 3T3-ephrinB1 cells were stimulated with either unfused Fc (control) or EphB2-Fc. Cells were fixed in absence of detergents, and immunostained for N-terminal epitopes of ephrinB1 to indicate its distribution on the cell surface. In a second step, cells were permeabilized and stained for total ephrinB1 using a different primary antibody against ephrinB1. Staining that appears exclusively after permeabilization represents the intracellular pool of ephrinB1. Stimulation of 3T3-ephrinB1 cells with EphB2-Fc at 37°C for 10min resulted in abundant intracellular ephrinB1 clusters, while the ephrinB1 pattern remained diffuse after stimulation with control Fc (red staining in **Figure 31 A, B**). To test whether the internal pool of ephrinB1 was endocytosed from the cell surface, stimulation was done at 12°C, because low temperatures are known to be non-permissive for vesicular trafficking (Harder et al., 1998). The 12°C temperature incubation did not block ephrinB1 clustering at the cell surface (although clusters appeared smaller than at 37°C), but blocked internalization (**Figure 31 C, D**). To analyze if the entire complex of EphB2-Fc bound to ephrinB1 was internalized, antibodies against the Fc portion of EphB2-Fc were used for staining. At 37°C, numerous Fc-positive vesicles appeared exclusively after permeabilization, whereas at 12°C, only few focal internalized clusters were seen close to the cell periphery (**Figure 31 E, F**).

As expected from published work on other RTKs (Sorkin and Von Zastrow, 2002), EphB2 receptors also undergo internalization upon stimulation with soluble ephrinB1-Fc. As shown in **Figure 32A-F**, stimulation of 3T3-EphB2 cells with soluble ephrinB1-Fc at 37°C, but not at 12°C, caused clustering and accumulation of intracellular EphB2 in complex with ephrinB1-Fc.

_____

Figure 31. EphrinB1 undergoes endocytosis upon engagement with EphB2 presented as soluble fusion protein. (**A-F**) Reverse endocytosis. NIH3T3 cells stably expressing full length ephrinB1 (3T3 ephrinB1) were stimulated with either control Fc protein (**A, A', A'', C**), or with EphB2-Fc (**B, B', B'', D, E, F**) at the indicated temperatures. After 15min, cells were fixed and ephrinB1 was immunolabeled on the surface (green label in **A, B, C, D;** and **A', B'**). The total pool of ephrinB1 was visualized after cell permeabilization (red label in **A, B, C, D;** and **A'', B''**). EphB2-Fc, bound to surface ephrinB1, was visualized with a FITC-conjugated antibody directed against human-Fc (green label in panels **E, F**). After permeabilization, EphB2-Fc was stained with a Texas-Red conjugated antibody directed against human-Fc (red label in panels **E, F**). Stimulation leads to internalization of clustered receptor ligand complexes.

NIH3T3 ephrinB1

A — Fc 37°C — surface ephrinB1 total ephrinB1

B — EphB2-Fc 37°C — surface ephrinB1 total ephrinB1

A' — Fc 37°C — surface ephrinB1

B' — EphB2-Fc 37°C — surface ephrinB1

A" — Fc 37°C — total ephrinB1

B" — EphB2-Fc 37°C — total ephrinB1

C — Fc 12°C — surface ephrinB1 total ephrinB1

D — EphB2-Fc 12°C — surface ephrinB1 total ephrinB1

E — EphB2-Fc 37°C — surface Fc total Fc

F — EphB2-Fc 12°C — surface Fc total Fc

_____
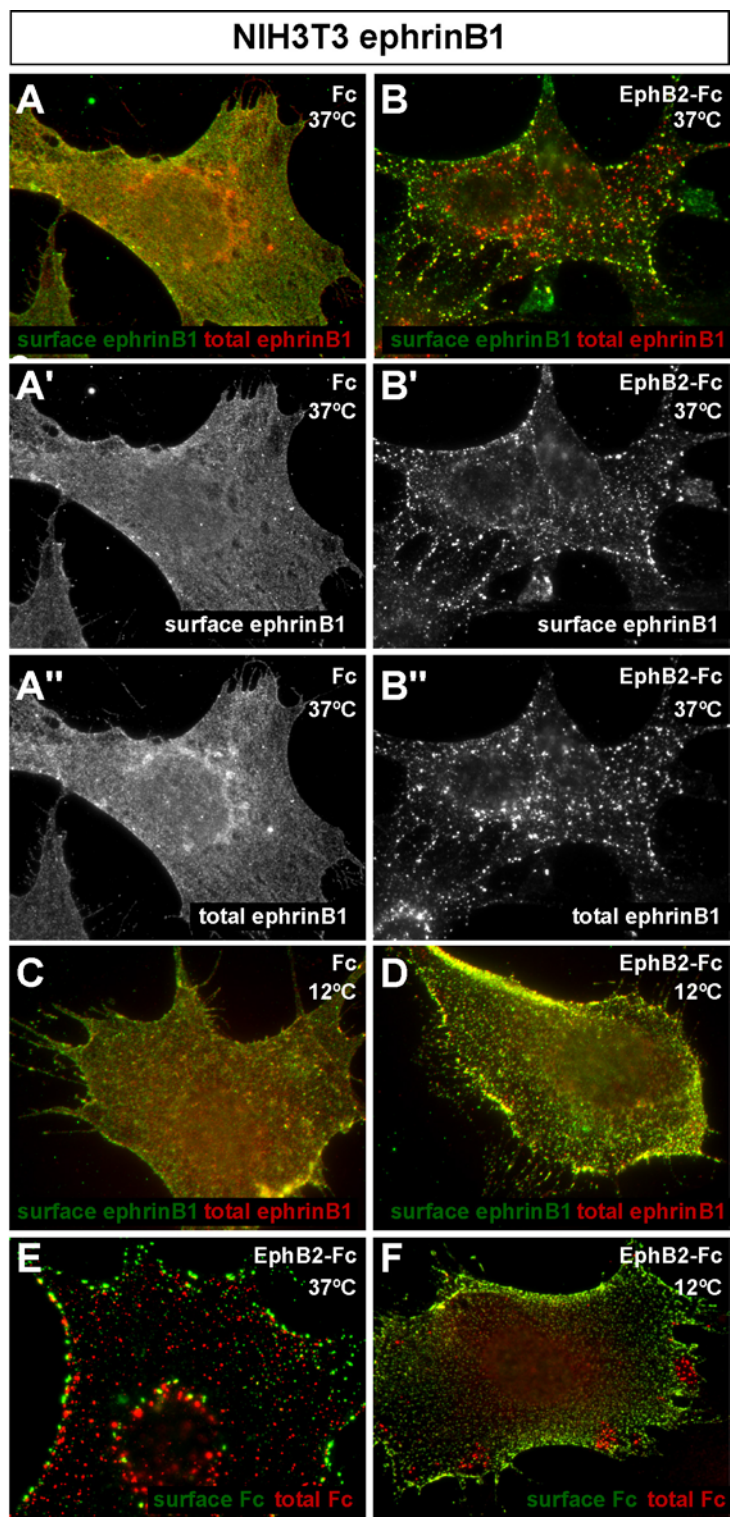
Figure 32. EphB2 undergoes endocytosis upon engagement with ephrinB1 presented as soluble fusion protein. (**A-F**) Forward endocytosis. NIH3T3 cells stably expressing full length EphB2 (3T3 EphB2) were stimulated with either control Fc protein (**A, A', A'', C**), or with ephrinB1-Fc (**B, B', B'', D, E, F**) at the indicated temperatures. After 15min, cells were fixed and surface EphB2 was immunolabeled (green label in **A, B, C, D;** and **A', B'**). The total pool of EphB2 was visualized after cell permeabilization (red label in **A, B, C, D;** and **A'', B''**). EphrinB1-Fc was stained against human Fc as above (**E, F**). Scale bars: 10μm.
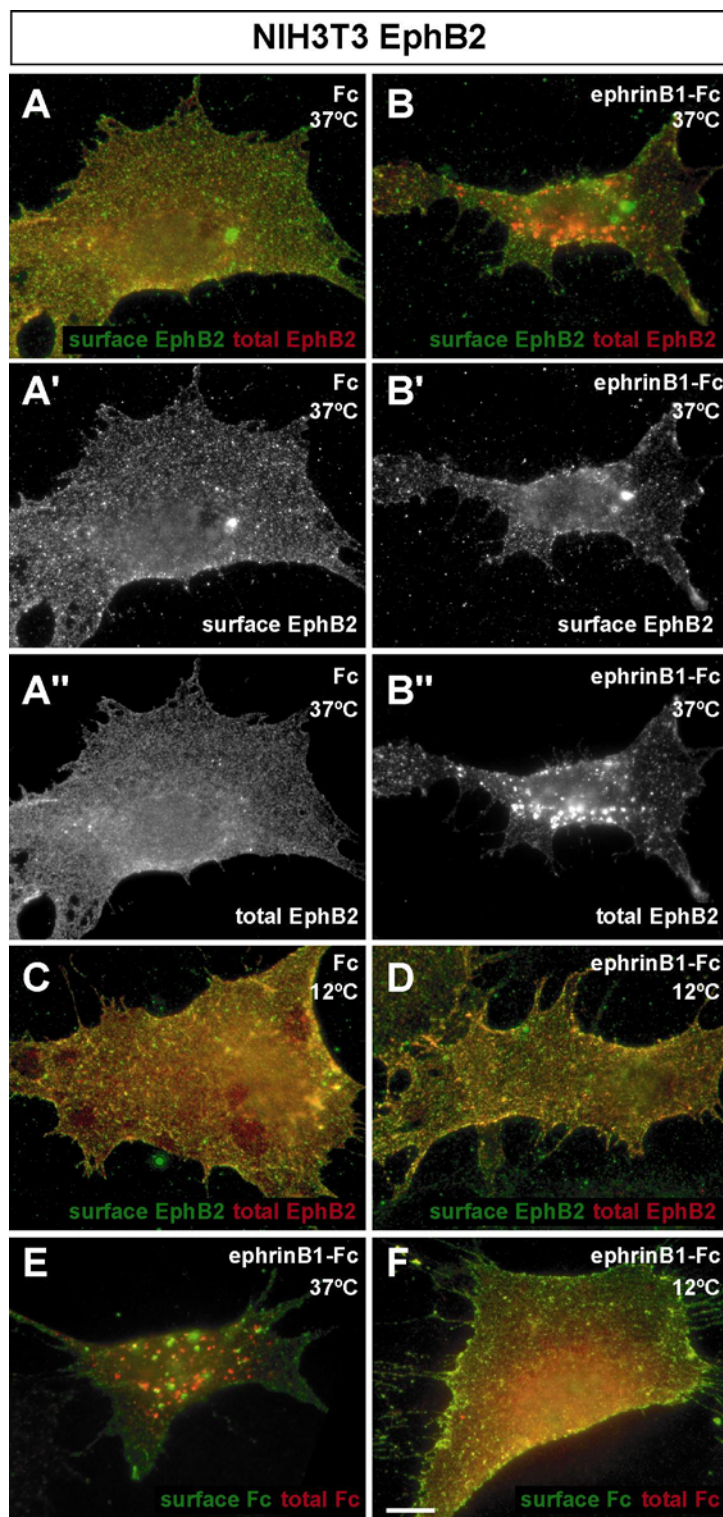
6.3.2. Regulated endocytosis of ephrinB and EphB proteins in primary telencephalic neurons

Clustering of endogenous ephrinB ligands and EphB2 receptors occurs in primary neurons and is important for signaling (chapter 6.1., Dalva et al., 2000) Primary mouse forebrain neurons which are known to express endogenous EphB receptors and ephrinB ligands (Brambilla et al., 1996; Dalva et al., 2000; Grunwald et al., 2001; Kullander et al., 2001; Shamah et al., 2001; Palmer et al., 2002) were dissected from E13.5 embryos and cultured for 2 days *in vitro* (DIV). Cells were stimulated with either EphB2-Fc or ephrinB1-Fc at $37^{o}C$ for 10min and stained with anti-Fc antibodies pre- and post-permeabilization. As shown in **Figure 33**, both reagents caused the rapid accumulation of internalized ligand-receptor complexes all over the cells (red staining). Consistent with rapid axonal transport of endocytosed vesicles, growth cones contain few small internalized clusters that increase in number and size with proximity to the cell bodies (compare red staining in **Figure 33E** with **33C** and **33J** with **33H**). Control Fc stimulated neurons do not show any Fc-positive clusters (**Figure 22D**). These results indicate that both endogenous ephrinB ligands and endogenous EphB receptors internalize, when clustered at the cell surface of primary neurons, by binding soluble forms of their binding partners.
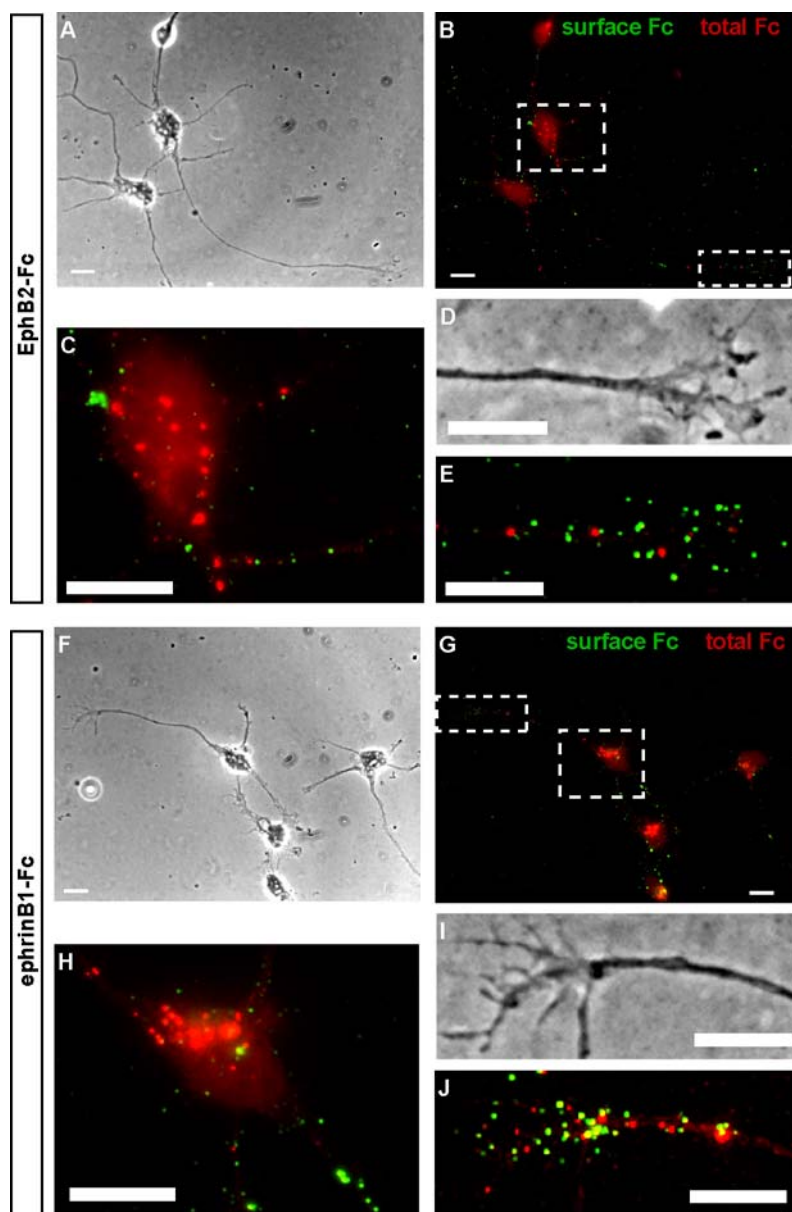
Figure 33. Endocytosis of EphB2-Fc and ephrinB1-Fc in primary telencephalic neurons. Neurons were dissected from E13.5 mouse embryonic forebrain, dissociated and cultured for 2 DIV to allow differentiation to occur. Cells were stimulated for 10min with either EphB2-Fc (panels **A-E**) or ephrinB1-Fc (panels **F-J**). Staining for surface and total Fc fusion proteins was done as described in **Figure 31**. **A, D, F, I**: Phase contrast images of stained neurons. Stippled boxes in panels **B** and **G** indicate those areas, which are zoomed in **C-E**, and **H-J**. Cell bodies are shown in panels **C** and **H**. Growth cones are shown in both, phase contrast (**D, I**) and after immunofluorescence (**E, J**). Note that internal clusters (red staining) are observed after ephrinB1-Fc and EphB2-Fc treatment both in growth cones and with increased size in cell bodies. Scale bars are 10μm in all panels.

6.3.3. EphrinB and EphB proteins co-cluster at sites of cell-to-cell contact and are endocytosed bidirectionally

Soluble ephrin-Fc and Eph-Fc fusion proteins are useful tools to specifically activate forward or reverse signaling in cells and tissues, but they may not recapitulate well the more localized physiological ephrin-Eph interactions at sites of cell-cell contact. Moreover, internalization may be facilitated, because the stimuli are soluble. To investigate if membrane-bound ephrinB-EphB complexes co-cluster and subsequently internalize, and if clustering is limited to sites of cell-cell contact, a cell-cell stimulation assay was developed. The assay consists of a sparse monolayer of adherent "recipient cells", cultured on glass cover slips. In a second step, "stimulator cells" are taken in suspension by a mild treatment which preserves the extracellular protein architecture, and added onto the recipient cells. After 10min, all cells are fixed and stained pre- and post-permeabilization as above. After stimulation of 3T3-ephrinB1 recipient cells with 3T3-EphB2 stimulator cells, rapid and localized co-clustering of ephrinB1 and EphB2 at the site of cell-cell contact near the plasma membranes of the two cells was observed (**Figure 34A, B** and **G, H**). Comparing the surface localization of ephrinB1 (**Figure 34F**) with its total distribution (**Figure 34G**) revealed that these clusters were partially endocytosed (red label in **Figure 34C, D**). The direction of internalization was mostly in a reverse manner, i.e. into the recipient 3T3-ephrinB1 cells, in part because its internalization machinery may have been more efficient than that of the freshly seeded stimulator cell. No internalization or clustering is observed when untransfected 3T3 cells are used as stimulator cells (data not shown). The pool of internalized ephrinB1 co-clusters with EphB2 (purple staining in **Figure 34A, B,** compares **3G** with **3H**). Immunostaining of total EphB2 was done with an antibody against the intracellular domain indicating that full length EphB2 was transcytosed into 3T3-ephrinB1 cells.
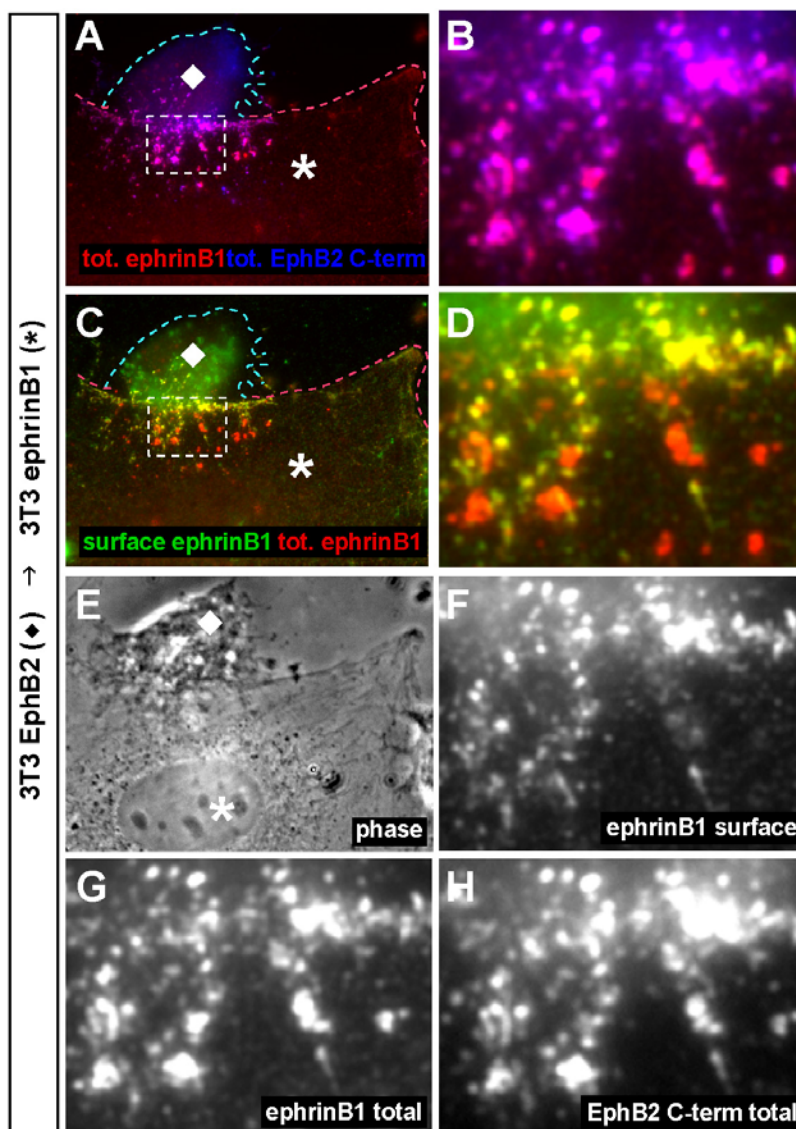
Figure 34: EphB2 and ephrinB1 cluster at sites of cell-cell contact and are endocytosed bidirectionally. Reverse endocytosis. 3T3-ephrinB1 recipient cells (asterisks) were cultured on glass cover slips and then stimulated with 3T3-EphB2 cells (diamonds). After 10min, cells were fixed and immunostained for surface ephrinB1 using an antibody directed against the ephrinB1 ectodomain (green label in **C-D**; and **F**). The total distribution of ephrinB1 was visualized after permeabilization of the cells (red label in **C-D**; and **G**). The total distribution of EphB2 was visualized with an antibody directed against the EphB2 cytoplasmic domain (blue label in **A-B**; and **H**). EphrinB1-EphB2 co-clusters are detected at the interface of the two cells and over the 3T3-ephrinB1 cell (purple color in **A** and **B**). Surface clusters are seen only at the direct contact sites of the two cells (yellow staining in C and **D**). Endocytosed ephrinB1 is seen only in the ephrinB1-expressing cell (red staining in **G** and **H**).
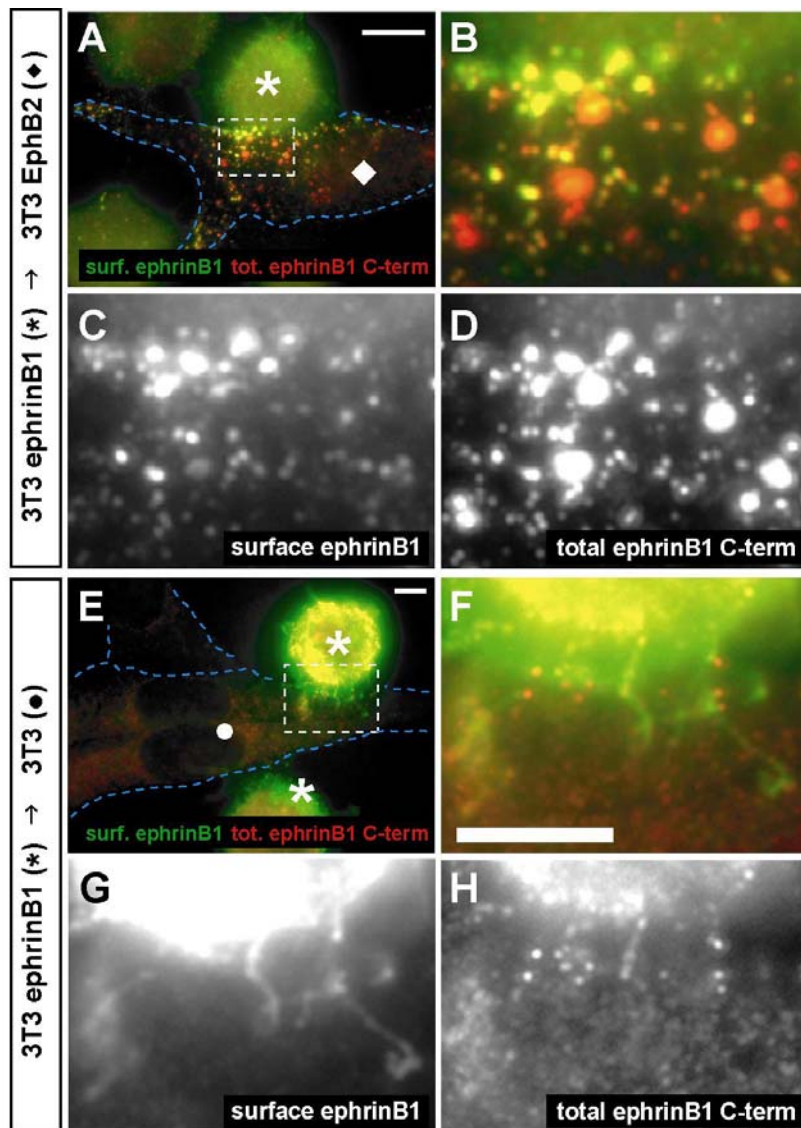
Figure 35: EphB2 and ephrinB1 cluster at sites of cell-cell contact and are endocytosed bidirectionally. Forward endocytosis and control. 3T3-EphB2 (diamond) or untransfected recipient cells (filled circle) were cultured on glass cover slips and stimulated with 3T3-ephrinB1 cells (asterisk). After 10min, cells were fixed and immunostained for surface ephrinB1 (green label in **A-B**, **E-F**; and **C**, **G**). After permeabilization of the cells, the total distribution of ephrinB1 was visualized with an antibody directed against the C-terminal tail (red label in **A-B**, **E-F**; and **D**, **H**). Surface clusters are seen exclusively at the interface of the two cells (yellow staining in **A** and **B**). Endocytosed full length ephrinB1 is seen in the EphB2 recipient cells (red staining in **A** and **B**). In control cultures, almost no clustering is observed with untransfected 3T3 cells (**E-H**). Scale bars are 5µm in all panels.

In the next experiment 3T3-ephrinB1 were used as stimulator cells and 3T3-EphB2 as recipient cells. EphrinB1 was internalized in a forward manner by 3T3-EphB2 cells (red label in **Figure 35A, B**, and compare **35C** with **35D**). Immunostaining of total ephrinB1 was done with an antibody against its C-terminus, indicating that full length ephrinB1 was transcytosed into the EphB2 cell. Co-clustering and internalization was strictly dependent on the presence of binding partners on neighboring cells. Seeding of 3T3-ephrinB1 cells onto wild-type 3T3 cells did not cause significant clustering and internalization of ephrinB1 (no red label in **Figure 35E-F**, compare **35G** with **35H**). In summary, localized clustering of EphB2 and ephrinB1 occurs at sites of intercellular interaction, followed by bidirectional endocytosis of complexes comprising full length receptors and ligands.

6.3.4. EphrinB/EphB-uptake and transport by primary neurons

To determine if membrane attached EphrinBs and EphBs are taken up in a regulated fashion by primary neurons, young immature forebrain neurons (E14.5 after 1DIV) were co-cultured with HeLa cells expressing an EphB2-YFP fusion protein. The YFP protein was inserted in frame into the cytoplasmic region of full length, kinase-active EphB2, a modification which did not interfere with the normal regulation and signaling function of EphB2 (J.K., R.K., unpublished). Neuronal growth cones touching HeLa-EphB2-YFP cells were imaged by time-lapse microscopy. **Figure 36A-B** shows a sequence of 7 images taken during a time period of 34min with a neuronal growth cone touching a transfected HeLa cell. During the first 10min, the growth cone collapses (**Figure 36A**; supplementary information on CD-Rom, **movie 1**). During collapse a small fluorescent cluster of EphB2 can be seen at the tip of a HeLa cell filopodium (**Figure 36B**, arrow). In subsequent images two clusters of EphB2 are taken up by the neuron and are retrogradely transported along the neurite. Endocytosis was never observed when neurons encountered HeLa cells expressing a membrane targeted version of YFP (memYFP) (data not shown). These results demonstrate that the full length EphB2 receptor is taken up by the neuron, likely due to ephrinB reverse endocytosis in the growth cones.
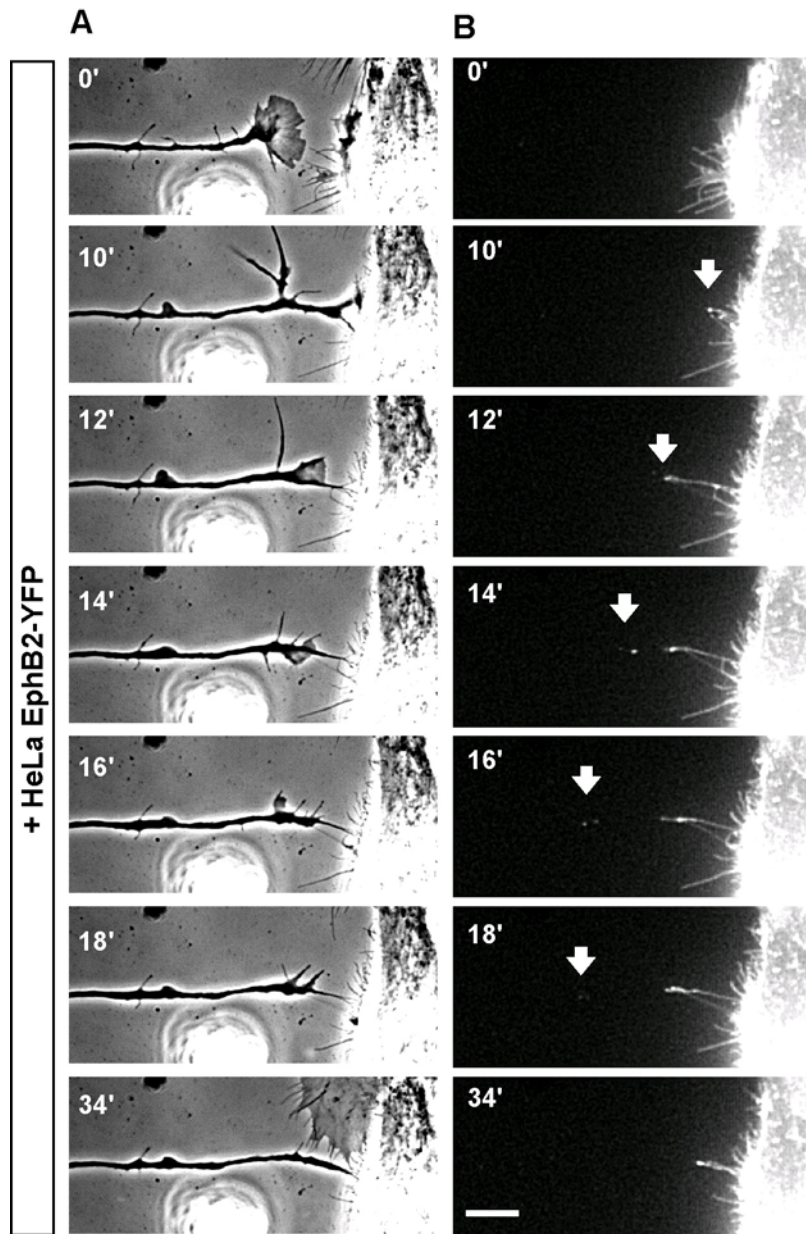
Figure 36. EphrinB1 and EphB2 uptake and transport by primary neurons. (A, B) Transcytosis of EphB2 by primary neurons. Forebrain neurons from E14.5 mouse embryos (1DIV) were co-cultured with HeLa cells transiently expressing EphB2-YFP. Growth cones were imaged by time-lapse microscopy at 1frame/min. The presented selection of images shows a nicely expanded neuronal growth cone before contact with a HeLa cell and collapse of the growth cone within 10min after contact. At the time of collapse, a fluorescent cluster of EphB2 forms at the tip of a single filopodium of the HeLa cell (arrow at 10min). The growth cone partially retracts and pulls the filopodium out. Two EphB2 clusters are retrogradely transported into the growth cone of the neuron. See also supplementary information on CD-Rom, **movie 1**. Scale bars: 10μm.

In the next experiment neurons were challenged with ephrinB1-expressing cells to monitor possible ephrinB1 uptake. Best results were obtained using hippocampal neurons, which had

matured in culture for 7 days. A 3T3 cell line expressing an N-terminally HA-tagged version of ephrinB1 was co-cultured with hippocampal neurons and uptake and retrograde transport of HA-ephrinB1 was visualized by immunostaining (**Figure 37A-D**). Near the contact site of a 3T3-HA-ephrinB1 cell, clusters of ephrinB protein can by visualized along the dendrite by immunostaining with an antibody against the C-terminus of ephrinB1 (**Figure 37C**). Most of these clusters also stain with an antibody against the HA epitope, suggesting that the neuron has transcytosed full length ephrinB1 from the 3T3 cell (**Figure 4B, D**). In no case HA-positive clusters were observed when neurons were co-cultured with untransfected 3T3 cells (**Figure 37E, F**).
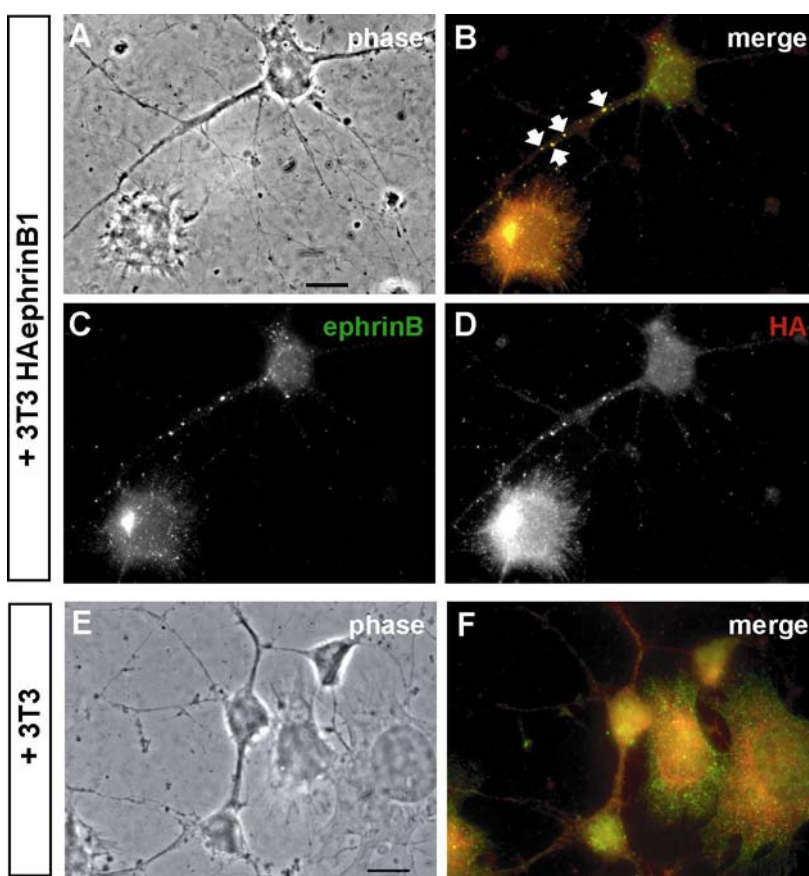
Figure 37. Uptake of ephrinB1 by primary neurons. Hippocampal neurons (E17.5, 7DIV) were cultured on laminin-coated glass cover slips and allowed to mature. Neurons were either stimulated with 3T3-HAephrinB1 cells (**A-D**) or with 3T3 cells (**E**, **F**). After 2h, cells were fixed, permeabilized and stained for ephrinB (panel **C**, and green label in **B**) and for the HA epitope tag (panel **D**, and red label in **B**). Clusters of ephrinB protein co-stain for HA indicating uptake of HAephrinB1 into the neuron. No clusters are seen when control 3T3 cells were co-cultured with untransfected 3T3 cells. Scale bars: 10μm.

6.3.5. Cytoplasmic determinants of EphrinB- and EphB-mediated endocytosis

To get some insights into the molecular mechanisms regulating endocytosis of the Eph/ephrin complex, it was investigated, if the cytoplasmic tails of ephrinB1 and EphB2 are required for bidirectional endocytosis. In the situation when both partners are full length, stimulation of a 3T3-ephrinB1 recipient cell with a 3T3-EphB2 stimulator cell causes the rapid (10min) internalization of ephrinB1 clusters near the contact site of the two cells predominantly into the 3T3-ephrinB1 recipient cell (large red clusters in **Figure 38A, B**). After 60min, internalized ephrinB1 is seen mostly in the 3T3-EphB2 cell (**Figure 38C, D**). If, however, the recipient cell expresses truncated ephrinB1-ΔC, strong ephrinB1 clustering is induced by the 3T3-EphB2 stimulator cell, but no internalization into the 3T3-ephrinB1-ΔC recipient cell occurs (no large red clusters in **Figure 38E, F**). At 60min instead, the adhered 3T3-EphB2 cell has internalized ephrinB1-ΔC (red clusters in **Figure 38G, H**). The cytoplasmic determinants required for ephrinB1 endocytosis are not yet known, since neither the block of tyrosine phosphorylation of ephrinB1 nor the block of its interaction with PDZ-domain proteins inhibited endocytosis (data not shown).
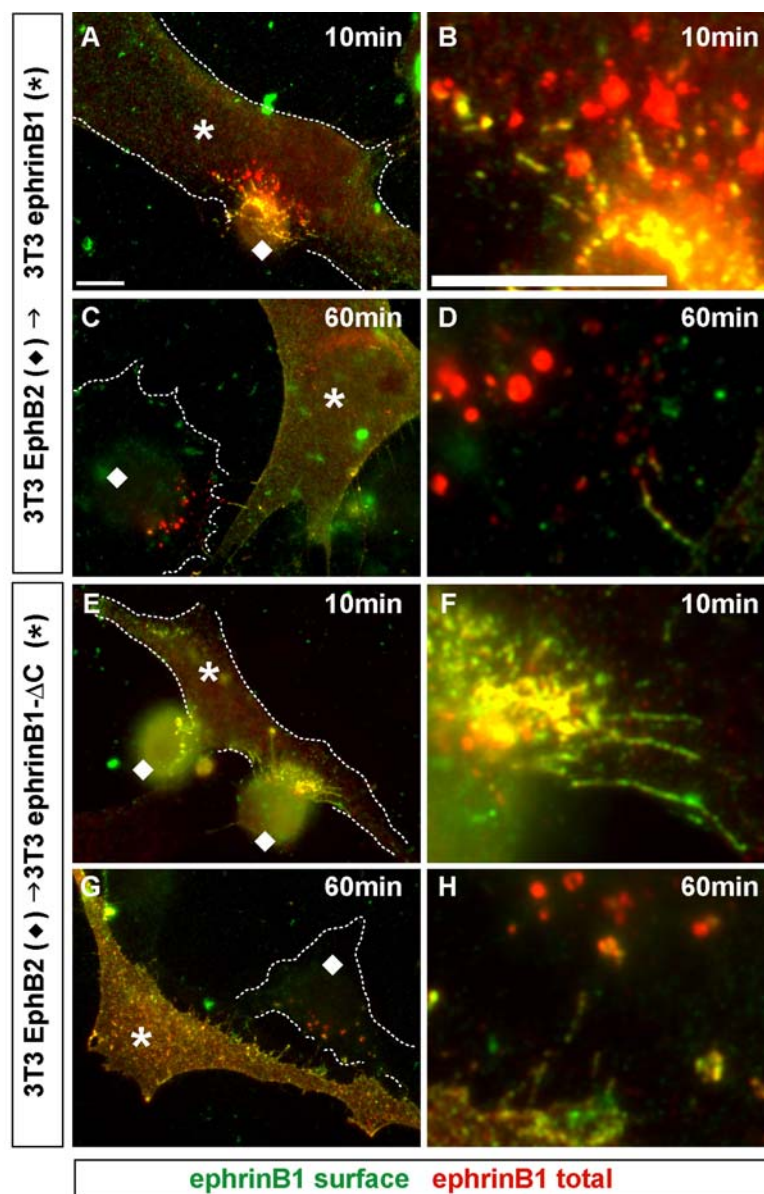
Figure 38: Reverse endocytosis requires cytoplasmic determinants. (**A-D**) 3T3-ephrinB1 recipient cells (asterisks) were pre-plated on glass cover slips and subsequently stimulated with 3T3-EphB2 cells (diamonds) as described above. Cells were fixed 10min (**A-B**) or 60min (**C-D**) after contact, and stained for surface (green) and total ephrinB1 (red). After 10min stimulation, ephrinB1 clusters are predominantly detected in the ephrinB1 cells. After 60min, ephrinB1 clusters are seen in 3T3-EphB2 stimulator cells. (**E-H**) 3T3-ephrinB1-ΔC recipient cells (asterisk) were pre-plated on glass cover slips and subsequently stimulated with 3T3-EphB2 cells (diamonds), for 10 and 60min. Fixation and staining were performed as above. At 10min, ephrinB1 clusters appear on the surface of the contact site between the cells in large membrane protrusions. No endocytosis into the 3T3-ephrinB1-ΔC recipient cell is observed (no red label in panel **F**). At 60min, ephrinB1-ΔC clusters are seen in 3T3-EphB2 stimulator cells (red label in Panels **G**, **H**). Scale bars: 10μm.

In the opposite situation in which the recipient cell expresses a truncated EphB2 receptor (EphB2-ΔC), trans-endocytosis of ephrinB1 clusters into the 3T3-EphB2-ΔC recipient cell is not observed at 10min (**Figure 39A, B**) and very rare even at 60min (**Figure 39C, D**). Instead, at 60min, numerous filopodia-like protrusions containing ephrinB1 are seen at the contact zone between the two cells and internalized ephrinB1 is seen in the 3T3-ephrinB1 stimulator cell (large red clusters in **Figure 39C, D**). To address the role of Eph-receptor kinase signaling, endocytosis was analyzed in recipient cells expressing a kinase-deficient EphB2 receptor (EphB2-KD). Similar to cells expressing truncated EphB2, transendocytosed ephrinB1 in cells expressing EphB2-KD was not detectable at 10min (**Figure 39E, F**). At 60min, endocytosis shifted again towards the ephrinB1 stimulator cells (large red clusters in **Figure 39G, H**). Occasional small red dots, as seen in EphB2-KD cells, were also observed in cells expressing EphB2-ΔC (data not shown).

In summary, these results indicate that the cytoplasmic tails of ephrinB1 and EphB2 are required for endocytosis. C-terminal truncation of one protein, however, does not impair endocytosis of its full length partner protein in the neighboring cell. EphB2 receptor mediated forward endocytosis requires the kinase activity of the receptor.
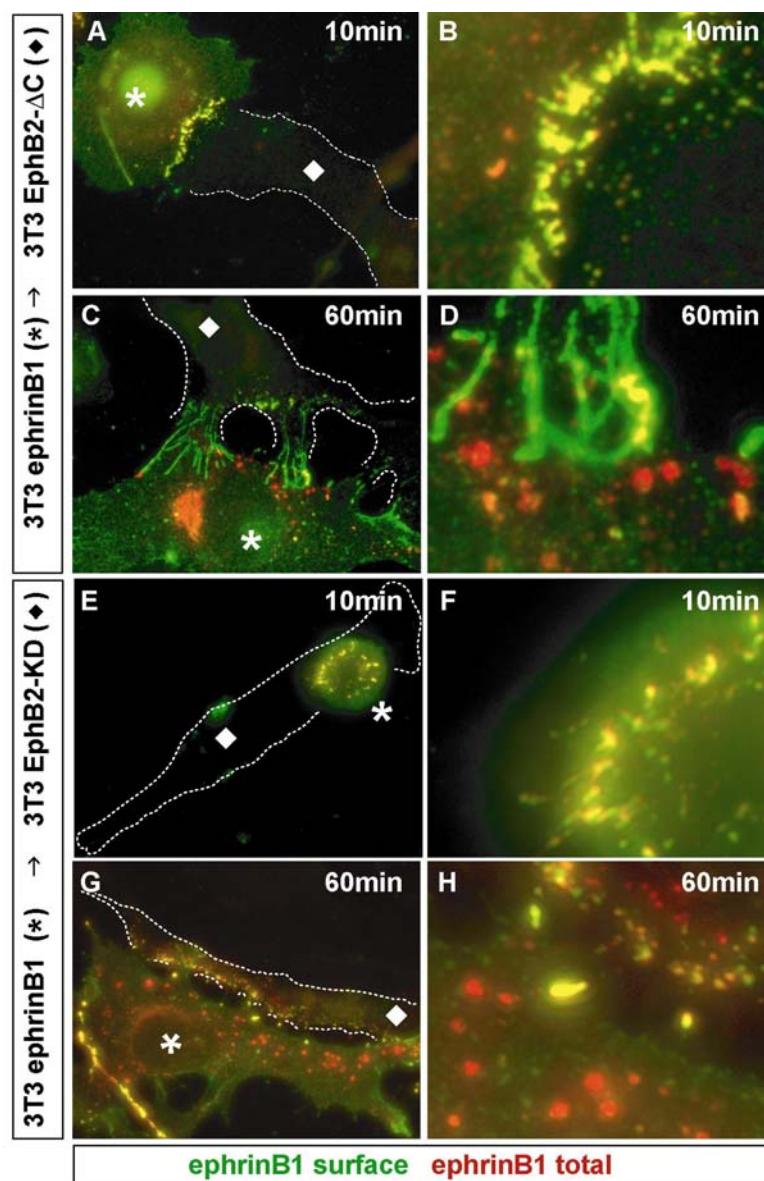
Figure 39. Forward endocytosis requires cytoplasmic determinants. (**A-D**) 3T3-EphB2-ΔC recipient cells (diamonds) were pre-plated on glass cover slips and subsequently stimulated with 3T3-ephrinB1 cells (asterisks) for 10min (**A**, **B**) or 60min (**C**, **D**). Cells were fixed and stained as described above. Intense staining of surface ephrinB1 is seen on the contact sites of both cells. Endocytosis into the 3T3-EphB2-ΔC recipient cell is largely reduced after 10min as well as after 60min co-culture. After 60min EphrinB1 clusters, unlike as in **Figure 38C-D**, are now seen in the 3T3-ephrinB1 stimulator cell (red label in panels **C**, **D**). (**E-H**) Recipient cells (diamonds) expressing a kinase inactive mutant EphB2 receptor (3T3-EphB2-KD) were stimulated as above with 3T3-ephrinB1 cells (asterisks) for 10min (**E**, **F**) or 60min (**G**, **H**). Endocytosis into 3T3-EphB2-KD cells is largely reduced (note that small endocytosed clusters are seen only at 60min). After 60min co-culture, large endocytosed clusters can be seen in the 3T3 ephrinB1 cells. Scale bars: 10µm.

6.3.6. Bidirectional endocytosis mediated by ephrinA ligands and EphA receptors

The next aim was to address if bidirectional endocytosis is a general phenomenon within the Eph and ephrin classes of protein families. EphrinA2 recipient cells were precultured on glass coverslips and stimulated with NIH3T3 control stimulator cells for 10min (**Figure 40A-B**) or with 3T3-EphA4 stimulator cells for 10min (**Figure40C-F**) or 60min (**Figure 40G-R**). Surface and total ephrinA2 was visualized using a similar immunostaining protocol as above (see Materials and Methods for details). In addition the total distribution of EphA4 was visualized. Stimulation with NIH3T3 control cells does not affect the distribution of EphrinA2, which is homogenous on the cell surface (**Figure 40A-B**). After 10min co-culture with EhA4 cells ephrinA2 clusters at the interface of the two cells (purple staining in **Figure 40E-F**). Many of these clusters become endocytosed as indicated by the red staining in **Figure 40C-D**. The clusters remain at the contact site of the two cells. This is different to the observation that endocytosed ephrinB1-EphB2 clusters spread into the recipient cells (**Figure 34A-D** or **Figure 38A-B**). Thus, the direction of endocytosis cannot be judged easily. After 60min, however, endocytosed clusters of ephrinA2 can be detected in both, the ephrinA2 cells as well as in the EphA4 cells (red staining in **Figure 40G-I** and compare **M** with **N** and **P** with **Q**).

Figure 40: Bidirectional endocytosis by ephrinA2 ligand and EphA4 receptor. NIH3T3 cells expressing a myc-tagged version of ephrinA2 (3T3 ephrinA2, asterisks) were cultured on glass cover slips and stimulated with 3T3 control cells (filled circles) for 10min (**A**, **B**) or with 3T3 EphA4 cells (diamonds) for 10min (**C-F**) or 60min (**G-R**). Cells were fixed and stained for ephrinA2 on the surface (green label in **A**, **C-D**, **G-I**; and **M**, **P**). After permeabilization cells were stained for the total distribution of ephrinA2 (red label in **A-L**; and **N**, **Q**) as well as for the total distribution of EphA4 (blue label in **B**, **E-F**, **J-L**; and **O**, **R**). (**A, D**) 10min stimulation with 3T3 control cells (marked by dashed lines) does not affect the subcellular distribution of ephrinA2. (The same is true after 60min co-culture, data not shown) (**B**, **C**, **E**, **F**) 10min stimulation with EphA4 cells leads to clustering of ephrinA2 at the cell-cell contact site. Red clusters indicate endocytosis of ephrinA2. Compare with **Figure 34A-D** or **Figure 38A-B**, where reverse endocytosis is detected by spreading of endocytosed clusters into the ligand cell. Instead, ephrinA2 clusters remain at the contact site between the two cells and therefore the direction of endocytosis cannot be judged easily. (**G-R**) After 60min co-culture, endocytosed clusters can be detected in both the EphA4 cells (**G-H**, **Q**) as well as in the ephrinA2 cells (**G**, **I**, **N**). Clusters of EphA4 only partially co-localize with ephrinA2 clusters (**K**, **L**; and compare **N** with **O** and **Q** with **R**), suggesting the degradation of EphA4. Scale bars: 10µm.

10min 3T3 (●) →
3T3 ephrinA2 (*)

10min 3T3 EphA4 (♦) →   3T3 ephrinA2 (*)

A — surface ephrinA2 tot. ephrinA2

B — total ephrinA2 total EphA4

C — surface ephrinA2 tot. ephrinA2

D

E — total ephrinA2 total EphA4

F

60min 3T3 EphA4 (♦) →   3T3 ephrinA2 (*)

G — surface ephrinA2 tot. ephrinA2

H

I

J — total ephrinA2 total EphA4

K

L

M — surface ephrinA2

N — total ephrinA2

O — total EphA4

P — surface ephrinA2

Q — total ephrinA2

R — total EphA4

97

The staining pattern of endocytosed ephrinA2 only slightly matches that of EphA4 (**Figure 40J-L** and compare **N** with **O** and **Q** with **R**). These results indicate that also ephrinA ligands and EphA receptors undergo bidirectional endocytosis at sites of cell-cell contact. The lack of complete co-staining of EphA4 with internalized ephrinA2 suggests that the receptor might be rapidly degraded after endocytosis.

6.3.7. Bidirectional endocytosis regulates a cell repulsion response and cell detachment

To determine if bidirectional endocytosis affects repulsive cell migration, an *in vitro* assay was developed in which cells expressing fluorescently tagged EphB2 receptor (EphB2-YFP) were co-cultured with cells expressing fluorescently tagged ephrinB1 (CFP-ephrinB1). To analyze cell repulsion, fluorescence time lapse recordings were conducted using a dimmed mercury light source which did not affect the viability and mobility of the cells within the observation times. HeLa cells were chosen, because they express low levels of endogenous ephrinB and EphB proteins and high levels of transfected proteins therefore allowing low exposure times. Furthermore, they show similar transcytosis of the EphB/ephrinB complex as NIH3T3 cells (data not shown) and they are very motile, when cultured on laminin in the presence of hepatocyte growth factor (HGF). Repulsion between two cells was scored positive when an advancing ruffling lamellipodium at the leading edge retracted immediately after cell contact. In almost all observed cases (11 out of 13 collisions) when a ruffling lamellipodium of an EphB2 cell collides with an ephrinB1 cell, strong co-clustering of receptor with ligand occurs within 1min. The initial clusters always appear in filopodia-like protrusions. During the retraction of EphB2 positive lamellipodia receptor-ligand complexes endocytose bidirectionally (**Figure 41A**; supplementary information on CD-Rom, **movie 2**). Only thin and diminished retraction fibers remain between the cells over time. Contacts of EphB2- or ephrinB1-transfected cells with untransfected cells in the same mixed culture do not result in clustering nor cell retraction (**Figure 41A** asterisk; supplementary information on CD-Rom, **movie 2**, and data not shown). Thus, in this reconstituted cell system, Eph-receptor mediated forward signaling leads to lamellipodia-retraction and forward endocytosis, whereas ephrinB-mediated reverse signaling only controls reverse endocytosis.

The next experiment addressed the role of the bidirectional mode of endocytosis during unilateral cell retraction. Dramatically different cell behavior was observed when ephrinB1 endocytosis was blocked by a C-terminal truncation. Upon contact, rapid receptor-ligand co-clustering occurs, but these clusters in part remain localized to the surface of the ligand expressing cell, where they grow to much larger complexes compared to full length ephrinB1 (**Figure 41B** left panels; supplementary information on CD-Rom, **movie 3** and compare **41F** with **41G**). The EphB2 cell engulfs the clusters vigorously, retracts strongly, and in most cases (8 out of 14) even rounds up, a behavior rarely (3 out of 11 cases) observed with wild-type ephrinB1 (**Figure 41B**, **E**; supplementary information on CD-Rom, **movie 3**). Hence, a mutation that blocks ephrinB1 endocytosis leads to a stronger EphB2 cell retraction response. This retraction behavior clearly depends on the cytoplasmic domain of EphB2. Under conditions when both ephrinB1 and EphB2 are C-terminally truncated, the cells strongly adhere to each other and large receptor- and ligand-bearing fascicles are formed at the contact zone (**Figure 41C**; supplementary information on CD-Rom, **movie 4**). These findings indicate that ephrinB and EphB proteins can act as adhesion molecules, if endocytosis and other signaling events are blocked.

In order to test how cells react to unidirectional ephrinB reverse signaling, cell behavior was investigated in the presence of truncated EphB2 and wild-type ephrinB1. As expected, ephrinB1 cells strongly endocytose receptor-ligand clusters, whereas EphB2-ΔC cells fail to endocytose these complexes (**Figure 41D**; supplementary information on CD-Rom, **movie 5**). The cells, however, neither retract nor adhere to each other. Cell behavior is in fact indistinguishable from untransfected cells, i.e. they migrate along each other (**Figure 41D**, phase images; supplementary information on CD-Rom, **movie 5**). EphrinB1 reverse endocytosis is therefore sufficient to terminate adhesion and to cause cell detachment. In comparison, EphB2 forward signaling also terminates adhesion by endocytosis, but in addition results in a strong repulsive response.

A EphB2-YFP CFP-ephrinB1

B EphB2-YFP CFP-ephrinB1-ΔC

C EphB2-YFP-ΔC CFP-ephrinB1-ΔC

D EphB2-YFP-ΔC CFP-ephrinB1

E

F

G

_____
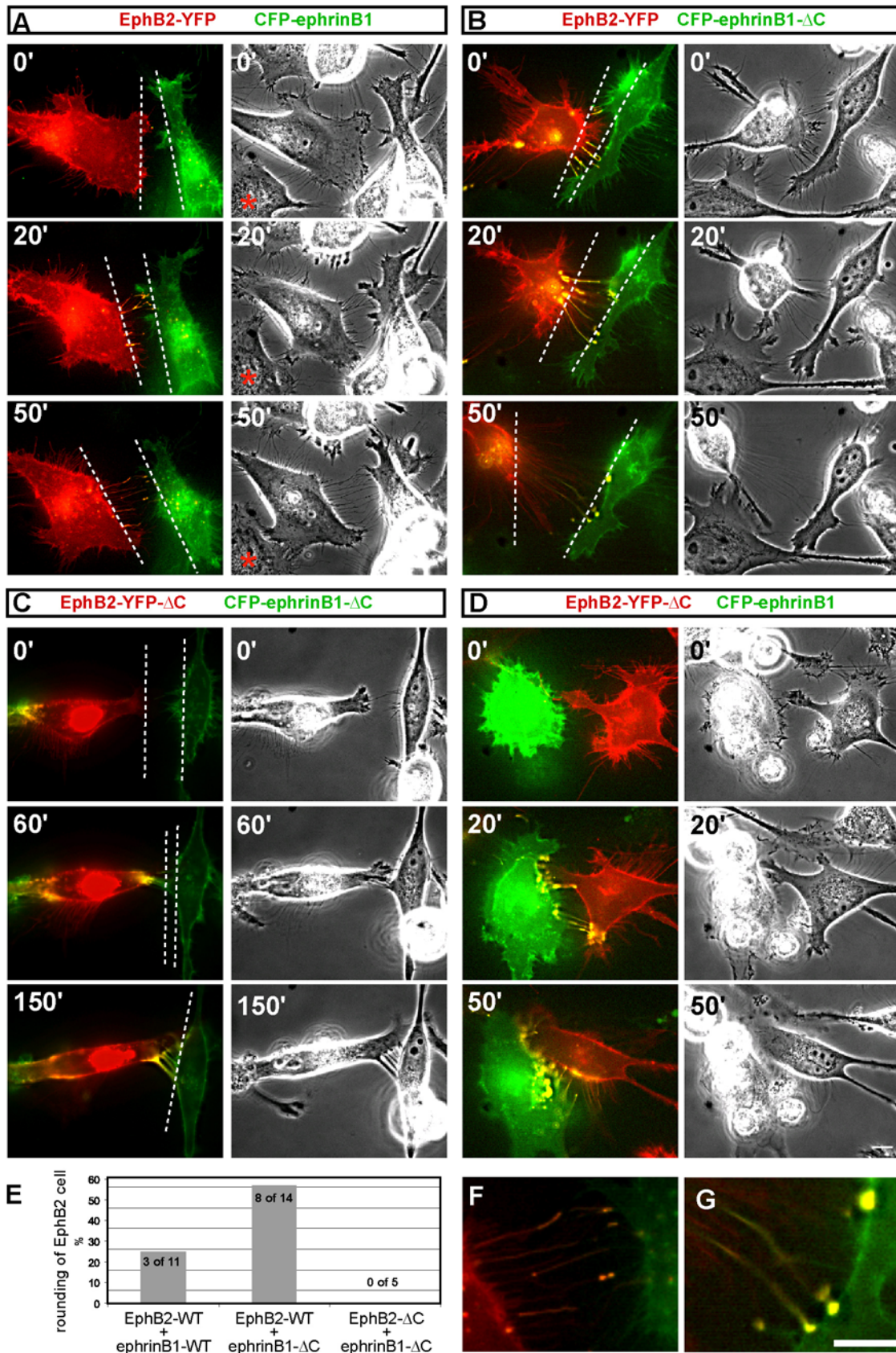
Figure 41. Endocytosis regulates the cell repulsion response by EphB2 and is sufficient for detachment. (**A**; supplementary information on CD-Rom, **movie 2**) HeLa cells were transiently transfected with full length EphB2-YFP and full length CFP-ephrinB1, and then co-cultured on laminin-coated glass cover slips in the presence of HGF to enhance motility. Cultures were imaged, acquiring sequentially couples of phase contrast and YFP-fluorescence images at a frequency of 1frame/min. In addition, every 10min a CFP-fluorescence image was taken. Time points of imaging are indicated in upper left corners. Left panels: Selected fluorescence images are shown with EphB2-YFP in red and CFP-ephrinB1 in green. Right panels: phase contrast images. Intense clustering of EphB2 and ephrinB1 is seen at the contact site between the two cells at 20min. The EphB2-YFP cell retracts a lamellipodium from the ephrinB1 cell (indicated by the distance between the two stippled lines). (**B**; supplementary information on CD-Rom, **movie 3**) Similar experiment as shown in panels A, except that C-terminally truncated CFP-ephrinB1-ΔC was used. Ephrin-Eph clusters (in yellow) are unidirectionally endocytosed into the EphB2-YFP-expressing cell. Intense yellow label is seen also on the surface of the CFP-ephrinB1-ΔC cell indicating lack of reverse endocytosis (see also panel **G**). Strong repulsion and rounding of EphB2-YFP-expressing cell is observed. (**C**; supplementary information on CD-Rom, **movie 4**) Similar experiment as shown in panels A, except that C-terminally truncated CFP-ephrinB1-ΔC and EphB2-YFP-ΔC were used. No repulsion is observed. Instead, cells strongly adhere to each other forming large fascicles filled with ephrin-Eph complexes. (**D**; supplementary information on CD-Rom, **movie 5**) Similar experiment as shown in panels **A**, except that wild-type CFP-ephrinB1 and EphB2-YFP-ΔC were used. Strong reverse endocytosis of ephrinB-EphB complexes, but otherwise normal cell behavior similar to untransfected cells is observed. Neither adhesion, nor repulsion is observed. (**E**) Quantification of cell rounding. Numbers of time lapse recordings used for the analysis are indicated. (**F, G**) Higher power images of 50 min-panels of A and B are shown. Note the accumulation of brightly fluorescing complexes on the surface of CFP-ephrinB1-ΔC-expressing cells (panel **G**). Scale bars: 10μm.

6.3.8. EphB2 forward endocytosis is required for efficient axon detachment

The work presented above shows that EphrinB1 reverse endocytosis is sufficient to mediate cell detachment. The subsequent experiment addressed the involvement of endocytosis in growth cone collapse and neurite withdrawal. In cultivated mouse forebrain neurons, growth cone collapse can be induced by co-culture with either ephrinB2- or EphB2-expressing cells, but not with untransfected cells or cells expressing a membrane-tagged version of EYFP (data not shown and **Figure 36**). However, cell surface clustering and endocytosis are much more pronounced in case of EphB2-YFP stimulator cells. Strong surface clustering allowed us to selectively observe ephrin-Eph-mediated growth cone collapse, as opposed to unspecific growth cone collapse. The blockade of EphB2 endocytosis in the stimulator cells interfered with axon detachment. As shown in **Figure 42A**, **B**, both EphB2-YFP and EphB2-YFP-ΔC expressing cells caused growth cone collapse within 5-10min of first contact. Therefore, unidirectional ephrinB reverse endocytosis is sufficient to allow collapse of the growth cone. In most cases, the contacting filopodia carrying small EphB2 clusters are pulled out by the retracting growth cone (**Figure 42A, B**). Using time lapse imaging, the maximal extension of the contacting filopodia just before detachment occurs was measured. The average expansion of filopodia, from its first cluster to its maximal extension was about twice as long in EphB2-YFP-ΔC- than EphB2-YFP-expressing cells (15.5 versus 8μm, respectively; $p < 0.002$; two-tailed t-test) (**Figure 42C**). Likewise, the time it took for filopodia to rupture was significantly longer in EphB2-YFP-ΔC- than EphB2-YFP-expressing cells ($p < 0.03$) (**Figure 42D**). Because the speed of filopodia extension was not different between the groups (**Figure 42E**), it can be concluded that axon detachment from EphB2-YFP-ΔC-expressing cells is delayed compared to EphB2-YFP-expressing cells. Our results suggest that forward endocytosis by EphB2 is required for efficient ephrinB-mediated axon detachment of forebrain neurons.
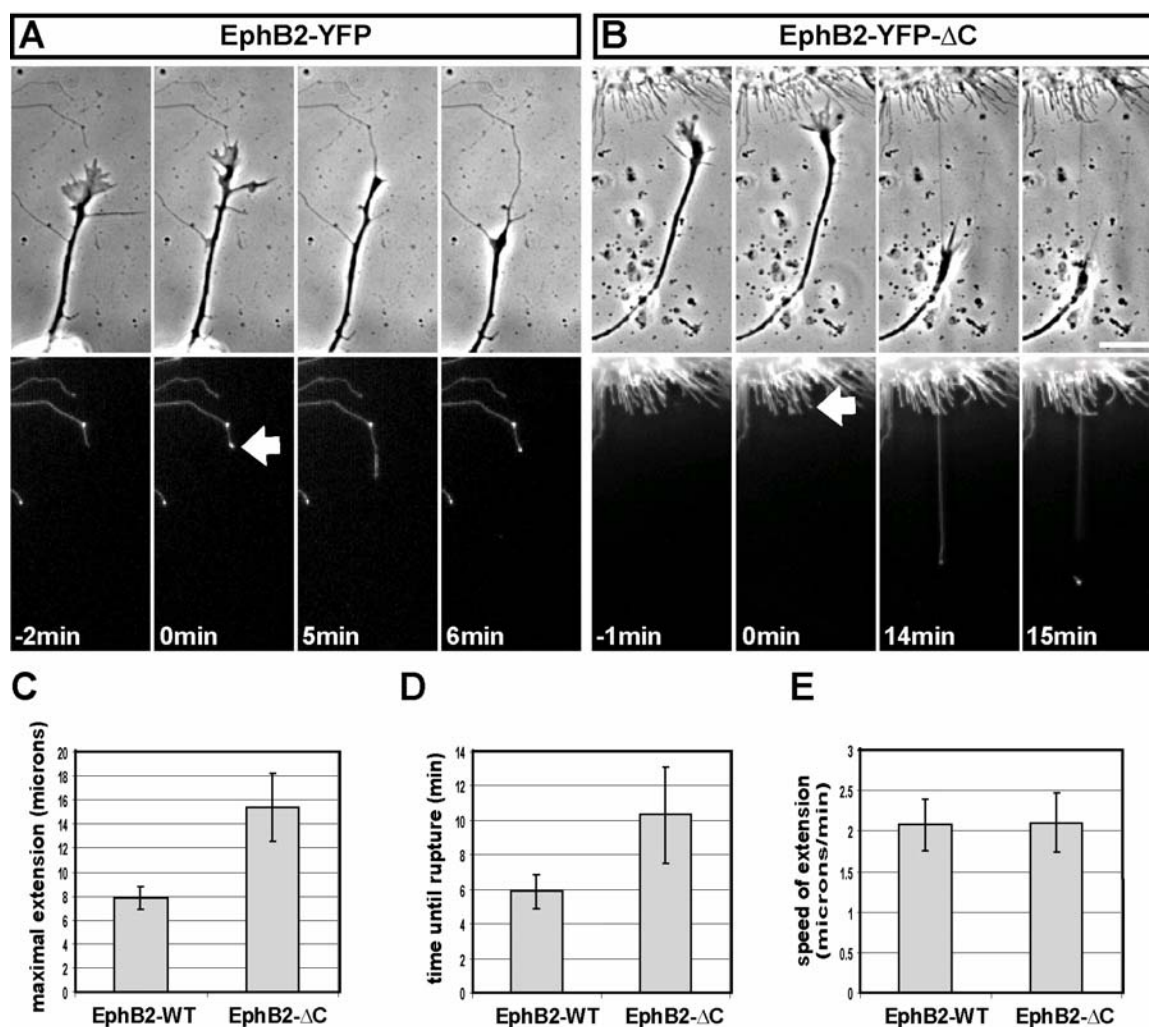
Figure 42. EphB2 C-terminal truncation impairs growth cone detachment. Primary forebrain neurons were co-cultured with HeLa cells expressing either EphB2-YFP (**A**) or EphB2-YFP-ΔC (**B**). After 1DIV, growth cones were imaged by time lapse microscopy at 1frame/min. (**A**) Growth cone (left panels: 2min before contact) collapses upon contact with a protrusion of a HeLa cell expressing EphB2-YFP (fluorescent cluster indicated by arrow). 5min after contact the collapsing growth cone pulls the HeLa filopodium to its maximal length. One minute later the filopodium detaches (6min). (**B**) Growth cone (left panels: one minute before contact) collapses upon contact with a protrusion of a HeLa cell expressing EphB2-YFP-ΔC (fluorescent cluster indicated by arrow). One filopodium is pulled out to its maximal length by the retracting growth cone after 14min before it ruptures after 15min. (**C**) Quantification of average maximal extension of filopodia, (**D**) average time until rupture, (**E**) average speed of filopodia extension in the two groups. Scale bar: 10μm.

6.3.9. Supplementary information on CD-Rom

(Supplementary information on CD-Rom, movie 1) EphB2 uptake and transport by primary neurons during growth cone collapse. Forebrain neurons from E14.5 mouse embryos (1DIV) were co-cultured with HeLa cells transiently expressing EphB2-YFP. Growth cones were imaged by time-lapse microscopy at 1frame/min (phase contrast on the left and YFP fluorescence on the right). The movie shows the collapse of a neuronal growth cone after contacting the HeLa cell. At the time of contact, a fluorescent cluster of EphB2 forms at the tip of a single protrusion of the HeLa cell. The growth cone partially retracts and pulls the protrusion out. EphB2 clusters are retrogradely transported into the neurite.

(Supplementary information on CD-Rom, movie 2) Repulsion of HeLa EphB2 cells and bidirectional endocytosis. HeLa cells were transiently transfected with full length EphB2-YFP and full length CFP-ephrinB1, and then co-cultured before time lapse imaging at 1frame/min (upper part: phase contrast, lower part YFP fluorescence). The movie shows a HeLa EphB2-YFP cell colliding with a HeLa CFP-ephrinB1 cell (see **Figure 41A**) via one of its lamellipodia. The lamellipodium retracts within 10min after contact and leaves some retraction fibers behind. At this time, clusters of EphB2-YFP form. After 10min, large vesicular structures pinch off from the clusters and move within the EphB2-YFP cell. Smaller vesicular structures pinch off from the retraction fibers and move into the CFP-ephrinB1 cell. Around 22min another lamellipodium collides with a untransfected HeLa cell (lower left corners) and neither retraction nor clustering occurs.

(Supplementary information on CD-Rom, movie 3) Enhanced repulsion in the absence of reverse endocytosis. HeLa cells were transiently transfected with full length EphB2-YFP and truncated CFP-ephrinB1-ΔC, and then co-cultured before time lapse imaging at 1frame/min (upper part: phase contrast, lower part YFP fluorescence). The movie shows a HeLa EphB2-YFP cell retracting from a HeLa CFP ephrinB1-ΔC cell (see **Figure 41B**) after contact. EphB2-YFP clusters form but vesicular structures only pinch off towards the EphB2-YFP cell. Large clusters remain at the periphery of the HeLa CFP-ephrinB1-ΔC cell. After 40min the HeLa EphB2-YFP cell rounds up.

(Supplementary information on CD-Rom, movie 4) Signaling inactive EphB2 and ephrinB1 initiate cell-cell adhesion sites. HeLa cells were transiently transfected with truncated EphB2-YFP-ΔC and truncated CFP-ephrinB1-ΔC, and then co-cultured before time lapse imaging at 1frame/min (upper part: phase contrast, lower part YFP fluorescence). The movie shows a HeLa EphB2-YFP-ΔC cell approaching a HeLa CFP-ephrinB1-ΔC cell (see **Figure 41C**). The HeLa EphB2-YFP-ΔC cell does not retract its lamellipodia. Cell-cell contact leads to enhanced co-clustering of EphB2-YFP-ΔC and CFP-ephrinB1-ΔC. Prolonged cell-cell contact leads to the formation of large fascicles bearing EphB2-YFP-ΔC and CFP-ephrinB1-ΔC that mediate strong cell to cell adhesion.

(Supplementary information on CD-Rom, movie 5) Reverse endocytosis is sufficient to convert adhesion to detachment. HeLa cells were transiently transfected with truncated EphB2-YFP-ΔC and full length CFP-ephrinB1, and then co-cultured before

time lapse imaging at 1frame/min (upper part: phase contrast, lower part YFP fluorescence). The movie shows a HeLa EphB2-YFP-ΔC cell approaching a HeLa CFP-ephrinB1 cell (see **Figure 41D**). The HeLa EphB2-YFP-ΔC cell does not retract its lamellipodia. Large EphB2-YFP-ΔC clusters form and are taken up by the HeLa CFP-ephrinB1 cell. The HeLa EphB2-YFP-ΔC cell detaches and continues to move. Endocytosis by the HeLa CFP-ephrinB1 cell is sufficient to remove the strong adhesion occurring in a situation when both, the receptor and the ligand are truncated (see **Figure 41C** and **supplementary information on CD-Rom, movie 4**).

7. Discussion

7.1. EphrinB phosphorylation and reverse signaling: Regulation by Src kinases and PTP-BL phosphatase

Early steps in ephrinB reverse signaling involve phosphorylation on tyrosine residues (Holland et al., 1996; Brückner et al., 1997) and interaction with PDZ proteins via its C-terminal tail (Dong et al., 1997; Torres et al., 1998; Brückner et al., 1999; Lin et al., 1999; Lu et al., 2001). At least *in vitro*, PDZ binding may in certain cases also be modulated by phosphorylation of ephrinB C-terminal tyrosine residues (Lin et al., 1999). The work presented in this thesis shows that engagement of ephrinB ligands with soluble EphB receptors led to SFK activation in a variety of cell types like fibroblasts, endothelial cells and primary cortical neurons. This indicates that SFKs are general signal transducers in ephrinB reverse signaling. SFKs bind to the cytoplasmic domain of ephrinBs and are required for its phosphorylation on tyrosine. Functionally, SFKs are required for ephrinB-mediated angiogenic responses in endothelial cells. The tyrosine phosphatase PTP-BL is implicated as a negative regulator of SFK activity and ephrinB phosphorylation. The kinetics of phosphorylation and of SFK and PTP-BL recruitment to complexes of activated ephrinBs suggest the presence of a switch mechanism that allows a shift from phosphotyrosine-dependent signaling to PDZ-dependent signaling.

7.1.1. Mechanisms of SFK activation in ephrin reverse signaling

Structure function analysis revealed insight into the molecular mechanisms how the activity of SFKs is regulated (Thomas and Brugge, 1997): SFKs are composed out of an N-terminal lipid modification motif, followed by an SH3 domain, an SH2 domain, a linker region containing a SH3 binding (P-X-X-P) motif, the kinase domain and a C-terminal regulatory motif. In the inactive state SFKs are in a closed conformation held together by two major intramolecular interactions: The SH3 domain binds to the linker region and the SH2 domain binds to a phosphorylated tyrosine residue in the regulatory C-terminal motif (Y529 in Src) (**Figure 43A**). Active SFKs are in an open conformation

where these inhibitory intramolecular interactions are disrupted. In addition, like many other tyrosine kinases, the kinase domain bears an activation loop (A-loop) containing another regulatory tyrosine residue (Y418 in Src). In the unphosphorylated state the A-loop is folded into the catalytic pocket thereby inhibiting kinase activity. When phosphorylated, the A-loop folds out of the kinase domain, permitting kinase activation (**Figure 43A**) (Kmiecik and Shalloway, 1987). Hallmarks of SFK activation therefore are 1) conformational changes caused by the dephosphorylation at the C-terminal regulatory tyrosine residue. 2) SH3 and SH2 interactions with activated cell surface receptors that compete with the intramolecular interactions and stabilize the active open conformation. 3) Phosphorylation of the A-loop tyrosine. A general scheme for SFK activation downstream of cell surface receptors has been evolved from studies of immune response receptors (IRRs), integrins and RTKs. Initially, receptor clustering or dimerization leads to the recruitment of SFKs. Subsequent associations with phosphorylated tyrosine residues, located in the ITAM (immunoreceptor tyrosine activation motif) motif of IRRs or the juxtamembrane region in RTKs, via the SH2 domain and P-X-X-P motif interactions via the SH3 domain stabilize the active open conformation. Many RTKs and other receptor associated tyrosine kinases can further activate SFKs by direct phosphorylation of the A-loop tyrosine. Tyrosine phosphatases that become activated downstream of the receptors can dephosphorylate the regulatory C-terminal tyrosine residue.

Induction of ephrinB/EphB-Fc complexes led to the rapid co-clustering of Src. The increased focal concentration of SFKs in these clusters may favor autophosphorylation at the A-loop tyrosine by basal kinase activity. Binding of SFKs to ephrinB may promote the active open conformation. The exact binding sites have not been determined but a candidate is a putative P-X-X-P motif within the cytoplasmic domain (**Figure 17**). Subsequent phosphorylation of ephrins may then provide additional binding sites for the SH2 domain promoting further stabilization of the open conformation. The proposed model is illustrated in **Figure 43B**.

Ephrins and Src are co-localized to lipid rafts. This may be a mechanism to ensure colocalization in the plasma membrane. However, raft disruption did not affect ephrinB Src co-clustering. However, basal ephrinB phosphorylation was greatly enhanced and

could be further increased by EphB-Fc stimulation. Lipid rafts are known to harbor a negative feedback loop for SFK activity: The SFK substrate Cbp (Csk binding protein) co-localizes with SFKs in rafts and recruits the negative regulator Csk (C-terminal Src Kinase) in a phosphorylation dependent manner. Subsequently, Csk phosphorylates SFKs at the C-terminal regulatory tyrosine residue leading to their inactivation (Cary and Cooper, 2000). Raft disruption by cholesterol depletion may specifically abolish this negative feedback loop leaving other mechanisms of SFK activation intact. PTP-BL was identified as another negative regulator of SFK activity and its colocalization in lipid rafts was demonstrated in this study. Raft disruption may have also abolished the recruitment of PTP-BL leading to enhanced ephrinB phosphorylation.

GPI-anchored ephrinA ligands were also shown to be recruited to rafts and stimulation with EphA-Fc led to Fyn kinase activation (Davy et al., 1999). Moreover, SFKs are activated downstream of Eph receptors (Ellis et al., 1996), therefore suggesting, together with our results, that SFKs may be important mediators of Eph/ephrin bidirectional signaling.
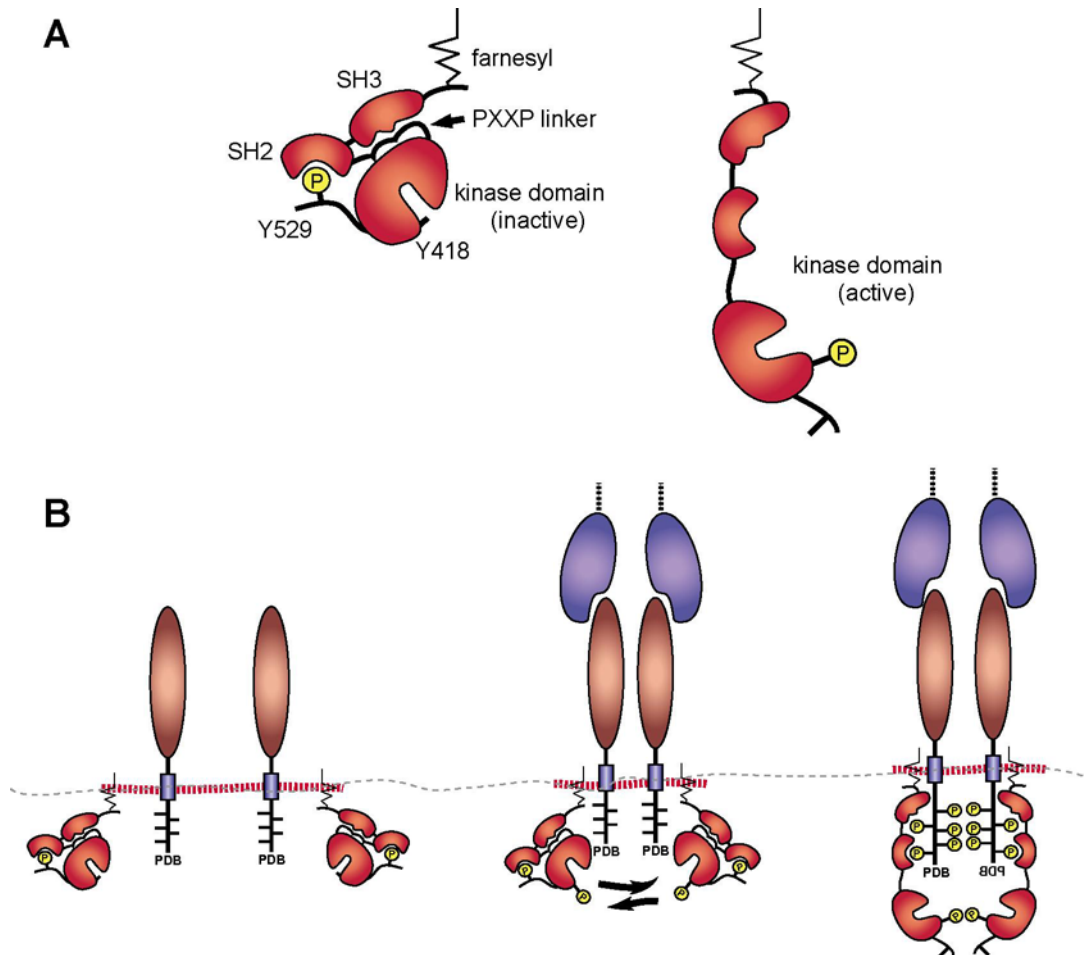
Figure 43. Model for SFK activation downstream of ephrinB ligands. (**A**) Domain structure of SFK shown in its inactive conformation (left). Intramolecular interactions between the SH2 domain and the C-terminal regulatory tyrosine residue (Y529in Src) and between the SH3 domain and the P-X-X-P linker region keep SFKs in this conformation. Another regulative A-loop tyrosine residue in the kinase domain (Y418 in Src) blocks the catalytic activity when in its unphosphorylated state. Activity of SFKs requires an open conformation (right). After phosphorylation the A-loop folds out of the catalytic pocket thereby permitting kinase activity.

(**B, left panel**) Unbound ephrinB ligands and inactive SFKs co-localize in lipid raft subdomains (red stippled line) at the plasma membrane. (**B, middle panel**) Binding of EphB receptors causes ephrinB ligands to cluster at the plasma membrane shown as a heterotetramer. Co-clustering of SFKs favors trans-autophosphorylation of the A-loop tyrosine by basal kinase activity. (**B, right panel**) Active SFKs phosphorylate ephrinB on tyrosine residues. SH2 and SH3 interactions between SFKs and ephrinBs promote the open active conformation. Although lipid rafts do not seem to be important for co-clustering and activation they may recruit other regulatory proteins (not shown).

7.1.2. *In vivo* phosphorylation sites in ephrinB ligands

The *in vivo* phosphorylated tyrosines in ephrinB ligands involved in the process of reverse signaling are currently unknown. In a recent study (Kalo et al., 2001), the authors have identified three tyrosines of ephrinB1 as major phosphorylation sites in transfected 293 cells stimulated with soluble EphB2-Fc and the same residues are *in vivo* phosphorylated in the embryonic retina. The work presented in this thesis confirmed with phosphospecific anti-ephrinB antibodies on lysates of cultured cells the phosphorylation of the tyrosines at positions –18 and/or –23 from the C-terminus.

7.1.3. Regulation of endothelial cell migration by ephrinB tyrosine phosphorylation and SFKs

A recent study demonstrates that the cytoplasmic domain of ephrinB2 is required for angiogenic remodeling *in vivo* (Adams et al., 2001), suggesting that ephrinB2 reverse signaling is crucial for endothelial cell communication. This work shows that SFKs are required for the *in vitro* angiogenic response induced by soluble EphB4-Fc. The data suggest that EphB4-Fc binding to endogenous ephrinB2 activates SFKs, which phosphorylate the cytoplasmic domain of ephrinB2. Further, EphB4-mediated co-clustering of ephrins and SFKs may engage SFKs with other substrates, which mediate sprouting independently of or in concert with the tyrosine-phosphorylated cytoplasmic domain of ephrinB.

The requirement of SFK activity is specific for the angiogenic response induced by EphB4-Fc. The responses of endothelial cells to other potent angiogenic factors such as the chemokine SDF-1, via its receptor CXCR4, and Ang-1, via its receptor Tie-2, were not affected by inhibition of SFKs in the assay. This suggests that distinct downstream signaling cascades are involved in the angiogenic process regulated by these different molecules. In addition to their established functions in cell proliferation, adhesion, and differentiation, SFKs have recently been shown to play important roles in angiogenesis. Dominant interfering mutants of Src blocked VEGF- but not bFGF-induced angiogenesis

in chick embryos and studies in mutant mice showed that SFKs are required for VEGF-induced blood vessel permeability (Eliceiri et al., 1999).

7.1.4. Are SFKs required for ephrinB reverse signaling *in vivo*?

Three SFKs, namely Src, Fyn, and Yes, are expressed in blood vessels (Bull et al., 1994; Kiefer et al., 1994) and in HUAECs (data not shown) and Src and Fyn are highly expressed in the developing nervous system (Maness et al., 1988). SFKs are functionally redundant in many systems. Whereas mice deficient in a single SFK gene displayed no severe phenotypes (Lowell and Soriano, 1996), mice with targeted mutations for all three kinases, Src, Fyn and Yes, showed severe developmental defects and lethality at embryonic day E9.5 (Klinghoffer et al., 1999), indicating that SFKs play crucial roles in early mammalian embryonic development. Conversely, single mutant mice lacking ephrinB2 suffer from early (E10.5) embryonic lethality (Wang et al., 1998; Adams et al., 1999). Therefore, genetic evidence for a requirement of SFKs in vascular development downstream of ephrinB ligands will require sophisticated conditional mutagenesis of ephrinB2, combined with multiple mutant alleles of Src, Fyn and Yes to overcome their functional redundancy.

7.1.5. The role of other kinases in ephrinB reverse signaling

SFKs are probably not the only kinases involved in ephrinB phosphorylation. Serum stimulation of endothelial cells also led to robust ephrin phosphorylation which was not sensitive to the Src inhibitor PP2. The identity of the serum-activated ephrin kinase is unclear. EphrinB1 has been shown to interact and be phosphorylated by FGF receptors when co-expressed in Xenopus embryos (Chong et al., 2000). Therefore FGF receptors in endothelial cells could be a candidate for the serum activated kinase in this study. Moreover, phosphoamino acid analysis of *in vitro* phosphorylated ephrinB1 revealed the presence of a serine/threonine kinase capable to phosphorylate ephrinB on serine residues. The functional consequences of serine phosphorylation will have to be further explored. It is possible that the sequences surrounding phosphoserine residues could

serve as docking sites for cytoplasmic effectors carrying interaction modules similar to 14-3-3 proteins (Pawson and Scott, 1997). Moreover, serine phosphorylation could modulate PDZ binding to ephrinB (see below).

7.1.6. Co-expression of PTP-BL with ephrinB ligands

The findings of this study implicate the PDZ-domain containing PTPase PTP-BL as an important component of the signaling apparatus downstream of ephrinB ligands. The co-expression studies in growth cones together with previously published in situ data (Thomas et al., 1998; Brückner et al., 1999) support the idea, that PTP-BL and ephrinB ligands act in concert in guiding peripheral axons during development. PTP-BL is targeted to membrane rafts in embryonic neurons, and interacts with the cytoplasmic domain of ephrinB1.

In cells stably expressing physiological levels of ephrinB1, the interaction between endogenous PTP-BL and ephrinB1 via its PDZ target site is not constitutive, but rather induced by EphB2 receptor engagement.

7.1.7. Regulated ephrinB-PDZ interactions with PTP-BL and GRIP2

Regulation of PDZ interactions is unusual and suggests functional relevance. The co-clustering of PTP-BL and ephrinB happens with delayed kinetics, in contrast to the rapid co-clustering of ephrinB and Src that occurs only two minutes after stimulation with the receptor. So far there is no indication that tyrosine phosphorylation within the PDZ binding motif of EphrinBs can positively promote the binding to PDZ domains. By contrast *in vitro* studies suggested that tyrosine phosphorylation in ephrinB may negatively regulate binding to at least some PDZ domains, as shown for the multiple PDZ-domain protein syntenin (Lin et al., 1999). In the same study, binding to the PDZ domain 5 of PTP-BL was not affected by phosphorylation. Thus, the mechanism of how PTP-BL becomes recruited to ephrinB ligands remains to be identified. It is possible that PTP-BL meets activated ephrinB ligands in endocytic compartments (see below).

Ephrin interacts with the multiple PDZ-domain containing protein GRIP2 also in a regulated manner. By contrast to PTP-BL this interaction occurs with rapid kinetics. However, it is independent of tyrosine phosphorylation. Mutation of a conserved serine residue close to the PDZ binding motif at position -9 abolished this interaction. EphrinB ligands bind to the domain PDZ6 in GRIP. Interestingly liprin-α, another binding partner of GRIP PDZ6 depends on a serine residue at position -9 in liprin-α (Wyszynski et al., 2002). This indicates a general function of this residue in PDZ binding. Serine phosphorylation appears to regulate various PDZ interactions. Phosphorylation within the PDZ binding motif of the glutamate receptor 2 (GluR2) subunit of AMPA receptors releases binding of GRIP molecules, while leaving binding to another PDZ-domain protein, PICK1, unaffected (Chung et al., 2000). In another described case phosphorylation of the β2-adrenergic receptor enhances the interaction with the PDZ protein EBP50 (Cao et al., 1999). However, in these two cases the phosphorylation site is located directly in the PDZ binding motif at position -3. The results of the presented study support the hypothesis that ephrinB molecules may positively regulate PDZ binding by phosphorylation of serine at position -9. Phosphorylation would be achieved by a serine kinase downstream of ephrinB reverse signaling. A serine/threonine kinase in complex with GRIP and ephrinB has been reported (Brückner et al., 1999). So far the presented data only indicate the requirement of serine -9 for ephrinB binding to GRIP. It would be of high interest to test if serine -9 is a major phosphorylation site *in vivo* and that phosphorylation of this residue indeed directly increases the affinity of the ephrinB cytoplasmic tail to PDZ domains.

7.1.8. PTP-BL is a negative regulator of ephrinB tyrosine phosphorylation

In vitro phosphatase assays on ephrinB immunoprecipitated from mouse embryos showed that PTP-BL is able to dephosphorylate the native phosphorylation sites of ephrinB ligands. By co-expression studies in HeLa cells it could be demonstrated that PTP-BL interacts with and dephosphorylates ephrinB in living cells. We have also shown that *in vitro* PTP-BL dephosphorylates Src at Y418, the autophosphorylation site required for Src activation, but not at Y529, the negative regulatory site phosphorylated by Csk.

Together with the known role of PTP-BL as Src antagonizer in a functional yeast growth assay (Superti-Furga et al., 1996), the presented data suggest that PTP-BL is a negative regulator of Src downstream of ephrinB ligands.

7.1.9. A 'switch mechanism' shifts ephrinB phosphotyrosine dependent signaling to PDZ-dependent signaling

The studies of this thesis led to the proposal of a 'switch model' of ephrinB reverse signaling: EphrinB engagement with its EphB receptors induces the rapid co-clustering of ephrinB and SFKs, causing SFK activation and ephrinB phosphorylation. Both active SFKs and phosphorylated ephrinB activate signaling pathways, either independently or in concert with each other, involving phosphotyrosine/SH2 interactions. With delayed kinetics, ephrinB clusters recruit PTP-BL, which dephosphorylates both Src and ephrinB, effectively turning off signaling by ephrinB and Src via phosphotyrosine. The recruitment of PTP-BL to ephrinB may not terminate ephrinB signaling completely, but rather shifts signaling from phosphotyrosine-dependent to PDZ-domain-dependent signaling. The switch model is illustrated in **Figure 44**.
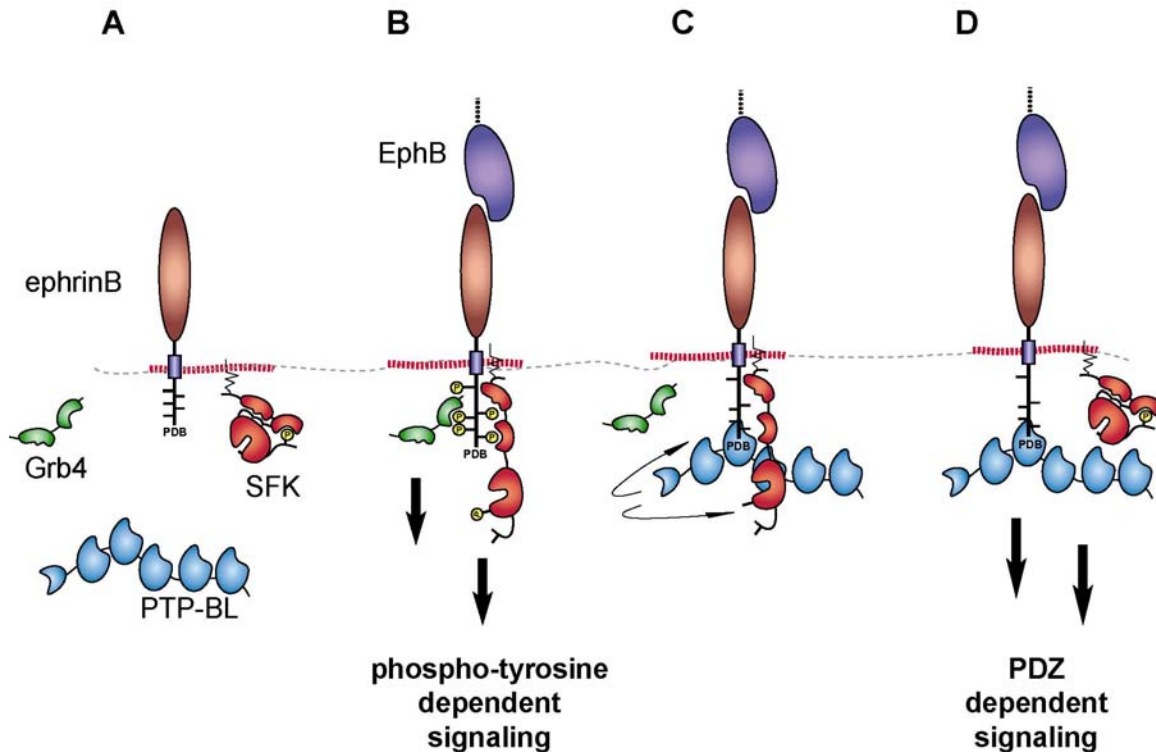
Figure 44. Switch model for ephrinB reverse signaling. (**A**) Signaling is switched off, when ephrinB does not encounter its receptor. (**B**) Engagement with EphB receptors induces rapid co-clustering and activation of SFKs. Subsequent tyrosine phosphorylation on ephrinB provides docking sites for SH2 adaptors like Grb4. SFKs and Grb4 mediate phosphotyrosine dependent signaling. (**C**) PTP-BL becomes recruited to the complex with delayed kinetics and dephosphorylates ephrinB and SFKs thereby attenuating phosphotyrosine dependent signaling. (**D**) PDZ interactions with ephrinB are long lasting leading to prolonged PDZ-dependent signaling.

7.1.10. Phosphotyrosine and PDZ-dependent signaling

Both phosphorylated ephrins and SFKs may activate parallel or converging signaling pathways leading to actin cytoskeleton rearrangements. Signaling via the SH2 adaptor Grb4 is described in detail in chapter 5.3.7.2. Moreover, it is also likely that other SH2 domain containing adaptors binding to phosphorylated ephrinB still remain to be identified. Active SFKs can elicit a variety of intracellular responses with effects on the cytoskeleton. SFKs phosphorylate an enormous variety of substrates including proteins involved in cell adhesion and cytoskeletal dynamics (Thomas and Brugge, 1997). For example, SFKs are known to regulate cell morphology, adhesion and migration by association with and phosphorylation of focal adhesion kinase (FAK) and p190 RhoGAP

(Brouns et al., 2001). Recent data by Cowan and Henkemeyer (Cowan and Henkemeyer, 2001) suggest FAK as a downstream phosphorylation target of ephrinB reverse signaling. Interestingly, mice deficient in p190 RhoGAP exhibit lack of the anterior commissure (Brouns et al., 2001), a phenotype associated with lack of ephrinB reverse signaling in EphB2$^{-/-}$ mice (Henkemeyer et al., 1996). It would be very interesting to test, if there is a functional link between these molecules in ephrinB reverse signaling.

A first example of ephrinB signaling via PDZ domain proteins was shown for cerebellar granule cells, which require the PDZ-RGS3 protein to respond to chemoattractants signaling through heterotrimeric G proteins (Lu et al., 2001) (See also chapter 5.3.7.2.).

PTP-BL contains five PDZ domains, which interact with other cytoplasmic proteins including the GTPase-activating protein PARG with specificity for Rho, and the PKC related kinase PRK2 an effector of both Rho and Rac (Saras et al., 1997; Vincent and Settleman, 1997; Gross et al., 2001). Rho family GTPases are important regulators of actin cytoskeleton dynamics in response to external stimuli and ephrinB-mediated axon guidance is thought to involve rapid changes in actin filament organization. The findings that PTP-BL and ephrinB ligands co-localize in neuronal growth cones suggest a role for these proteins in regulating the cytoskeleton during neurite outgrowth. Thus, it will be very interesting for future studies to analyze the role of the Src/p190 RhoGAP and the PTP-BL/PRK2, PARG pathways downstream of ephrinB ligands and how these proteins contribute to both ephrinB "phosphotyrosine dependent" and "PDZ-domain dependent" signaling linked to rearrangements of the actin cytoskeleton.

7.2. EphB/ephrinB bidirectional endocytosis terminates adhesion allowing contact mediated repulsion

This study addressed the role of endocytosis in ephrinB-EphB-mediated cell-cell repulsion. Four important observations were made: 1) EphrinB-EphB endocytosis can be bidirectional and the relative contribution of reverse versus forward endocytosis may largely depend on the cellular context. 2) Endocytosis is regulated by mechanisms that engage the cytoplasmic domains of EphBs and ephrinBs. 3) Endocytosis involves the entire ligand-receptor complex,

i.e. one of the interacting partners is transcytosed in full length from one cell to its neighbor. 4) Block of endocytosis of either ephrinB or EphB changes cell repulsion behavior and axon detachment. These findings provide insight into a mechanism of how cell-cell contact induced high affinity interactions between two transmembrane molecules can result in cell repulsion responses leading to detachment and withdrawal.

7.2.1. Trans-endocytosis of membrane attached proteins

Endocytosis of protein complexes involving the intercellular (trans-) interaction of two transmembrane proteins is unusual and so far only documented for three receptor systems (Sorkin and Von Zastrow, 2002). In two described cases, endocytosis of transmembrane proteins was shown to be unidirectional. In *Drosophila*, the seven transmembrane ligand, Boss, is internalized into the R7 photo-receptor precursor cell upon trans-interaction with the sevenless tyrosine kinase receptor. The entire Boss protein enters the sev-expressing cell and endocytosis occurs only in the forward direction (Cagan et al., 1992). The receptor patched-1 (Ptc-1) is able to retrieve membrane-bound forms of sonic hedgehog (Shh) from adjacent cells, a process that is unidirectional and may be linked to Shh signal transduction (Incardona et al., 2000). In the third described case, endocytosis is bidirectional, but involves proteolytic cleavage of one of the proteins: Notch receptor binding to its membrane-anchored ligand, Delta, triggers proteolytic shedding of the Notch ectodomain and endocytosis of the Notch-Delta protein complex into the Delta-expressing cell. Notch signaling in the Notch-expressing cell occurs after a second cleavage event that releases the Notch cytoplasmic domain that translocates to the nucleus (Parks et al., 2000).

7.2.2. Bidirectional endocytosis of Eph receptors and ephrin ligands: A tug of war.

Endocytosis of ephrinB-EphB complexes can occur in a bidirectional fashion. The direction of endocytosis may depend on several parameters including ligand/receptor protein levels, experimental design and cellular context. NIH3T3 and HeLa cells ectopically expressing

EphB and ephrinB are capable of mediating ephrinB reverse and EphB forward endocytosis, which was further confirmed by time-lapse imaging of random encounters of mixed cultures of ephrinB and EphB expressing HeLa cells (**Figure 41** and supplementary information on CD-Rom, **movie 2**). In a parallel study the authors showed that Swiss 3T3 and primary human endothelial (HUVECs) cells, when engaging in ephrinB-EphB trans-interactions primarily undergo forward endocytosis (Marston et al., 2003). However, in that case the experimental setup was different. Endocytosis and repulsion were studied several hours after microinjection of cells with expression constructs. Prolonged cell-cell contact may favor forward endocytosis by receptor expressing cells as was also observed with NIH3T3 cells (**Figure 38**), and therefore could also explain why reverse endocytosis was not observed in the accompanying study. In contrast, very immature primary neurons from mouse forebrain when engaged in growth cone-cell contact show little forward, but rather pronounced ephrinB reverse endocytosis (**Figures 36**, **42** and data not shown). Similar results were obtained with primary neurons from Xenopus retina when stimulated with soluble Fc fusion proteins (Mann, in press)

Other parameters that influence the direction of endocytosis are cell spreading and EphB forward signaling. One of the experimental setups in the presented work involved the stimulation with cells that had been removed from their substrate and therefore were deprived of a functional cytoskeleton. In this case, endocytosis was predominant in the pre-plated recipient cells independently whether or not they expressed ephrinB1 or EphB2. It is possible that the recipient cells have an advantage in their organization of endocytic and membrane trafficking machinery over the freshly seeded stimulator cells since the endocytic machinery might be linked to the actin cytoskeleton (Qualmann and Kessels, 2002). After the stimulator cells had spread out, endocytosis was favored in the EphB2 forward direction suggesting that in this tug-of-war EphB2 signaling is dominant over ephrinB signaling, at least in fibroblasts. Weakening the receptor's ability to signal by C-terminal truncation or blocking its kinase activity shifted endocytosis towards ephrinB reverse signaling. On the ligand side, the cytoplasmic determinants that drive reverse endocytosis are not yet known. Neither signaling via tyrosine residues nor the PDZ domain seems to be required to mediate endocytosis. The tug-of-war between ephrinB and EphB molecules is illustrated in **Figure 45**.
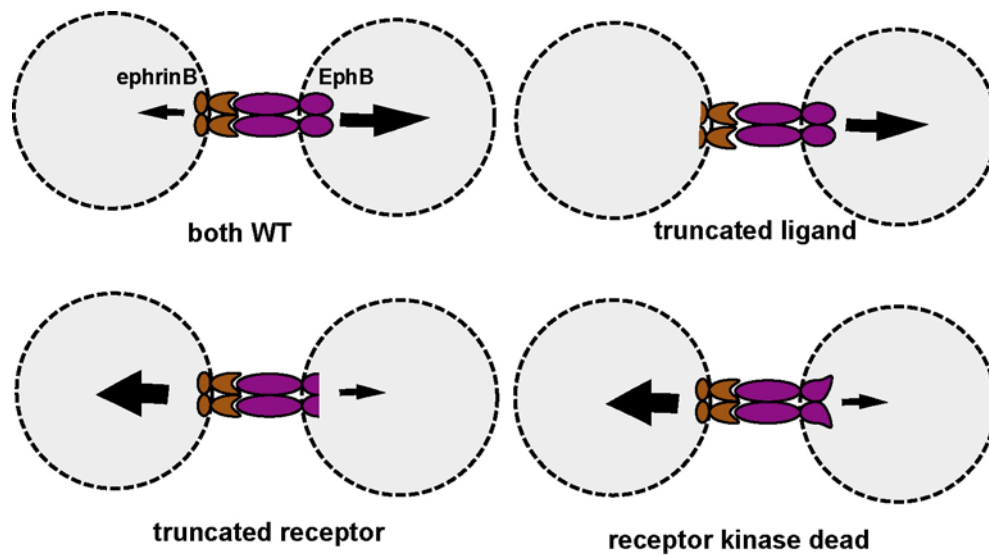
Figure 45. EphB ephrinB bidirectional endocytosis: A Tug of war. Contact between ephrinB1 and EphB2 cells leads to bidirectional endocytosis (upper left panel). Forward endocytosis into the EphB2 cells is predominant when both ligand and receptor are wild-type (upper left panel). C-terminal truncation of the ligand completely abolishes endocytosis in reverse direction but leaving forward endocytosis intact (upper right panel). C-terminal truncation or inactivation of the kinase activity of the receptor shifts the predominant direction of endocytosis into the ligand cell (lower panels).

7.2.3. Endocytosis of full length transmembrane Eph/ephrin complexes

Independently of the cell type and the specific cellular response, the results of this study have shown that the endocytosed complex contains full length proteins indicating that one of the partners had to be transcytosed from one cell to its neighbor. In a parallel study the authors could demonstrate the concomitant transfer of a GFP marker hooked up to the inner leaflet of the plasma membrane. This suggests that internalization of the ephrinB-EphB complex includes pieces of the plasma membrane (Marston et al., 2003). No colocalization of ephrinB-EphB clusters with known markers of endocytic pathways including clathrin and caveolin and the early endosomal marker EEA1 could be seen (data not shown). Although clathrin mediated endocytosis has been shown to be capable to transcytose a transmembrane ligand in the case of boss/sevenless (Chang et al., 2002) it is unlikely to take place in Eph/ephrin bidirectional endocytosis. Clathrin coated pits have an average diameter of approximately 120nm. Caveolin and other clathrin and caveolin independent mechanisms even involve smaller membrane invaginations (Conner and Schmid, 2003). By contrast

surface and intracellular clusters of Eph/ephrin complexes appear at variant sizes of up to 1μm. Endocytosis is preceded by the formation of large membrane protrusions. Phagocytosis and macropinocytosis can lead to the invagination of particles, even of much larger size than 1μm, and involves actin driven membrane protrusions for initial engulfment. Actin protrusions required activity of the Rho family GTPases Rac and Cdc42 (Chimini and Chavrier, 2000; Nichols and Lippincott-Schwartz, 2001). The study of Marston et al. demonstrates the involvement of Rac in EphB mediated forward endocytosis. Thus, the underlying mechanism of Eph/ephrin endocytosis may resemble phagocytosis or macropinocytosis. Endocytosis of a transmembrane protein including plasma membrane may ultimately result in the formation of multivesicular bodies (**Figure 46**).
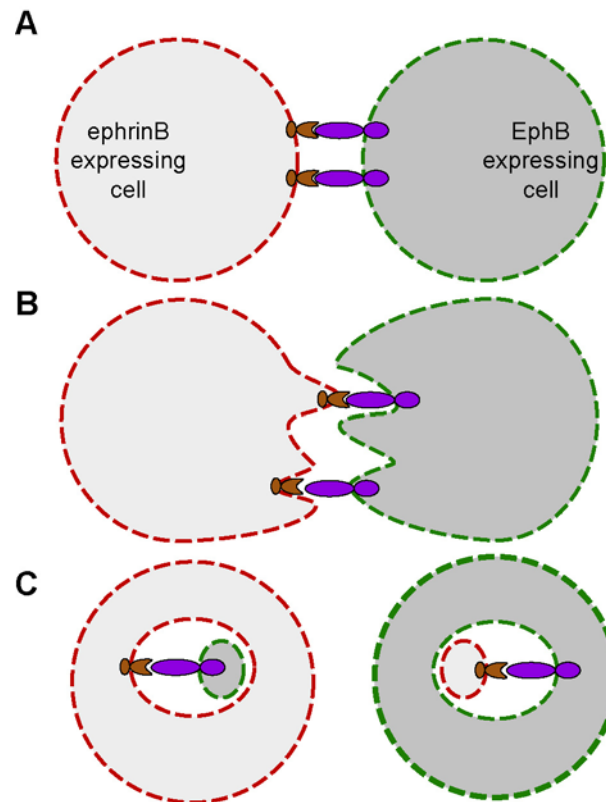
Figure 46. Model for bidirectional endocytosis of transmembrane receptor ligand complexes.
(**A**) Contact between ephrinB (left) and EphB (right) expressing cells. (**B**) EphrinB reverse and EphB forward signaling leads to clustering in membrane protrusions followed by the invaginations of receptor/ligand complexes. (**C**) Entire transmembrane complexes are endocytosed either into the EphB or the ephrinB cell, including pieces of plasma membrane, leading to the formation of multivesicular bodies.

7.2.4. Endocytosis mediated by ephrinA reverse signaling

Bidirectional endocytosis is not unique to the B-class of Eph receptors and their ligands, as this study demonstrates for ephrinA2 and EphA4 in NIH3T3 cells. Endocytosis of ephrinA2 not only occurred into the EphA4 cells but also into the ephrinA2 cells, despite the fact that ephrinA2 lacks a cytoplasmic domain. EphrinA ligands, however, can signal in reverse by yet poorly understood mechanisms (Davy et al., 1999; Davy and Robbins, 2000; Huai and Drescher, 2001). Apparently these mechanisms also lead to endocytosis of EphA receptors. Clusters of endocytosed ephrinA2 in part lack positive staining for EphA4 receptor. EphA4 may become rapidly degraded or recycled after endocytosis.

7.2.5. Endocytosis regulates EphB receptor signaling

In HeLa cells EphB2 receptor forward signaling induces forward endocytosis of EphB2/ephrinB1 complexes and in addition a lamellipodial retraction response, whereas ephrinB1 reverse signaling only mediates reverse endocytosis (summarized in **Figure 47**). The absence of reverse endocytosis causes a gain-of-function phenotype, i.e. enhancement of repulsion by EphB receptor forward signaling. Instead of initiating only a transient withdrawal of lamellipodia, the EphB2 cells deadhere and round up from the substratum. It is likely that persistent ephrinB clusters on the surface of the ephrinB-positive cell lead to enhanced activation of EphB2 receptors on the neighboring cell. EphB2 receptors may continue to signal after endocytosis as was shown for internalized EGF and NGF (TrkA) receptors (Burke et al., 2001; Barker et al., 2002). Consistent with this idea, we observed that internal clusters containing EphB2 stain positive for phosphotyrosine (data not shown).
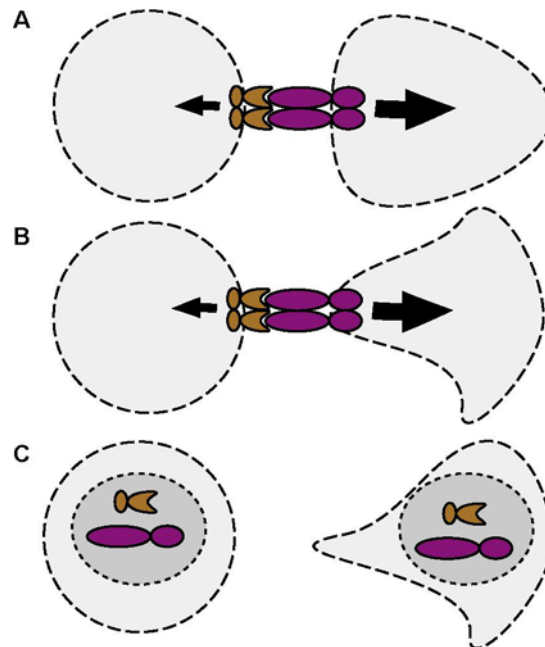
Figure 47. Cellular responses of EphB/ephrinB signaling in HeLa cells. (A) EphrinB cell (left) in contact with a migrating EphB cell (right). Cell-cell contact induces clustering and bidirectional signaling into both cells (arrows). **(B)** Signaling by EphB triggers a retraction response of the EphB cell. **(C)** Removal of receptor/ligand complexes by either the EphB or ephrinB endocytosis is required to allow detachment. Bidirectional endocytosis is required for proper attenuation of EphB receptor signaling.

7.2.6. A physical contribution of endocytosis to lamellipodial retraction and growth cone collapse?

The rapid retraction of lamellipodia and collapse of growth cones may physically require the concomitant endocytosis and reorganization of plasma membrane (Fournier et al., 2000; Jurney et al., 2002). What are the relative contributions to the retraction response of endocytosis and other effectors of Eph signaling, e.g. rearrangements of the actin cytoskeleton? Is signaling to the cytoskeleton sufficient for cell retraction or must it act in concert with endocytosis? Endocytosis alone cannot be sufficient to mediate cellular repulsion, because HeLa-ephrinB1 cells endocytose efficiently but do not retract after contact with EphB2 cells. On the other hand it is unlikely that cytoskeletal rearrangements alone lead to such dramatic changes in cell shape within minutes. Detailed knowledge about the

molecular mechanisms of how Ephs/ephrins regulate their internalization will provide tools to specifically interfere with endocytosis while leaving other signaling mechanisms intact.

7.2.7. Contact mediated repulsion requires mechanisms that permit detachment

A recent study reported that ephrinA ligands are recognized and cleaved by ADAM-type metalloproteinases following binding of ephrinA by clustered EphA receptors (Hattori et al., 2000). Growth cones of hippocampal neurons collapsed and neurites withdrew after contact with ephrinA2 expressing cells. When the cells expressed a mutated uncleavable form of ephrinA2, growth cones still collapsed but withdrawal was greatly delayed. These studies demonstrated that contact-repulsion requires mechanisms that allow detachment. In the case of EphA/ephrinA mediated growth cone guidance regulated ectodomain shedding provides an efficient way to overcome adhesion (**Figure 48**). Metalloproteinase cleavage of endogenous ephrinB ligands is induced by phorbol ester treatment, a stimulus that promotes ectodomain shedding of a variety of transmembrane proteins. EphrinB cleavage by EphB receptor engagement was, however, very inefficient in primary cells and sometimes not detectable (G.A. Wilkinson, R.K., unpublished). The experiments presented in this thesis cannot exclude that ephrinB ligands at least in part become cleaved after contact between ephrinB- and EphB-cells. However, the demonstration of full length proteins in the internalized ephrinB-EphB complexes suggests that a major fraction of these proteins stays intact during endocytosis. In the experimental setups used in this work ephrinB cleavage may have only a minor if any contribution in terminating cell adhesion. Surprisingly, preliminary data on ephrinAs suggest that they also trigger endocytosis. It is possible that proteolysis and endocytosis play parallel roles in EphA/ephrinA-mediated cell-cell communication.
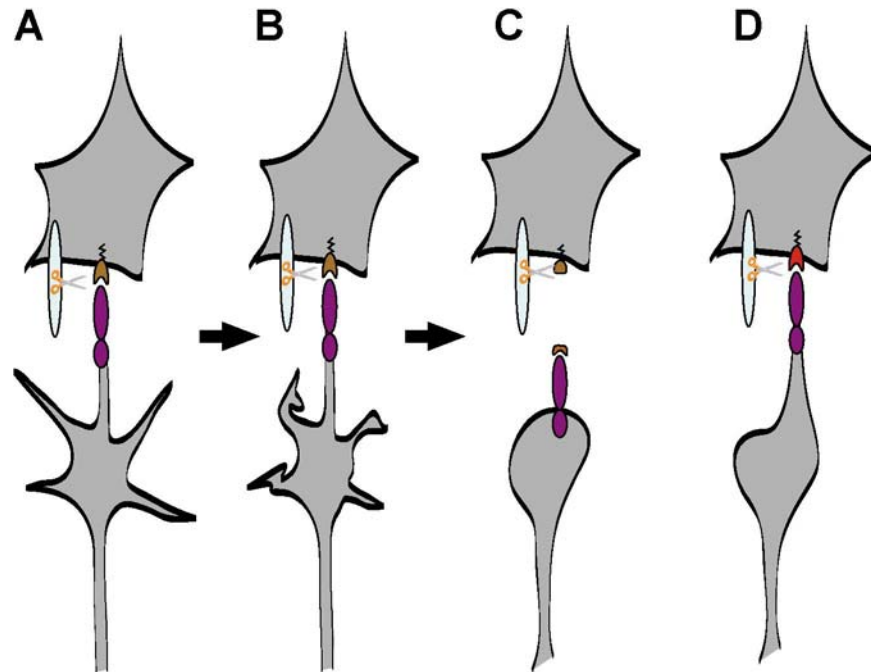
Figure 48. Regulated ectodomain shedding of ephrinA ligands permits neurite withdrawal. (**A**) Growth cones expressing EphA receptor contacting an intermediate target cell that expresses ephrinA ligand in complex with an ADAM-type metalloprotease. (**B**) EphA forward signaling induces growth cone collapse. (**C**) During collapse EphA binding activates the metalloprotease that cleaves the ectodomain of ephrinA. Adhesion between growth cone and intermediate target cell is abolished permitting withdrawal of the growth cone. (**D**) When the intermediate target cell expresses a mutant uncleavable form of ephrinA growth cone collapse still can occur but adhesion between EphA and ephrinA delays withdrawal.

Interfering with repulsion and bidirectional endocytosis by C-terminal truncations on both sites results in a remarkable abnormal adhesion between the cells (**Figure 41C**; supplementary information on CD-Rom, **movie 4**), that could be explained by the high affinity between receptor and ligand. Unidirectional reverse endocytosis alone efficiently switches adhesion to detachment by the removal of Eph/ephrin complexes from the surface (**Figure 41D**; supplementary information on CD-Rom, **movie 5**). In the case of reverse signaling mediated growth cone collapse in cortical neurons, however, detachment occurs in a delayed fashion when endocytosis is unidirectional, and thereby less efficient. Thus, endocytosis provides a powerful mechanism to permit cell-cell repulsion and withdrawal initiated by the intercellular trans-interaction of two transmembrane (TM) contact repellents (**Figure 49**). Similar mechanisms might be relevant in other guidance systems, such like TM semaphorins acting through neuropilins and plexins.
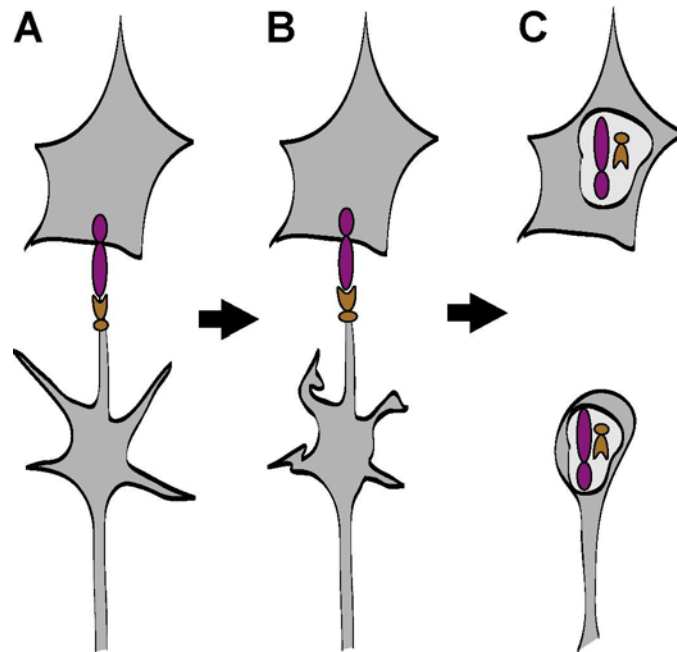
Figure 49. Growth cone collapse mediated by ephrinB reverse signaling requires bidirectional endocytosis. (**A**) Growth cone expressing ephrinB ligand in contact with an intermediate target cell that expresses EphB receptor. (**B**) EphrinB reverse signaling induces growth cone collapse. (**C**) Bidirectional endocytosis removes high affinity receptor ligand complexes allowing deadhesion and neurite withdrawal.

7.3. Concluding remarks

In conclusion, the work presented in this thesis demonstrates that cell-cell communication mediated by Eph/ephrins can result in bidirectional endocytosis of the Eph/ephrin ligand-receptor complex. In addition to previously described ligand ectodomain shedding (Hattori et al., 2000), endocytosis is shown to act as an additional mechanism for cell and axon detachment during repulsive guidance. Both mechanisms may be relevant for other repulsive guidance systems.

It would be very interesting for future studies, to track the intracellular fate of Eph receptors and ephrin ligands after endocytosis. As shown for other surface receptors, forward and reverse signaling by EphBs and ephrinBs might continue from intracellular compartments. Such trans-endocytosis would ultimately allow Eph receptors to signal within a cell, which

originally only expressed its ligand. Since endocytosis occurs bidirectionally, the same consideration is valid for ephrinB ligand reverse signaling.

Attenuation of forward and reverse signaling may occur from endocytic compartments. This thesis work shows that PTP-BL is a negative regulator of ephrinB reverse signaling. Kinetic studies of Src and PTP-BL recruitment suggest that colocalization occurs after endocytosis. Intracellular membrane traffic could explain the delayed recruitment of PTP-BL. Endocytosed clusters of activated ephrinB and Src may be targeted to intracellular organelles where PTP-BL is constitutively located. Once PTP-BL meets its substrates it can inactivate phosphotyrosine dependent signaling. This would have the consequence that the suggested phase of PDZ dependent signaling would occur from these intracellular organelles.

Similar mechanisms of signal attenuation have been demonstrated for activated EGFR. After endocytosis, EGFR is sorted to the surface of the endoplasmic reticulum where it becomes dephosphorylated by the phosphatase PTP1B (Haj et al., 2002). This could be relevant for other RTKs including Eph receptors.

8. Materials and Methods

8.1. Materials

8.1.1. Buffers and solutions

8.1.1.1. Media and antibiotics for bacterial culture

LB (Luria-Bertani-) media	10g Bacto-Trypton
	5g Yeast extract
	5g NaCl
	add H_2O to 1l, adjust pH to 7.5
LB plates	supplement with 15g/l agar

Antibiotics	diluted 1:1000
Ampicillin	Stock 100mg/ml inH_2O
Kanamycinsulfate	Stock 50mg/l in H_2O

8.1.2. Media and supplements for tissue culture

DMEM	Dulbecco's Modified Eagle medium (Invitrogen)
DMEM CS G418	DMEM, 10% Calf serum, 0.292mg/ml L-glutamine, 100U/ml penicillin, 100μg/ml streptomycin, 350μg/ml geneticin sulfate (G418).
DMEM CS Hygro	DMEM, 10%Calf serum, 0.292mg/ml L-glutamine, 100U/ml penicillin, 100μg/ml streptomycin, 400μg/ml hygromycin.

DMEM FBS G418	DMEM, 10% Foetal bovine serum, 0.292mg/ml L-Glutamine, 100U/ml Penicillin, 100µg/ml Streptomycin, 350µg/ml geneticin sulfate (G418).
DMEM CS Hygro G418	DMEM, 10%Calf serum, 0.292mg/ml L-glutamine, 100U/ml penicillin, 100µg/ml streptomycin, 400µg/ml hygromycin, 350µg/ml geneticin sulfate (G418).
DMEM CS ZeoR Dox	DMEM, 10% CS, 0.292mg/ml L-glutamine, 100U/ml penicillin, 100µg/ml streptomycin, 400µg/ml zeosin, 1mM L-histidinol dihydrochlorid, 5µg/ml doxycycline

8.1.2.2. Media and supplements for primary culture of neurons

Neurobasal medium/B27	500ml of neurobasal medium (Invitrogen) were supplemented with 10ml of B27 supplement (Invitrogen).
MEM	Minimal essential medium (Invitrogen)
N-MEM	MEM, 0.6% glucose, 110µg/ml pyruvic acid, 0.292mg/ml L-glutamine
N2 supplement	MEM containing: Insulin (500µg/l), human transferrin (10mg/l), progesterone (0.63µg/l), putrescin (1611µg/l), selenit (0.52µg/l).
N2-MEM	N-MEM, 10%N2, 0.1g/ml chicken egg albumin.
HS-MEM	MEM, 10% HS, 0.6% glucose, 0.292mg/ml L-glutamine.
Borate Buffer	1.24g boric acid, 1.9g Borax ad 400ml H_2O, pH8.5.
HBSS	500ml of Hank's buffered salt solution (Invitrogen) were supplemented to final concentrations of 100U/ml penicillin, 100µg/ml streptomycin and with 3.5ml 1M Hepes (pH7.2) and 3.5ml 1M $MgCl_2$.

8.1.2.3. Media and supplements for endothelial cell culture

EGM	Endothelial cell growth medium (Clonetics) was supplemented with bovine pituitary brain extract (Clonetics) and 1ng/ml bFGF (Sigma)

8.1.2.4. Solutions for Biochemistry

Laemmli stacking gel (10ml):	1.3ml	30% w/v acrylamid/bis 25:1
	2.6ml	0.5M Tris HCl pH6.8, 0.4% SDS
	6.1ml	H_2O
	100µl	10% APS
	10µl	TEMED
10% Laemmli separating gel (10ml):	3.3ml	30% w/v acrylamid/bis 25:1
	2.6ml	1.5M Tris HCl pH8.8, 0.4% SDS
	4ml	H_2O
	50µl	10% APS
	5µl	TEMED
5x Laemmli electrophoresis buffer (10l):	154.5g Tris base 721g glycine 50g SDS	
10x Transfer buffer (2.5l):	60.5g tris base 281.5g glycine 25g SDS	
Anderson stacking gel buffer (7.45ml):	1.25ml	30% w/v acrylamide
	1ml	1% bisacrylamide
	0.9ml	1M Tris HCl pH6.8
	4.3ml	H_2O
	50µl	10% APS
	5µl	TEMED
15% Anderson separating gel (20ml):	10ml	30% w/v acrylamide
	1.7ml	1% bisacrylamide
	5ml	1.5M Tris HCl pH8.8
	3.15ml	H_2O
	200µl	10% APS
	20µl	TEMED
5x Anderson electrophoresis buffer (2l):	60g Tris Base 288g glycine 10g SDS	

Stripping buffer:	5mM sodium phosphate buffer pH7.25 2mM β-mercaptoethanol 2% SDS
4x Sample buffer for non-reducing conditions:	4ml 10% SDS 16.ml 1M Tris pH6.8 2ml glycerol 1.9ml H_2O 0.1% bromophenol blue
4x Sample buffer for reducing conditions:	50μl β-mercaptoethanol /ml 4x sample buffer

8.1.3. Bacteria

Escherichia coli XL1-blue (Stratagene)	*recA1, endA1, gyrA96, thi1, hsdR17, supE44, relA1, lac[F'proAB lacIZ M15, Tn10(tet^R)]*
Escherichia coli TG-1	*supE hsd 5thi (lac-proAB) F ' [traD36 proAB+ lacI9 lacZ M15]*

8.1.4. Plasmids

8.1.4.5. EphB2 expression constructs

Expression constructs encoding full length and truncated flagEphB2, and for EphA4 are described (Dalva et al., 2000). An expression construct encoding kinase deficient mouse EphB2 was generated by site directed mutagenesis leading to exchange of lysine 660 to arginine using the Promega kit. To generate an expression construct encoding EphB2-YFP, EYFP (Clontech) was cloned in frame into the juxtamembrane region of flagEphB2. The flanking amino acid sequence (single letter code) of the EphB2 juxtamembrane region is …GFERADSE-(EYFP)-YTDKLQHY… . To generate an expression construct encoding EphB2-YFP-ΔC (pJK18) a restriction site was inserted by site directed mutagenesis into flagEphB2. The remaining amino acid sequence of the EphB2 cytoplasmic domain is GFERADSE followed by the EYFP sequence.

8.1.4.6. HA-ephrinB1 expression constructs

Expression constructs of HA-ephrinB1, HA-ephrinB1-ΔC and HA-ephrinB1-6F were generated by subcloning from pJP104, pJP105 (Brückner et al., 1999) and pKB21 respectively into pcDNA3.1/Hygro using EcoRI and XhoI restriction sites. HA-ephrinB1_S-9A was generated from HA-ephrinB1 by site directed mutagenesis using the Promega kit.

To generate expression constructs encoding ECFP-HA-ephrinB1 (pJK30) or ECFP-HA-ephrinB1ΔC (pJK32), the ECFP coding region of pECFP-N1 (Clontech) was cloned into pJP136 or pJP139 (Brückner et al., 1999) using SalI and BsrGI restriction sites. To generate EphB2-YFP (pJK12),

A bacterial expression construct encoding the cytoplasmic domain of ephrinB1 fused to GST was described (Brückner et al., 1997).

8.1.4.7. PTP-BL expression constructs

PTP-BL expression plasmids were provided by Dr. Kai Erdmann (Ruhr Universität Bochun). The expression vector for the truncated PTP-BL construct was generated by subcloning the coding region corresponding to amino acids 1103-2460 of PTP-BL into the expression vector pcDNA3. The expression vector for truncated PTP-BL-CS was generated as described above but cysteine 2285 was replaced by serine using PCR derived site directed mutagenesis.

GST-PTP-BL phosphatase domain and GST-PTP-BL-CS (inactive) phosphatase domain were provided by Dr. Volker Eulenburg and Dr. Kai Erdmann (Ruhr Universität Bochun).

8.1.5. Chemicals and commercial kits

(γ-^{32}P)ATP (Amersham)
100x L-glutamine (Invitrogen)
100x penicillin / streptomycin. (Invitrogen)
30% Acrylamid/Bis 25:1 (Biorad)
Antifade kit (Molecular Probes)
Aprotinin (Sigma)
Benzamidine (Sigma)
Biorad D_c Protein Assay (Biorad)
ß-Glycerophosphate (Sigma)
ß-Mercaptoethanol (Sigma)
Calf serum (CS) (Invitrogen)
Chicken albumin (Sigma) 1g/ml in N-MEM
Dimethyl sulfoxide (DMSO) (Sigma)
Dithiothreitol (DTT)
Doxycycline (Sigma)
ECL Western Blot detection reagent (Amersham)
EDTA (Sigma)
EphB-Fc (R&D)
Foetal bovine serum (FBS) (Invitrogen)
Geneticin sulfate (G418) (Invitrogen)
Glutathione (Sigma)
Glutathione-sepharose beads (Pharmacia)
Human Fc fragment (Dianova)
Human transferrin (Sigma)
Hygromycin (Roche)
Isopropyl-β-D-thiogalactopyranoside (IPTG) (Sigma)
L-histidinol dihydrochlorid (Aldrich)
Lipofectamine (Invitrogen)
Lipofectamine plus reagent (Invitrogen)
Lysozyme (Sigma)
Methyl-β-cyclodextrin (MßCD, Sigma)
Mouse-laminin (Invitrogen)
Mouse-laminin (Invitrogen)
Normal Donkey Serum (Dianova)
Normal Goat Serum (Dianova)
NP-40 (Roche)
Optiprep (Nycomed Pharma)
Papain (Sigma), 1mg/ml, stored at 4°C.
phenylmethylsulfonyl fluoride (PMSF) (Sigma)
Poly-D-lysine (Sigma)
Poly-L-lysine (Sigma)

Poly-ornithine (Sigma)	
PonceauS solution (Serva)	
PP2 (Calbiochem)	
PP3 (Calbiochem)	
Progesterone (Sigma)	
Protein A-Sepharose 4B (Pharmacia)	
Protein G-Sepharose 4B (Pharmacia)	
Putrescin (Sigma)	
Pyruvic acid (Sigma)	
Site directed mutagenesis kit (Promega)	
Sodium-Selenit (Sigma)	
SU6656 (Provided by Sara A. Courtneidge, Sugen)	
TEMED (Biorad)	
Thrombin	
Triton X-100, analytical grade (Serva)	
Trypsin inhibitor (Roche)	
Trypsin/EDTA (Invitrogen)	
Tween 20 (Biorad)	
Zeosin (Invitrogen)	

8.1.6. Antibodies

Primary antibodies:

Affinity purified mouse anti-HA (12CA5, Roche)	Immunocytochemistry: 8μg/ml surface ephrinB1 staining in **Fig. 31A-D; 35A-C, E-G, 39A-H** total ephrinB1 staining in **Fig**. **33A-D, G; 36B, D, F; 38A-H** Western Blotting: 1:1000 Immunoprecipitation: 4μg/IP
Affinity purified goat anti-ephrinB1 (AF473, R&D)	Immunocytochemistry: 0.4μg/ml Surface ephrinB1 staining in **Fig. 34C, D, F** and **38A-H**.
Affinity purified rabbit anti-ephrinB1 (C-18, Santa Cruz)	Immunocytochemistry: 1μg/ml Total ephrinB1 in **Fig. 31A-D**; **35A-B**, **D-F**, **H**; **37B-C, F, 39A-H**
Affinity purified goat anti-EphB2 (AF467, R&D)	Immunocytochemistry: 4μg/ml Surface EphB2 in **Fig. 32A-D**
Rabbit serum anti-(SAM)EphB2 (Grunwald et al., 2001)	Immunocytochemistry: 1:2000. Total EphB2 staining in **Fig. 32G-J** and **34A, B, H**

Rabbit serum anti-EphA4 globular domain (J. Egea, R.K., unpublished)	Immunocytochemistry: 1:100 Total EphA4 staining in **Fig. 40B, E-F, J-L, O, R**
Mouse ascities anti-myc (clone 9E10)	Immunocytochemistry: 1:100 Surface myc-ephrinA2 labeling in **Fig. 40A, C-D, G-I, M, P** Western Blotting 1:1000
Mouse anti-myc (clone 9E10) Cy3 conjugated (Sigma)	Immunocytochemistry: 1:50 Total ephrinA2 labeling in **Fig. 40A-L, N, Q**
Mouse anti-myc (clone 9E10) agarose beads (Sigma)	Immunoprecipitation: 10μl/IP
FITC- or TR-conjugated goat anti human Fc$_\gamma$ (Jackson ImmunoResearch)	Immunocytochemistry: 7.5μg/ml Surface and total anti-Fc: **Fig. 22C-D; 31E-F, 32E-F** and **Fig. 33**
Goat anti human Fc$_\gamma$ (Jackson ImmunoResearch)	1/10 (w/w) for preclustering of Fc-fusion proteins
Mouse hybridoma cell supernatant anti-Src (clone 2-17)	Immunocytochemistry: Ascities 1:100 Total Src staining in **Fig. 22C-D, 26A** Immunoprecipitation ?μl/IP
Affinity purified rabbit anti-Fyn (fyn-14) Santa Cruz Biotechnology)	Western Blotting 1:000 Immunoprecipitation 4μl/IP
Affinity purified rabbit anti-cst1 (Biosource Deutschland GmbH)	Western Blotting 1:000
Affinity purified rabbit anti phospho-(pY416) Src (Cell Signaling Technology)	Western Blotting 1:000
Affinity purified rabbit anti phospho-(pY529) Src (Biosource Deutschland GmbH)	Western Blotting 1:000
Rabbit serum anti-ephrinB (#200). (Brückner et al., 1997)	Immunocytochemistry: 1:100 Total ephrinB labeling in **Fig. 22B** Western Blotting: 1:1000
Rabbit serum anti-ephrinB (#23) (Brückner et al., 1997)	Immunoprecipitation: 10μl/IP
EphB2-Fc (R&D)	Immunocytochemistry: 10μg/ml Total ephrinB labeling in **Fig. 24D** and **26A**
Affinity purified rabbit anti-phospho-(pY -18/-23)-ephrinB (Cell Signaling)	Western Blotting: 1:2000
Affinity purified rabbit anti-PTP-BL (Erdmann et al., 2000)	Immunocytochemistry: 1:40 Total PTP-BL labeling in **Fig. 27A**
Affinity purified mouse anti-phosopho-tyrosine (clone 4G10) (UBI)	Western Blotting 1:2000

Affinity purified goat anti human Fc (Dianova)	Western blotting 1:2000 Fc-clustering1:10 w/w

Secondary antibodies:

Donkey anti-mouse-Cy3, -Cy5 (Jackson ImmunoResearch)	Immunocytochemistry: 3.75µg/ml
Donkey anti-rabbit-Cy3, -Cy5 (Jackson ImmunoResearch)	Immunocytochemistry: 3.75µg/ml
Donkey anti-goat-Alexa488 (Molecular Probes)	Immunocytochemistry: 10µg/ml
Goat anti-mouse-Alexa488 (Molecular Probes)	Immunocytochemistry: 10µg/ml
Donkey anti rabbit-Alexa488 (Molecular Probes)	Immunocytochemistry: 10µg/ml
Goat anti-mouse antibody HRP conjugate (Amersham)	Western Blotting 1:3000
ProteinA HRP conjugate (Amersham)	Western Blotting 1:3000

8.1.7. Cell lines

NIH3T3 (Bristol Mayer Squibbs)	Mouse fibroblasts	DMEM CS
HUAEC (Provided by G. Martiny-Baron and B. Barleon)	Human umbilical chord arterial endothelial cells	EGM
ACE (Urban Deutsch, Münster)	Bovine Adrenal Cortex derived Endothelial cells	DMEM FBS
NIH3T3 ephrinB1 (Brambilla et al., 1995)	Mouse fibroblasts stably expressing human ephrinB1	DMEM CS G418
NIH3T3 EphB2 (Brambilla et al., 1995)	Mouse fibroblasts stably expressing chicken EphB2	DMEM CS G418
HeLa	Human cervix carcinoma cells	DMEM FBS
HeLa ephrinB1 and HeLa-B1ΔYKV	Human cervix carcinoma cells stably expressing	DMEM FCS G418

(Kai Erdmann, Ruhr University Bochum)	ephrinB1 constructs	
3T3 HA-ephrinB1 (clone MZ2-5)	Mouse fibroblasts stably expressing human HA-ephrinB1	DMEM CS Hygro
3T3 HA-ephrinB1-ΔC (clone MZ1-6-1)	Mouse fibroblasts stably expressing human HA-ephrinB1-ΔC	DMEM CS Hygro
3T3 HA-ephrinB1 + myc-GRIP2 (clone MZ4-6)	Mouse fibroblasts stably expressing human HA-ephrinB1 and myc-GRIP2	DMEM CS Hygro G418
3T3 HA-ephrinB1-ΔC + myc-GRIP2 (clone MZ5-23)	Mouse fibroblasts stably expressing human HA-ephrinB1-ΔC and myc-GRIP2	DMEM CS Hygro G418
3T3 HA-ephrinB1-6F (clone MZ7-23)	Mouse fibroblasts stably expressing human HA-ephrinB1-6F	DMEM CS Hygro
3T3 myc-GRIP2 (clone MZ6-1)	Mouse fibroblasts stably expressing human myc-GRIP2	DMEM CS G418
3T3 HA-ephrinB1-6F + myc-GRIP2 (clone MZ8-7)	Mouse fibroblasts stably expressing human HA-ephrinB1-6F + myc-GRIP2	DMEM CS Hygro G418
3T3 HA-ephrinB1_S-9A + myc-GRIP2 (clone MZ13-8)	Mouse fibroblasts stably expressing human HA-ephrinB1_S-9A + myc-GRIP2	DMEM CS Hygro G418
3T3 myc-ephrinA2 (Hattori et al.)	Mouse fibroblasts stably expressing myc-ephrinA2	DMEM CS ZeoR Dox

8.1.8. Other materials and equipment

Cloning cylinders (SIGMA)

Live-cell-dishes with a glass bottom (Mattek Corporation; P35G-0-14-C)

Micro-carrier (MC) Cytodex 3 beads (Sigma)

Bovine fibrinogen (>95% of protein clottable) (Sigma)

Zeiss Axiovert 200M inverted epifluorescence microscope

Zeiss Axioplan epifluorescence microscope

CO$_2$-incubation chamber (EMBL)

AttoArc2 System (Zeiss)

Coolsnap-fx digital camera (Photometrics)

SpotRT digital camera (Diagnostics Instruments)

SW40 rotor (Beckman)

SW60 rotor (Beckman)

Immobilon PVDF membrane (Millipore)

Nitrocellulose membrane, 0.45µm pore size (Schleicher & Schuell)

Semidry blotting apparatus

Biorad gel system

8.2. Cell Culture

8.2.1. Generation of stable cell lines from NIH3T3 cells

Cells of the parental cell lines (NIH3T3, MZ2-5, MZ1-6 or MZ6-1) were seeded into 10cm tissue culture dishes. Cells were transfected after reaching a confluency of approximately 60%. DNA was linearized by restriction enzyme, twice ethanol precipitated and resuspended in sterile H$_2$O. 5µg of DNA were used for transfection with lipofectamine following the manufacturer's instructions. After 2days cells were passaged at serial dilutions (1:10-1:1000) into 10cm tissue culture dishes and kept under selection with G418 or Hygromycin supplemented growth medium for 10-20 days. Single colonies of clones were isolated by trypsinization in cloning cylinders following transfer into 24well tissue culture clusters. Each clone was expanded and checked for expression by immunocytochemistry or western-blotting.

8.2.2. Transfection of cells

NIH3T3 cells were transiently transfected with FlagEphB2-ΔC and FlagEphB2-KD using lipofectamine plus reagent. HeLa cells were transfected following a conventional Ca-phosphate-DNA precipitation procedure (Sambrook et al., 1989).

8.2.3. Sprouting assays

ACE cells were cultured on beads as described (Nehls and Drenckhahn, 1995). In brief, gelatin-coated cytodex-3 microcarriers (MCs) were suspended in DMEM/20%FCS and cells were added to a final concentration of 30cells/MC. After an attachment period of 4h beads were diluted and cultured for 2days at 37°C and 5% CO_2 under gentle agitation. When cells reached confluency, the MCs were embedded as follows: Bovine fibrinogen (>95% of protein clottable) was dissolved in PBS (2.5mg/ml) together with 200U/ml aprotinin. Growth factors and inhibitors were added at the indicated concentrations. The solution was passed through a 0.2μm filter and added to 35mm cell culture dishes. Cell-coated MCs were added at a density of 150MCs/ml. Clotting was induced by addition of 0.625u/ml thrombin. The 1.5ml gels were equilibrated with DMEM/20% FCS that was replaced after 60min by fresh medium. After 7days, the number of capillary sprouts with length exceeding the diameter of the MC bead was determined for every 50 MC beads / sample.

8.2.4. Primary culture of neurons for immunocytochemistry and time lapse imaging

Chick embryonic sensory DRG neurons (E9) were isolated and cultured as described (Lindsay et al., 1985). Cells were plated on polyornithine/laminin coated glass coverslips and cultured in low serum for at least 4h before fixation.

Hippocampal and cortical neurons were taken from E13.5, E14.5 and E17.5 embryos. Embryos were taken out of the uterus and kept in ice cold HBSS buffer. Embryo heads were cut off and the scull opened to take out the brain. Brain cortices were cut off from the midbrain and brainstem and the meninges was pulled off. For hippocampal cultures the striatum was cut out and the hippocampus was separated from the cortex. Hippocampi and cortices were incubated in HBSS with 1/10 papain solution for 10min at 37°C. The digestion reaction was stopped using 10mg/ml trypsin inhibitor in HBSS. The tissue was washed 3 times in Neurobasal medium. Cells were dissociated by trituration with glass Pasteur pipettes with narrowed tips. 10ml of cell suspension was centrifuged for 3min at 800rpm to remove debris. The cell pellet was resuspended in Neurobasal medium supplemented with B27. Cells were plated on glass coverslips or on live-cell-dishes precoated with 1mg/ml Poly-D-lysine in borate buffer over night and 10μg/ml mouse laminin in PBS for 2h at 37°C. Cells were cultured in medium supplemented with 1/3 (v/v) of conditioned growth medium obtained from at least 7day old high density E17.5 cortical neuron cultures ($3 \cdot 10^6$ cells / 10cm dish) prepared the same way as above with the exception that the dishes were not coated with laminin. Depending on the length of culture and the experiment, different numbers of cells were plated and incubated for 0.5-7 days at 37°C, 5% CO_2.

For co-culture with NIH3T3 cells hippocampal neurons were cultured for 7days. NIH3T3 cells were seeded as described below at a density of 2000 cells/cm^2. After 2h cells were fixed.

For time lapse experiments of neurons with HeLa cells, we used live-cell-dishes with a glass bottom coated as above. Transfected HeLa cells were seeded as described below in growth medium at a density of 25-50000 cells/dish and left to attach over night. Cells were then washed 3x with D-PBS+Ca^{2+},Mg^{2+} and left in Neurobasal/B27 medium supplemented with 1/3 (v/v) conditioned medium. Neurons were plated at a density of 500000 cells/dish. After 4-36h *in vitro*, time lapse movies were taken.

8.2.5. Primary culture of telencephalic neurons for biochemistry

Mass cultures of cortical neurons were prepared by a modified procedure based on (de Hoop et al., 1998). Forebrain hemispheres from mouse E14.5 embryos were dissected in warm HBSS as above. Cortices were washed with HBSS and then dissociated with Trypsin/EDTA solution for 15min at 37°C. Trypsin was blocked by 2 washes in prewarmed HS-MEM medium. Cells were triturated as above and plated in tissue culture dishes precoated with 1mg/ml poly-L-lysine in borate buffer over night at 37°C and HS-MEM for an additional over night period at 37°C. Approximately 4-6 hemispheres were used per 10cm dish. Cells were left for 5h to attach and then medium was changed to N2-MEM without insulin. Neurons were left for 2 days to differentiate, washed three times in warm HBSS and then stimulated.

8.2.6. Stimulation of cells

All cell types were stimulated with EphB-Fc or Fc (Biochemistry: 1μg/ml, Immunocytochemistry: 4μg/ml), which had been pre-clustered (except **Figure 31-33**) for 1h at room temperature using 1/10 (w/w) goat anti-human IgG (Jackson Immunoresearch). Before stimulation, all cell types except cortical neurons were starved for 16h in medium containing 0.5% serum. Transient stimulation was carried out as above, but after 10min of EphB2-Fc addition, cells were washed three times with DMEM and were then left in medium containing 0.5% serum for the indicated time before lysis.
For rafts-disruption by cholesterol depletion, cells were starved as above and then washed three times with DMEM. Before stimulation they were incubated for 10min in DMEM containing 10mM Methyl-β-cyclodextrin (MßCD) under slight agitation. Stimulation was carried out under the same conditions for 10min.
For inhibition of SFKs, the specific inhibitor, PP2 or its negative control PP3, were resuspended in DMSO and added to the cells, at the indicated concentrations, together with the EphB-Fc receptor bodies. SU6656 was dissolved in DMSO at a concentration of

10mM, diluted in pre-warmed stimulation medium and added to the cells, at the indicated concentrations, 1h prior stimulation with EphB-Fc.

8.2.7. Cell-cell stimulation assays

For cell-cell stimulation experiments with NIH3T3 cells, recipient cells were seeded at low density (12500 cells/cm^2) on glass cover slips and left to attach before starvation in low serum medium (0.5% CS) over night. Stimulator cells were grown to 60% confluency, washed once with D-PBS without Ca^{2+}Mg^{2+} (Dulbecco's-PBS, Invitrogen) containing 2mM EDTA, and then left for 5min in the same solution. Cells were gently rinsed from the dishes, washed twice in D-PBS+Ca^{2+}Mg^{2+}, and seeded onto recipient cells (25000cells/cm^2). For co-cultures of transfected HeLa cells, EphB2-YFP cells were seeded as above on live-cell-dishes coated with laminin at a density of 25-50000 cells/dish 1day before imaging. 30min before imaging CFP-ephrinB1 cells were seeded at a density of 50-100000/dish and cell migration was stimulated with 20ng/ml HGF.

8.2.8. Time lapse imaging

Live cell imaging was performed at a Zeiss Axiovert 200M microscope equipped with a temperature-controlled CO$_2$-incubation chamber set to 37°C, 65% humidity, 5%CO$_2$ (neurons) or 7% CO$_2$ (HeLa) and an AttoArc2 System set to 20%. Images were acquired with a Coolsnap-fx camera. Sequential couples of phase contrast and YFP images were acquired at a rate of 1frame/minute. In case of HeLa cell experiments additionally one CFP image was taken every 10min.

8.3. Biochemistry

8.3.1. Generation of GST-fusion proteins

Recombinant GST-cytoB1 was expressed in *Escherichia coli* TG-1. Fresh overnight LB-ampicillin (100mg/ml) cultures were diluted 10-fold with fresh medium and incubated at 37°C until the A600 was 0.4–0.5. Induction was for 6h at 23°C using 0.1mM isopropyl-β-D-thiogalactopyranoside (IPTG). The cells were harvested, washed with cold phosphate-buffered saline (PBS) and lysed in 50mM Tris, pH 7.5, 150mM NaCl, 1mM EDTA, 1mM phenylmethylsulfonyl fluoride (PMSF), 1mM benzamidine, 0.05% NP-40 and 0.5mg/ml lysozyme, for 30min at 4°C. After sonication and centrifugation at 10 000 g for 15min, the supernatant was mixed with glutathione–Sepharose (Pharmacia) for 30min at 4°C. Beads were washed in lysis buffer containing neither NP-40 nor lysozyme and the GST fusion proteins were eluted with 10mM glutathione in 50mM Tris, pH 7.5, 50mM NaCl and 1mM DTT.

Fractions containing the purified GST fusion proteins were dialyzed overnight against 20–50mM Tris, pH 7.5–8.0, 50mM NaCl, 0.1mM EDTA, 0.5mM DTT, 5% glycerol and stored in aliquots at –70°C.

8.3.2. Immunoblotting, immunoprecipitation and GST pull-down experiments

For immunoblotting, protein samples were separated by 10% SDS-PAGE or 15% Anderson PAGE and transferred to nitrocellulose membranes. For PTP-BL samples were separated by 6% SDS-PAGE. The membranes were blocked for 2h at room temperature in 7.5% non-fat milk in PBS plus 0.1% Tween-20. Anti-phosphotyrosine blots were performed using 4G10. For reprobing, membranes were stripped with 5mM sodium-phosphate buffer, pH 7.5, 2% SDS, 2mM ß-mercaptoethanol, where indicated.

For immunoprecipitation, cells were lysed in lysis buffer (50mM Tris-HCl, pH 7.5, 0.5-1% Triton X-100, 150mM NaCl, 10mM NaPPi, 20mM NaF, 1mM sodium orthovanadate, 1mM PMSF, 2.5mM benzamidine and 10μg/ml each leupeptin and

aprotinin) and centrifuged at 10000*g* for 10min. For immunodepletion of SFKs, lysates from HUAECs were incubated with 2μg of anti-cst1 prebound to 20μl of proteinA-Sepharose. SFKs immunoprecipitations from cortical neurons were performed with monoclonal antibodies anti Src (2-17) and anti-Fyn (fyn-14) prebound to protein G-Sepharose 4B (Pharmacia). Polyclonal serum anti-ephrinB #23 was used for immunoprecipitation of ephrinB ligands from cortical neurons. Antibody #23 was covalently coupled to protein A-Sepharose as described (Harlow and Lane, 1988). Immunoprecipitations of ephrinB1 from NIH3T3-ephrinB1 cell lysates were done with a specific goat anti-ephrinB1 antibody. 4μg of antibody prebound to protein G beads were used per IP. After 2h at 4°C, immunoprecipitates were washed, denatured and analyzed by SDS-PAGE under non-reducing conditions.

For EphB2-Fc precipitation, cells were lysed in NP-40 lysis buffer (0.5 % NP40, 140mM NaCl, 1mM $MgCl_2$, 1mM $CaCl_2$, 1mM sodium orthovanadate, 20mM Tris/HCl pH 7.4 and protease inhibitors), diluted 1:1 with lysis buffer without NP-40. 2.5μg of EphB2-Fc, prebound to proteinG-beads, were used per precipitation. Precipitates were washed twice with diluted lysis buffer and bound proteins were analyzed for EphrinB and PTP-BL by SDS-PAGE and Western-blotting. For co-precipitation of PTP-BL with ephrinB1 10cm dishes of HeLa-B1 or HeLa-B1ΔYKV cells were transfected with an expression construct encoding for a fusion protein consisting of the five PDZ domains of PTP-BL and an N-terminally fused EGFP. 48h later cells were lysed and subjected to EphB2-Fc precipitation as described above.

For GST pull-down experiments, 5μg of bacterially produced GST or GST-cytoB1 were prebound to 20μl of glutathione-sepharose beads and then incubated in E12.5 embryo head lysates (1 mg of protein). After 2h at 4ºC, the beads were washed three times in lysis buffer (50mM Hepes pH 7.5, 150mM NaCl, 10% glycerol, 1% Triton X-100, 1.5mM $MgCl_2$, 1mM EGTA, 10mM NaPPi, 20mM NaF, 1mM sodium orthovanadate, 1mM PMSF, 2.5mM benzamidine and 10μg/ml each leupeptin and aprotinin) and analyzed by immunoblotting for the presence of PTP-BL.

8.3.3. Purification of membranes and rafts from mouse embryos and cortical neurons

For the analysis of detergent-insoluble complexes in flotation gradients, a membrane fraction was prepared at 4ºC as follows. Five heads from E12.5 mouse embryos or three 10cm dishes of cortical neurons were homogenized in a Dounce homogenizer with 1ml of ice-cold homogenization buffer (TNE: 25mM Tris pH 7.4, 150mM NaCl, 2.5mM EDTA containing 250mM sucrose, plus inhibitors as described above). The extract was passed five times through a 22G needle, ten times through 27G needle and centrifuged for 5min (3000 rpm, 4ºC). The supernatant was adjusted to 40% Optiprep and overlaid in a SW40 centrifuge tube with 7ml of 30% and 3ml of 5% Optiprep in TNE buffer. After centrifugation for 4h (24000 rpm, 4ºC; SW40 rotor), the floated membranes were collected in 600µl from the 5%/30% interface. Membranes were adjusted to 0.5% Triton X-100 for ephrinB1 and Src flotations and to 0.1% for PTP-BL flotations following extraction for 30min on ice. The extracted membranes were adjusted to 35% of Optiprep and overlaid in a SW60 centrifuge tube with 2.5ml 30% Optiprep and 400µl of 5% Optiprep in TNE buffer. After centrifugation for 4h (40000 rpm, 4ºC; SW60 rotor) seven fractions were collected from the top. After incubation with 1% Triton X-100 at room temperature, the fractions were immunoprecipitated with anti-ephrinB polyclonal antiserum (#23) for the detection of ephrinB ligands or total protein was precipitated with tricarboxylic acid (TCA) and analyzed by SDS-PAGE and Western-blotting for detection of Src and PTP-BL.

8.3.4. *In vitro* kinase assays

In vitro kinase assays with total lysates were performed in a final volume of 20µl of kinase buffer (80mM ß-glycerophosphate, pH 7.5, 20mM EGTA, 15mM MgCl$_2$, 1mM DTT, 1mM PMSF, 2.5mM benzamidine and 2µg/ml each leupeptin and aprotinin) containing 4µg total protein from the lysate, 50µM unlabeled ATP, 10µCi of (γ-^{32}P)ATP (5000 Ci/mmol) and 3µg of GST-cytoB1. After 30min at room temperature, the

phosphorylation reactions were terminated by addition of sample buffer and were analyzed by SDS-PAGE and autoradiography.

For kinase assays in pull-down experiments, 3μg of GST-cytoB1 or GST alone were prebound to 20μl of glutathione-Sepharose beads and then incubated in 1ml (1mg total protein) of cell lysates. After 2h rocking at 4°C, the beads were washed three times with kinase buffer and used for kinase assay in a final volume of 12μl of kinase buffer containing 50μM cold ATP and 10μCi of (γ-^{32}P)ATP (5000Ci/mmol). After 30min at room temperature samples were analyzed by SDS-PAGE and autoradiography.

Kinase assays were also performed in immunoprecipitates from NIH3T3-ephrinB1 cells stimulated with Fc and EphB2-Fc. EphrinB1 was immunoprecipitated as described below and, after washing the immunocomplexes three times with kinase buffer, kinase assays were performed on the beads as described above for pull-down experiments.

8.3.5. Phosphoamino acid analysis

For phosphoamino acid analysis, GST-cytoB1 was phosphorylated in a pull-down assay from NIH3T3-ephrinB1 cells stimulated with EphB2-Fc. After SDS-PAGE, proteins were transferred to a PVDF membrane and the band corresponding to phosphorylated GST-cytoB1 was cut out. Phosphoamino acids were analyzed by HCl hydrolysis of the protein followed by thin-layer chromatography using standard procedures (Kamps, 1991).

8.3.6. *In vitro* phosphatase assay

GST-PTP-BL and GST-PTP-BL Cys→Ser mutant were expressed in bacteria and purified as described (Erdmann et al., 2000). Tyrosine phosphorylated Src and ephrinB were immunoprecipitated from E12.5 mouse embryos with monoclonal antibodies anti Src (2-17) and polyclonal sera anti-ephrinB (#23) and the immunoprecipitates were incubated with 500ng GST-fusion proteins in 25mM Hepes, pH 7.5, 5mM EDTA, 10mM DTT. Immunoprecipitates were separated by SDS-PAGE and phosphotyrosine content

146

was determined using the anti-phosphotyrosine antibody 4G10 (UBI). For detection of phosphorylation of specific tyrosine residues in Src, anti-pY416 and anti-pY529 polyclonal antibodies were used. Total levels of Src phosphorylation and Src were detected using 4G10 and pan-Src polyclonal antibody respectively.

8.3.7. In gel kinase assay

For in gel kinase assays lysates were taken in 2x SDS-sample buffer supplemented with 10mM NaF, 0.4mM Na_3VO_4, 10mM EDTA pH8 and a cocktail of protease inhibitors. Samples were separated by SDS-PAGE on 10% Laemmli gels, which were polymerized in the presence of 100μg/ml of GST-cytoB1 or GST alone. After electrophoresis, the proteins were fixed by 2x 45min washing with 100ml 50mM Hepes pH7.6, 20% 2-Propanol. The gels were washed 2x30min in buffer A (50mM Hepes ph 7.6, 5mM β-mercaptoethanol). Proteins in the gel were denatured by incubation in 200ml of 6M urea in buffer A for 1h at RT. For renaturation gels were washed sequentially for 20min at 4°C in buffer A containing 0.05% Tween20 and 3M, 1.5M and 0.75M urea respectively, followed by 5 washes without urea at 4°C. Before kinase reaction gels were preincubated for 20min at 37°C under slight agitation in 30ml of kinase buffer: 40mM Hepes pH7.6, 20mM β-glycerophosphate, 20mM p-Nitrophenyl phosphate, 0.1mM Sodium Vanadate, 2mM DTT, 5mM $MgCl_2$). Kinase reaction was performed under moderate agitation for 1-1.5h at 30°C in 20ml of kinase buffer containing 50μM ATP and 100μCi (γ-^{32}P)ATP. Kinase reaction was stopped by washing in 5% TCA, 1% Pyrophosphate, 2mM ATP buffered to pH 5.7 with Na_2HPO_4 (to prepare 5l approximately 263g are added). Gels were washed by changing the solution several times until radioactivity in the gel was barely around background.

8.4. Immunocytochemistry

8.4.1. Immunostaining of cells

For normal immunocytochemistry of total protein distributions, cell were fixed with 4% PFA, 4% sucrose in D-PBS for 15min at RT, rinsed once with D-PBS, then incubated with 50mM NH$_4$Cl in D-PBS for 10min at RT, and rinsed again before permeabilization for 5min with ice cold 0.1% Triton X-100 in D-PBS at 4°C. After washing, blocking was done for 30min at RT or over night at 4°C. Primary antibodies for total stainings were applied for 60min at RT. After washing, secondary antibodies were incubated for 30min at RT. After washing, samples were mounted using the ProLong antifade kit. Images were acquired using an epifluorescence microscope equipped with a digital camera (SpotRT).

Chick embryonic sensory DRG neurons (E9) were fixed in warm 4% PFA for 20min, blocked with 2% BSA, and incubated with EphB2-Fc (10μg/ml) for 1h. After permeabilization with 0.2% NP-40 for 10min at room temperature, samples were processed for PTP-BL and anti-Fc staining as above.

8.4.2. Immunofluorescence internalization assay

Cell were fixed with 4% PFA, 4% sucrose in D-PBS for 15min at RT, rinsed once with D-PBS, then incubated with 50mM NH$_4$Cl in D-PBS for 10min at RT, and rinsed again before blocking for 30min at RT with 2%BSA, 4% donkey and/or 4% goat serum. Primary antibodies for surface labeling were applied for 60min at RT. Cells were washed 3x5min with D-PBS. In case of myc-ephrinA2 surface labeling a secondary anti-mouse antibody was applied for 30min and cells were washed 3x5min. Cells were permeabilized for 5min with ice cold 0.1% Triton X-100 in D-PBS at 4°C. After washing, blocking was done for 30min at RT or over night at 4°C. Primary antibodies for total stainings were applied for 60min at RT. After washing secondary antibodies were incubated for 30min at RT. After washing, samples were mounted using the ProLong antifade kit. Images

were acquired using an epifluorescence microscope equipped with a digital camera. All fluorescence images of fixed cells except in **Figure 31** are maximum projections of 2-10 focal planes generated by the MetaMorph software.

9. Curriculum Vitae

Manuel Zimmer, born 11.09.1971 in Osnabrück, Germany. Parents: Wendelin and Margarete Zimmer.

30/09/98: 'Diplom Biochemie' at Freie Universität Berlin, Germany.

    Degree received: 'Sehr gut'.

    Title of diploma thesis:

    In vivo phosphorylation sites in the Muscle Specific Receptor Tyrosine Kinase (MuSK).

    Performed in the lab of Dr. Steve Burden, Skirball Institute, New York

01/08/01: Continuation of PhD.-studies in the laboratory of Dr. Rüdiger Klein at Max-Planck Institute of Neurobiology, Munich, Germany.

01/10/98 to 31/07/01: Begin of PhD.-studies in the laboratory of Dr. Rüdiger Klein at European Molecular Biology Laboratories (EMBL), Heidelberg, Germany.

01/3/98 to 30/09/98: Diploma studies in the laboratory of Dr. Steven J. Burden at Skirball Institute for Biomolecular Medicine, New York, USA.

01/03/93-30/09/98: University studies of Biochemistry at Freie Universität Berlin, Germany.

01/08/91 to 31/10/1992: Community Service.

03/06/91: 'Abitur' at Ernst-Moritz-Arndt-Gymnasium, Osnabrück, Germany.

10. Bibliography

Adams, R. H., F. Diella, S. Hennig, F. Helmbacher, U. Deutsch and R. Klein (2001). "The cytoplasmic domain of the ligand ephrinB2 is required for vascular morphogenesis but not cranial neural crest migration." Cell **104**: 57-69.

Adams, R. H., G. A. Wilkinson, C. Weiss, F. Diella, N. W. Gale, U. Deutsch, W. Risau and R. Klein (1999). "Roles of ephrinB ligands and EphB receptors in cardiovascular development: demarcation of arterial/venous domains, vascular morphogenesis and sprouting angiogenesis." Genes and Development **13**: 295-306.

Aderem, A. and D. M. Underhill (1999). "Mechanisms of phagocytosis in macrophages." Annu Rev Immunol **17**: 593-623.

Arpin, M., M. Algrain and D. Louvard (1994). "Membrane-actin microfilament connections: an increasing diversity of players related to band 4.1." Curr Opin Cell Biol **1994**: 136-141.

Bamburg, J. R., D. Bray and K. Chapman (1986). "Assembly of microtubules at the tip of growing axons." Nature **321**(6072): 788-90.

Barker, P. A., N. K. Hussain and P. S. McPherson (2002). "Retrograde signaling by the neurotrophins follows a well-worn trk." Trends Neurosci **25**(8): 379-81.

Bashaw, G. J., T. Kidd, D. Murray, T. Pawson and C. S. Goodman (2000). "Repulsive axon guidance: Abelson and Enabled play opposing roles downstream of the roundabout receptor." Cell **101**(7): 703-15.

Becker, E., U. Huynh-Do, S. Holland, T. Pawson, T. O. Daniel and E. Y. Skolnik (2000). "Nck-interacting Ste20 kinase couples Eph receptors to c-Jun N-terminal kinase and integrin activation." Mol Cell Biol **20**(5): 1537-45.

Blake, R. A., M. A. Broome, X. Liu, J. Wu, M. Gishizky, L. Sun and S. A. Courtneidge (2000). "SU6656, a selective Src family kinase inhibitor, used to probe growth factor signaling." Molecular and Cellular Biology **20**(23): 9018-9027.

Bonhoeffer, T. and R. Yuste (2002). "Spine motility. Phenomenology, mechanisms, and function." Neuron **35**(6): 1019-27.

Bossing, T. and A. H. Brand (2002). "Dephrin, a transmembrane ephrin with a unique structure, prevents interneuronal axons from exiting the Drosophila embryonic CNS." Development **129**(18): 4205-18.

Brambilla, R., K. Bruckner, D. Orioli, A. D. Bergemann, J. G. Flanagan and R. Klein (1996). "Similarities and differences in the way transmembrane-type ligands interact with the Elk subclass of Eph receptors." Mol Cell Neurosci **8**(2-3): 199-209.

Brambilla, R., A. Schnapp, F. Casagranda, J. P. Labrador, A. D. Bergemann, J. G. Flanagan, E. B. Pasquale and R. Klein (1995). "Membrane-bound LERK2 ligand can signal through three different Eph-related receptor tyrosine kinases." EMBO Journal **14**: 3116-3126.

Brittis, P. A., Q. Lu and J. G. Flanagan (2002). "Axonal protein synthesis provides a mechanism for localized regulation at an intermediate target." Cell **110**(2): 223-35.

Brouns, M. R., S. F. Matheson and J. Settleman (2001). "p190 RhoGAP is the principal Src substrate in brain and regulates axon outgrowth, guidance and fasciculation." Nat Cell Biol **3**: 361-367.

Brown, J. and P. C. Bridgman (2003). "Role of myosin II in axon outgrowth." J Histochem Cytochem **51**(4): 421-8.

Brückner, K., J. P. Labrador, P. Scheiffele, A. Herb, F. Bradke, P. H. Seeburg and R. Klein (1999). "EphrinB ligands recruit GRIP family PDZ adaptor proteins into raft membrane microdomains." Neuron **22**: 511-524.

Brückner, K., E. B. Pasquale and R. Klein (1997). "Tyrosine phosphorylation of transmembrane ligands for Eph receptors." Science **275**: 1640-1643.

Bull, H. A., P. M. Brickell and P. M. Dowd (1994). "Src-related kinases are physically associatedwith the surface antigen CD36 in human dermal microvascular endothelial cells." FEBS Lett **351**: 41-44.

Burke, P., K. Schooler and H. S. Wiley (2001). "Regulation of epidermal growth factor receptor signaling by endocytosis and intracellular trafficking." Mol Biol Cell **12**(6): 1897-910.

Cagan, R. L., H. Kramer, A. C. Hart and S. L. Zipursky (1992). "The bride of sevenless and sevenless interaction: internalization of a transmembrane ligand." Cell **69**(3): 393-9.

Cao, T. T., H. W. Deacon, D. Reczek, A. Bretscher and M. von Zastrow (1999). "A kinase-regulated PDZ-domain interaction controls endocytic sorting of the beta2-adrenergic receptor." Nature **401**(6750): 286-90.

Cary, L. A. and J. A. Cooper (2000). "Molecular switches in lipid rafts." Nature **404**(6781): 945, 947.

Castellani, V., A. Chedotal, M. Schachner, C. Faivre-Sarrailh and G. Rougon (2000). "Analysis of the L1-deficient mouse phenotype reveals cross-talk between Sema3A and L1 signaling pathways in axonal guidance." Neuron **27**(2): 237-49.

Chang, H. C., S. L. Newmyer, M. J. Hull, M. Ebersold, S. L. Schmid and I. Mellman (2002). "Hsc70 is required for endocytosis and clathrin function in Drosophila." J Cell Biol **159**(3): 477-87.

Charron, F., E. Stein, J. Jeong, A. P. McMahon and M. Tessier-Lavigne (2003). "The morphogen sonic hedgehog is an axonal chemoattractant that collaborates with netrin-1 in midline axon guidance." Cell **113**(1): 11-23.

Chida, D., T. Kume, Y. Mukouyama, S. Tabata, N. Nomura, M. L. Thomas, T. Watanabe and M. Oishi (1995). "Characterization of a protein tyrosine phosphatase (RIP) expressed at a very early stage of differentiation in both mouse erythroleukemia and embryonal carcinoma cells." FEBS Lett **358**: 233-239.

Chimini, G. and P. Chavrier (2000). "Function of Rho family proteins in actin dynamics during phagocytosis and engulfment." Nat Cell Biol **2**(10): E191-6.

Chin-Sang, I. D., S. E. George, M. Ding, S. L. Moseley, A. S. Lynch and A. D. Chisholm (1999). "The ephrin VAB-2/EFN-1 functions in neuronal signaling to regulate epidermal morphogenesis in C. elegans." Cell **99**(7): 781-90.

Chisholm, A. and M. Tessier-Lavigne (1999). "Conservation and divergence of axon guidance mechanisms." Curr Opin Neurobiol **9**(5): 603-15.

Chishti, A. H., A. C. Kim, S. M. Marfatia, M. Lutchman, M. Hanspal, H. Jindal, S. C. Liu, P. S. Low, G. A. Rouleau, N. Mohandas, J. A. Chasis, J. G. Conboy, P. Gascard, Y. Takakuwa, S. C. Huang, E. J. J. Benz, A. Bretscher, R. G. Fehon, J. F. Gusella, V. Ramesh, F. Solomon, V. T. Marchesi, S. Tsukita, S. Tsukita, K. B. Hoover and e. al. (1988). "The FERM domain: a unique module involved in the linkage of cytoplasmic proteins to the membrane." Trends Biochem Sci 23(8):281-2 **23**: 281-282.

Chong, L. D., E. K. Park, E. Latimer, R. Friesel and I. O. Daar (2000). "Fibroblast growth factor receptor-mediated rescue of x-ephrin B1-induced cell dissociation in Xenopus embryos." Mol Cell Biol **20**(2): 724-34.

Chung, H. J., J. Xia, R. H. Scannevin, X. Zhang and R. L. Huganir (2000). "Phosphorylation of the AMPA receptor subunit GluR2 differentially regulates its interaction with PDZ domain-containing proteins." J Neurosci **20**(19): 7258-67.

Colavita, A. and J. G. Culotti (1998). "Suppressors of ectopic UNC-5 growth cone steering identify eight genes involved in axon guidance in Caenorhabditis elegans." Dev Biol **194**(1): 72-85.

Conner, S. D. and S. L. Schmid (2003). "Regulated portals of entry into the cell." Nature **422**(6927): 37-44.

Contractor, A., C. Rogers, C. Maron, M. Henkemeyer, G. T. Swanson and S. F. Heinemann (2002). "Trans-synaptic Eph receptor-ephrin signaling in hippocampal mossy fiber LTP." Science **296**(5574): 1864-9.

Cooke, J. E. and C. B. Moens (2002). "Boundary formation in the hindbrain: Eph only it were simple." Trends Neurosci **25**(5): 260-7.

Cowan, C. A. and M. Henkemeyer (2001). "The SH2/SH3 adaptor Grb4 transduces B-ephrin reverse signals." Nature **413**(6852): 174-9.

Dalva, M. B., M. A. Takasu, M. Z. Lin, S. Shamah, L. Hu, N. W. Gale and M. E. Greenberg (2000). "EphB receptors interact with NMDA receptors and regulate excitatory synapse formation." Cell **in press**.

Dalva, M. B., M. A. Takasu, M. Z. Lin, S. M. Shamah, L. Hu, N. W. Gale and M. E. Greenberg (2000). "EphB receptors interact with NMDA receptors and regulate excitatory synapse formation." Cell **103**(6): 945-56.

Davy, A., N. W. Gale, E. W. Murray, R. A. Klinghoffer, P. Soriano, C. Feuerstein and S. M. Robbins (1999). "Compartmentalized signaling by GPI-anchored ephrin-A5 requires the Fyn tyrosine kinase to regulate cellular adhesion." Genes Dev **13**: 3125-3135.

Davy, A. and S. M. Robbins (2000). "Ephrin-A5 modulates cell adhesion and morphology in an integrin-dependent manner." EMBO J **19**: 5396-5405.

de Curtis, I. (2001). "Cell migration: GAPs between membrane traffic and the cytoskeleton." EMBO Rep **2**(4): 277-81.

de Hoop, M. J., L. Meyn and C. G. Dotti (1998). Culturing hippocampal neurons and astrocytes from fetal rodent brain. Cell Biology: A Laboratory Handbook. J. E. Celis. London, Academic Press. **1:** 154-163.

Dickson, B. J. (2002). "Molecular mechanisms of axon guidance." Science **298**(5600): 1959-64.

Dong, H., R. J. O'Brien, E. T. Fung, A. A. Lanahan, P. F. Worley and R. L. Huganir (1997). "GRIP: a synaptic PDZ domain-containing protein that interacts with AMPA receptors." Nature **386**: 279-284.

Edwards, D. C. and G. N. Gill (1999). "Structural features of LIM kinase that control effects on the actin cytoskeleton." J Biol Chem **274**(16): 11352-61.

Edwards, D. C., L. C. Sanders, G. M. Bokoch and G. N. Gill (1999). "Activation of LIM-kinase by Pak1 couples Rac/Cdc42 GTPase signalling to actin cytoskeletal dynamics." Nat Cell Biol **1**(5): 253-9.

Eliceiri, B. P., R. Paul, P. L. Schwartzberg, J. D. Hood, J. Leng and D. A. Cheresh (1999). "Selective requirement for Src kinases during VEGF-induced angiogenesis and vascular permeability." Mol Cell **4**: 915-924.

Ellis, C., F. Kasmi, P. Ganju, E. Walls, G. Panayotou and A. D. Reith (1996). "A juxtamembrane autophosphorylation site in the Eph family receptor tyrosine kinase, Sek, mediates high affinity interaction with p59fyn." Oncogene **12**: 1727-1736.

Erdmann, K. S., J. Kuhlmann, V. Lessmann, L. Herrmann, V. Eulenburg, O. Muller and R. Heumann (2000). "The Adenomatous Polyposis Coli-protein (APC) interacts with the protein tyrosine phosphatase PTP-BL via an alternatively spliced PDZ domain." Oncogene **19**: 3894-3901.

Ethell, I. M., F. Irie, M. S. Kalo, J. R. Couchman, E. B. Pasquale and Y. Yamaguchi (2001). "EphB/syndecan-2 signaling in dendritic spine morphogenesis." Neuron **31**(6): 1001-13.

Ethell, I. M. and Y. Yamaguchi (1999). "Cell surface heparan sulfate proteoglycan syndecan-2 induces the maturation of dendritic spines in rat hippocampal neurons." J Cell Biol **144**(3): 575-86.

Fournier, A. E., F. Nakamura, S. Kawamoto, Y. Goshima, R. G. Kalb and S. M. Strittmatter (2000). "Semaphorin3A enhances endocytosis at sites of receptor-F-actin colocalization during growth cone collapse." J Cell Biol **149**(2): 411-22.

Gale, N. W., P. Baluk, L. Pan, M. Kwan, J. Holash, T. M. DeChiara, D. M. McDonald and G. D. Yancopoulos (2001). "Ephrin-B2 selectively marks arterial vessels and neovascularization sites in the adult, with expression in both endothelial and smooth-muscle cells." Dev Biol **230**(2): 151-60.

Gale, N. W., S. J. Holland, D. M. Valenzuela, A. Flenniken, L. Pan, T. E. Ryan, M. Henkemeyer, K. Strebhardt, H. Hirai, D. G. Wilkinson, T. Pawson, S. Davis and G. D. Yancopoulos (1996). "Eph receptors and ligands comprise two major specificity subclasses, and are reciprocally compartmentalized during embryogenesis." Neuron **17**: 9-19.

Gale, N. W. and G. D. Yancopoulos (1999). "Growth factors acting via endothelial cell-specific receptor tyrosine kinases: VEGFs, angiopoietins, and ephrins in vascular development." Genes and Development **13**: 1055-1066.

George, S. E., K. Simokat, J. Hardin and A. D. Chisholm (1998). "The VAB-1 Eph receptor tyrosine kinase functions in neural and epithelial morphogenesis in C. elegans." Cell **92**: 633-643.

Gerety, S. S., H. U. Wang, Z. F. Chen and D. J. Anderson (1999). "Symmetrical mutant phenotypes of the receptor EphB4 and its specific transmembrane ligand ephrinB2 in cardiovascular development." Mol Cell **4**: 403-414.

Gerlai, R. (2001). "Eph receptors and neural plasticity." Nat Rev Neurosci **2**(3): 205-9.

Giordano, S., S. Corso, P. Conrotto, S. Artigiani, G. Gilestro, D. Barberis, L. Tamagnone and P. M. Comoglio (2002). "The semaphorin 4D receptor controls invasive growth by coupling with Met." Nat Cell Biol **4**(9): 720-4.

Gomez, T. M., E. Robles, M. Poo and N. C. Spitzer (2001). "Filopodial calcium transients promote substrate-dependent growth cone turning." Science **291**(5510): 1983-7.

Gomez, T. M. and N. C. Spitzer (1999). "In vivo regulation of axon extension and pathfinding by growth-cone calcium transients." Nature **397**(6717): 350-5.

Gonzalez-Gaitan, M. (2003). "Signal dispersal and transduction through the endocytic pathway." Nat Rev Mol Cell Biol **4**(3): 213-24.

Gross, C., R. Heumann and K. S. Erdmann (2001). "The protein kinase C-related kinase PRK2 interacts with the protein tyrosine phosphatase PTP-BL via a novel PDZ domain binding motif." FEBS Lett **496**(2-3): 101-4.

Grunwald, I. C. and R. Klein (2002). "Axon guidance: receptor complexes and signaling mechanisms." Curr Opin Neurobiol **12**(3): 250-9.

Grunwald, I. C., M. Korte, D. Wolfer, G. A. Wilkinson, K. Unsicker, H. P. Lipp, T. Bonhoeffer and R. Klein (2001). "Kinase-Independent Requirement of EphB2 Receptors in Hippocampal Synaptic Plasticity." Neuron **32**(6): 1027-40.

Grunwald, I. C., M. Korte, D. Wolfer, G. A. Wilkinson, K. Unsicker, H. P. Lipp, T. Bonhoeffer and R. Klein (2001). "Kinase-independent requirement of EphB2 receptors in hippocampal synaptic plasticity." Neuron **32**(6): 1027-40.

Gu, C. and S. Park (2001). "The EphA8 receptor regulates integrin activity through p110gamma phosphatidylinositol-3 kinase in a tyrosine kinase activity-independent manner." Mol Cell Biol **21**(14): 4579-97.

Gu, C. and S. Park (2003). "The p110 gamma PI-3 kinase is required for EphA8-stimulated cell migration." <u>FEBS Lett</u> **540**(1-3): 65-70.

Haj, F. G., P. J. Verveer, A. Squire, B. G. Neel and P. I. Bastiaens (2002). "Imaging sites of receptor dephosphorylation by PTP1B on the surface of the endoplasmic reticulum." <u>Science</u> **295**(5560): 1708-11.

Hakeda-Suzuki, S., J. Ng, J. Tzu, G. Dietzl, Y. Sun, M. Harms, T. Nardine, L. Luo and B. J. Dickson (2002). "Rac function and regulation during Drosophila development." <u>Nature</u> **416**(6879): 438-42.

Harder, T., P. Scheiffele, P. Verkade and K. Simons (1998). "Lipid domain structure of the plasma membrane revealed by patching of membrane components." <u>J Cell Biol</u> **141**(4): 929-42.

Harlow, E. and D. Lane (1988). <u>Antibodies. A laboratory manual</u>. Cold Spring Harbor, NY, Cold Spring Harbor Laboratory.

Hattori, M., M. Osterfield and J. G. Flanagan (2000). "Regulated cleavage of a contact-mediated axon repellent." <u>Science</u> **289**(5483): 1360-5.

Hedgecock, E. M., J. G. Culotti and D. H. Hall (1990). "The unc-5, unc-6, and unc-40 genes guide circumferential migrations of pioneer axons and mesodermal cells on the epidermis in C. elegans." <u>Neuron</u> **4**(1): 61-85.

Helmchen, F. (2002). "Raising the speed limit--fast Ca(2+) handling in dendritic spines." <u>Trends Neurosci</u> **25**(9): 438-41.

Hendriks, W., J. Schepens, D. Bachner, J. Rijss, P. Zeeuwen, U. Zechner, H. Hameister and B. Wieringa (1995). "Molecular cloning of a mouse epithelial protein-tyrosine phosphatase with similarities to submembranous proteins." <u>J Cell Biochem</u> **59**: 418-430.

Henkemeyer, M., D. Orioli, J. T. Henderson, T. M. Saxton, J. Roder, T. Pawson and R. Klein (1996). "Nuk controls pathfinding of commissural axons in the mammalian central nervous system." <u>Cell</u> **86**(1): 35-46.

Hering, H. and M. Sheng (2001). "Dendritic spines: structure, dynamics and regulation." <u>Nat Rev Neurosci</u> **2**(12): 880-8.

Himanen, J. P., K. R. Rajashankar, M. Lackmann, C. A. Cowan, M. Henkemeyer and D. B. Nikolov (2001). "Crystal structure of an Eph receptor-ephrin complex." <u>Nature</u> **414**(6866): 933-8.

Hing, H., J. Xiao, N. Harden, L. Lim and S. L. Zipursky (1999). "Pak functions downstream of Dock to regulate photoreceptor axon guidance in Drosophila." Cell **97**(7): 853-63.

Holland, S. J., N. W. Gale, G. Mbamalu, G. D. Yancopoulos, M. Henkemeyer and T. Pawson (1996). "Bidirectional signaling through the EPH-family receptor Nuk and its transmembrane ligands." Nature **383**: 722-725.

Hong, K., L. Hinck, M. Nishiyama, M. M. Poo, M. Tessier-Lavigne and E. Stein (1999). "A ligand-gated association between cytoplasmic domains of UNC5 and DCC family receptors converts netrin-induced growth cone attraction to repulsion." Cell **97**(7): 927-41.

Hong, K., M. Nishiyama, J. Henley, M. Tessier-Lavigne and M. Poo (2000). "Calcium signalling in the guidance of nerve growth by netrin-1." Nature **403**(6765): 93-8.

Hu, H. M., TF. Goodman, CS. (2001). "Plexin B mediates axon guidance in Drosophila by simultaneously inhibiting active Rac and enhancing RhoA signaling." Neuron **32**: 39-51.

Huai, J. and U. Drescher (2001). "An ephrin-A-dependent signaling pathway controls integrin function and is linked to the tyrosine phosphorylation of a 120-kDa protein." J Biol Chem **276**: 6689-6694.

Huynh-Do, U., C. Vindis, H. Liu, D. P. Cerretti, J. T. McGrew, M. Enriquez, J. Chen and T. O. Daniel (2002). "Ephrin-B1 transduces signals to activate integrin-mediated migration, attachment and angiogenesis." J Cell Sci **115**(Pt 15): 3073-81.

Incardona, J. P., J. H. Lee, C. P. Robertson, K. Enga, R. P. Kapur and H. Roelink (2000). "Receptor-mediated endocytosis of soluble and membrane-tethered Sonic hedgehog by Patched-1." Proc Natl Acad Sci U S A **97**(22): 12044-9.

Irie, F. and Y. Yamaguchi (2002). "EphB receptors regulate dendritic spine development via intersectin, Cdc42 and N-WASP." Nat Neurosci **5**(11): 1117-8.

Jurney, W. M., G. Gallo, P. C. Letourneau and S. C. McLoon (2002). "Rac1-mediated endocytosis during ephrin-A2- and semaphorin 3A-induced growth cone collapse." J Neurosci **22**(14): 6019-28.

Kalo, M. S., H. H. Yu and E. B. Pasquale (2001). "In vivo tyrosine phosphorylation sites of activated ephrin-B1 and ephB2 from neural tissue." J Biol Chem **276**(42): 38940-8.

Kamiguchi, H. and V. Lemmon (2000). "Recycling of the cell adhesion molecule L1 in axonal growth cones." J Neurosci **20**(10): 3676-86.

Kamiguchi, H. and F. Yoshihara (2001). "The role of endocytic l1 trafficking in polarized adhesion and migration of nerve growth cones." J Neurosci 21(23): 9194-203.

Kamps, M. P. (1991). "Determination of phosphoamino acid composition by acid hydrolysis of protein blotted to Immobilon." Methods Enzymol 201: 21-7.

Keleman, K., S. Rajagopalan, D. Cleppien, D. Teis, K. Paiha, L. A. Huber, G. M. Technau and B. J. Dickson (2002). "Comm sorts robo to control axon guidance at the Drosophila midline." Cell 110(4): 415-27.

Kennedy, T. E., T. Serafini, J. R. de la Torre and M. Tessier-Lavigne (1994). "Netrins are diffusible chemotropic factors for commissural axons in the embryonic spinal cord." Cell 78(3): 425-35.

Kidd, T., K. S. Bland and C. S. Goodman (1999). "Slit is the midline repellent for the robo receptor in Drosophila." Cell 96(6): 785-94.

Kiefer, F., I. Anhauser, P. Soriano, A. Aguzzi, S. A. Courtneidge and E. F. Wagner (1994). "Endothelial cell transformation by polyomavirus middle T antigen in mice lacking Src-related kinases." Curr Biol 4: 100-109.

Kilsdonk, E. P., P. G. Yancey, G. W. Stoudt, F. W. Bangerter, W. J. Johnson, M. C. Phillips and G. H. Rothblat (1995). "Cellular cholesterol efflux mediated by cyclodextrins." J Biol Chem 270(29): 17250-6.

Kirchhausen, T. (2000). "Clathrin." Annu Rev Biochem 69: 699-727.

Klinghoffer, R. A., C. Sachsenmaier, J. A. Cooper and S. Soriano (1999). "Src family kinases are required for integrin but not PDGFR signal transduction." EMBO J 18: 2459-2471.

Kmiecik, T. E. and D. Shalloway (1987). "Activation and suppression of pp60c-src transforming ability by mutation of its primary sites of tyrosine phosphorylation." Cell 49: 65-73.

Knobel, K. M., E. M. Jorgensen and M. J. Bastiani (1999). "Growth cones stall and collapse during axon outgrowth in Caenorhabditis elegans." Development 126(20): 4489-98.

Koblizek, T. I., C. Weiss, G. D. Yancopoulos, U. Deutsch and W. Risau (1998). "Angiopoietin-1 induces sprouting angiogenesis in vitro." Curr Biol 8: 529-532.

Koleske, A. J. (2003). "Do filopodia enable the growth cone to find its way?" Sci STKE 2003(183): pe20.

Kullander, K., N. K. Mather, F. Diella, M. Dottori, A. W. Boyd and R. Klein (2001). "Kinase-dependent and kinase-independent functions of EphA4 receptors in major axon tract formation in vivo." Neuron **29**(1): 73-84.

Kullander, K., N. K. Mather, F. Diella, M. Dottori, A. W. Boyd and R. Klein (2001). "Kinase-dependent and kinase-independent functions of EphA4 receptors in major axon tract formation in vivo." Neuron **29**(1): 73-84.

Kypta, R. M., Y. Goldberg, E. T. Ulug and S. A. Courtneidge (1990). "Association between the PDGF receptor and members of the src family of tyrosine kinases." Cell **62**: 481-492.

Lanier, L. M., M. A. Gates, W. Witke, A. S. Menzies, A. M. Wehman, J. D. Macklis, D. Kwiatkowski, P. Soriano and F. B. Gertler (1999). "Mena is required for neurulation and commissure formation." Neuron **22**(2): 313-25.

Lewis, A. and P. Bridgman (1992). "Nerve growth cone lamellipodia contain two populations of actin filaments that differ in organization and polarity." J. Cell Biol. **119**(5): 1219-1243.

Lin, D., G. D. Gish, Z. Songyang and T. Pawson (1999). "The carboxyl terminus of B class ephrins constitutes a PDZ domain binding motif." J Biol Chem **274**: 3726-3733.

Lindsay, R. M., H. Thoenen and B. Y.-A. (1985). "Placode and neural crest-derived sensory neurons are responsive at early
developmental stages to brain-derived neurotrophic factor." Dev. Biol. **112**: 319-328.

Lowell, C. A. and P. Soriano (1996). "Knockouts of Src-family kinases: Stiff bones, wimpy T cells, and bad memories." Genes and Development **10**: 1845-1857.

Lu, Q., E. E. Sun, R. S. Klein and J. G. Flanagan (2001). "Ephrin-B reverse signaling is mediated by a novel PDZ-RGS protein and selectively inhibits G protein-coupled chemoattraction." Cell **105**: 69-79.

Lundquist, E. A., P. W. Reddien, E. Hartwieg, H. R. Horvitz and C. I. Bargmann (2001). "Three C. elegans Rac proteins and several alternative Rac regulators control axon guidance, cell migration and apoptotic cell phagocytosis." Development **128**(22): 4475-4488.

Luo, L. (2000). "Rho GTPases in neuronal morphogenesis." Nat Rev Neurosci **1**(3): 173-80.

Maekawa, K., N. Imagawa, M. Nagamatsu and S. Harada (1994). "Molecular cloning of a novel protein-tyrosine phosphatase containing a membrane-binding domain and GLGF repeats." FEBS Lett **337**: 200-206.

Maness, P. F., M. Aubry, C. G. Shores, L. Frame and K. H. Pfenninger (1988). "c-src gene product in developing rat brain is enriched in nerve growth cone membranes." Proc Natl Acad Sci USA **85**: 5001-5005.

Mann, F., Miranda, E.,Weinl, C.,Harmer, E. and Holt, C. E (in press). "B-type Eph receptors and ephrins induce growth cone collapse through distinct intracellular pathways." J. Neurobiology.

Marston, D. J., S. Dickinson and C. D. Nobes (2003). "Rac-dependent trans-endocytosis of ephrinBs regulates Eph-ephrin contact repulsion." Nat Cell Biol **5**(10): 879-888.

McLaughlin, T., R. Hindges and D. D. O'Leary (2003). "Regulation of axial patterning of the retina and its topographic mapping in the brain." Curr Opin Neurobiol **13**(1): 57-69.

Mellitzer, G., Q. Xu and D. G. Wilkinson (1999). "Eph receptors and ephrins restrict cell intermingling and communication." Nature **400**(6739): 77-81.

Mellman, I. and R. M. Steinman (2001). "Dendritic cells: specialized and regulated antigen processing machines." Cell **106**(3): 255-8.

Miao, H., E. Burnett, M. Kinch, E. Simon and B. Wang (2000). "Activation of EphA2 kinase suppresses integrin function and causes focal-adhesion-kinase dephosphorylation." Nat Cell Biol **2**(2): 62-9.

Ming, G. L., H. J. Song, B. Berninger, C. E. Holt, M. Tessier-Lavigne and M. M. Poo (1997). "cAMP-dependent growth cone guidance by netrin-1." Neuron **19**(6): 1225-35.

Murai, K. K. and E. B. Pasquale (2002). "Can Eph receptors stimulate the mind?" Neuron **33**(2): 159-62.

Nagasawa, T., K. Tachibana and T. Kishimoto (1998). "A novel CXC chemokine PBSF/SDF-1 and its receptor CXCR4: their functions in development, hematopoiesis and HIV infection." Semin Immunol **10**: 179-85.

Nehls, V. and D. Drenckhahn (1995). "A novel, microcarrier-based in vitro assay for rapid and reliable quantification of three-dimensional cell migration and angiogenesis." Microvasc Res **50**(3): 311-22.

Newsome, T. P., S. Schmidt, G. Dietzl, K. Keleman, B. Asling, A. Debant and B. J. Dickson (2000). "Trio combines with dock to regulate Pak activity during photoreceptor axon pathfinding in Drosophila." Cell **101**(3): 283-94.

Nichols, B. J. and J. Lippincott-Schwartz (2001). "Endocytosis without clathrin coats."
        Trends Cell Biol **11**(10): 406-12.

O'Connor, T., J. Duerr and D. Bentley (1990). "Pioneer growth cone steering decisions
        mediated by single filopodial contacts in situ." J. Neurosci. **10**(12): 3935-3946.

O'Leary, D. D. and D. G. Wilkinson (1999). "Eph receptors and ephrins in neural
        development." Curr Opin Neurobiol **9**(1): 65-73.

Orioli, D., M. Henkemeyer, G. Lemke, R. Klein and T. Pawson (1996). "Sek4 and Nuk
        receptors cooperate in guidance of commissural axons and in palate formation."
        Embo J **15**(22): 6035-49.

Palmer, A. and R. Klein (2003). "Multiple roles of ephrins in morphogenesis, neuronal
        networking, and brain function." Genes Dev **17**(12): 1429-50.

Palmer, A., M. Zimmer, K. S. Erdmann, V. Eulenburg, A. Porthin, R. Heumann, U.
        Deutsch and R. Klein (2002). "EphrinB phosphorylation and reverse signaling:
        regulation by Src kinases and PTP-BL phosphatase." Mol Cell **9**(4): 725-37.

Parks, A. L., K. M. Klueg, J. R. Stout and M. A. Muskavitch (2000). "Ligand endocytosis
        drives receptor dissociation and activation in the Notch pathway." Development
        127(7): 1373-85.

Pasterkamp, R. J., J. J. Peschon, M. K. Spriggs and A. L. Kolodkin (2003). "Semaphorin
        7A promotes axon outgrowth through integrins and MAPKs." Nature **424**(6947):
        398-405.

Pawson, T. and J. D. Scott (1997). "Signaling through scaffold, anchoring, and adaptor
        proteins." Science **278**(5346): 2075-80.

Pelkmans, L. and A. Helenius (2002). "Endocytosis via caveolae." Traffic **3**(5): 311-20.

Penzes, P., A. Beeser, J. Chernoff, M. R. Schiller, B. A. Eipper, R. E. Mains and R. L.
        Huganir (2003). "Rapid Induction of Dendritic Spine Morphogenesis by trans-
        Synaptic EphrinB-EphB Receptor Activation of the Rho-GEF Kalirin." Neuron
        37(2): 263-74.

Pollard, T. D. and G. G. Borisy (2003). "Cellular motility driven by assembly and
        disassembly of actin filaments." Cell **112**(4): 453-65.

Qualmann, B. and M. M. Kessels (2002). "Endocytosis and the cytoskeleton." Int Rev
        Cytol **220**: 93-144.

Raper, J. A. (2000). "Semaphorins and their receptors in vertebrates and invertebrates."
        Curr Opin Neurobiol **10**(1): 88-94.

Ridley, A. J. (2001). "Rho proteins: linking signaling with membrane trafficking." Traffic **2**(5): 303-10.

Riento, K. and A. J. Ridley (2003). "Rocks: multifunctional kinases in cell behaviour." Nat Rev Mol Cell Biol **4**(6): 446-56.

Robles, E., A. Huttenlocher and T. M. Gomez (2003). "Filopodial calcium transients regulate growth cone motility and guidance through local activation of calpain." Neuron **38**(4): 597-609.

Rohatgi, R., L. Ma, H. Miki, M. Lopez, T. Kirchhausen, T. Takenawa and M. W. Kirschner (1999). "The interaction between N-WASP and the Arp2/3 complex links Cdc42-dependent signals to actin assembly." Cell **97**(2): 221-31.

Rohm, B., B. Rahim, B. Kleiber, I. Hovatta and A. W. Puschel (2000). "The semaphorin 3A receptor may directly regulate the activity of small GTPases." FEBS Lett **486**(1): 68-72.

Sambrook, J., E. F. Fritsch and T. Maniatis (1989). Molecular Cloning: A Laboratory Manual. Plainview, NY, Cold Spring Harbour Lab. Press.

Saras, J., L. Claesson-Welsh, C. H. Heldin and L. J. Gonez (1994). "Cloning and characterization of PTPL1, a protein tyrosine phosphatase with similarities to cytoskeletal-associated proteins." J Biol Chem **269**: 24082-24089.

Saras, J., P. Franzen, P. Aspenstrom, U. Hellman, L. J. Gonez and C. H. Heldin (1997). "A novel GTPase-activating protein for Rho interacts with a PDZ domain of the protein-tyrosine phosphatase PTPL1." J Biol Chem **272**: 24333-24338.

Sato, T., S. Irie, S. Kitada and J. C. Reed (1995). "FAP-1: a protein tyrosine phosphatase that associates with Fas." Science **268**: 411-415.

Schaefer, A. W., N. Kabir and P. Forscher (2002). "Filopodia and actin arcs guide the assembly and transport of two populations of microtubules with unique dynamic parameters in neuronal growth cones." J. Cell Biol. **158**(1): 139-152.

Scully, A. L., M. McKeown and J. B. Thomas (1999). "Isolation and characterization of Dek, a Drosophila eph receptor protein tyrosine kinase." Mol Cell Neurosci **13**(5): 337-47.

Shamah, S. M., M. Z. Lin, J. L. Goldberg, S. Estrach, M. Sahin, L. Hu, M. Bazalakova, R. L. Neve, G. Corfas, A. Debant and M. E. Greenberg (2001). "EphA receptors regulate growth cone dynamics through the novel guanine nucleotide exchange factor ephexin." Cell **105**(2): 233-44.

Shewan, D., A. Dwivedy, R. Anderson and C. E. Holt (2002). "Age-related changes underlie switch in netrin-1 responsiveness as growth cones advance along visual pathway." <u>Nat Neurosci</u> **5**(10): 955-62.

Shin, D., G. Garcia-Cardena, S. Hayashi, S. Gerety, T. Asahara, G. Stavrakis, J. Isner, J. Folkman, M. A. Gimbrone, Jr. and D. J. Anderson (2001). "Expression of ephrinB2 identifies a stable genetic difference between arterial and venous vascular smooth muscle as well as endothelial cells, and marks subsets of microvessels at sites of adult neovascularization." <u>Dev Biol</u> **230**(2): 139-50.

Simons, K. and D. Toomre (2000). "Lipid Rafts and signal transduction." <u>Nat Rev Mol Cell Biol</u> **1**: 31-39.

Song, H.-j., G.-l. Ming, Z. He, M. Lehmann, L. McKerracher, M. Tessier-Lavigne and M.-m. Poo (1998). "Conversion of Neuronal Growth Cone Responses from Repulsion to Attraction by Cyclic Nucleotides." <u>Science</u> **281**(5382): 1515-1518.

Song, H. J., G. L. Ming and M. M. Poo (1997). "cAMP-induced switching in turning direction of nerve growth cones." <u>Nature</u> **388**(6639): 275-9.

Sorkin, A. and M. Von Zastrow (2002). "Signal transduction and endocytosis: close encounters of many kinds." <u>Nat Rev Mol Cell Biol</u> **3**(8): 600-14.

Stein, E., A. A. Lane, D. P. Cerretti, H. O. Schoecklmann, A. D. Schroff, R. L. Van Etten and T. O. Daniel (1998). "Eph receptors discriminate specific ligand oligomers to determine alternative signaling complexes, attachment, and assembly responses." <u>Genes Dev</u> **12**(5): 667-78.

Superti-Furga, G., K. Jonsson and S. A. Courtneidge (1996). "A functional screen in yeast for regulators and antagonizers of heterologous protein tyrosine kinases." <u>Nature Biotechnology</u> **14**: 600-605.

Takasu, M. A., M. B. Dalva, R. E. Zigmond and M. E. Greenberg (2002). "Modulation of NMDA receptor-dependent calcium influx and gene expression through EphB receptors." <u>Science</u> **295**(5554): 491-5.

Tanaka, E. and J. Sabry (1995). "Making the connection: cytoskeletal rearrangements during growth cone guidance." <u>Cell</u> **83**(2): 171-6.

Tepass, U., D. Godt and R. Winklbauer (2002). "Cell sorting in animal development: signalling and adhesive mechanisms in the formation of tissue boundaries." <u>Curr Opin Genet Dev</u> **12**(5): 572-82.

Thomas, S. M. and J. S. Brugge (1997). "Cellular functions regulated by Src family kinases." <u>Annu Rev Cell Dev Biol</u> **13**: 513-609.

Thomas, T., A. K. Voss and P. Gruss (1998). "Distribution of a murine protein tyrosine phosphatase BL-beta-galactosidase fusion protein suggests a role in neurite outgrowth." Dev Dyn **212**: 250-257.

Torres, R., B. L. Firestein, H. Dong, J. Staudinger, E. N. Olson, R. L. Huganir, D. S. Bredt, N. W. Gale and G. D. Yancopoulos (1998). "PDZ proteins bind, cluster and synaptically co-localize with Eph receptors and their ephrin ligands." Neuron **21**: 1453-1463.

Vikis, H. G., W. Li, Z. He and K.-L. Guan (2000). "The semaphorin receptor plexin-B1 specifically interacts with active Rac in a ligand-dependent manner." PNAS **97**(23): 12457-12462.

Vincent, S. and J. Settleman (1997). "The PRK2 kinase is a potential effector target of both Rho and Rac GTPases and regulates actin cytoskeletal organization." Mol Cell Biol **17**(4): 2247-56.

Wahl, S., H. Barth, T. Ciossek, K. Aktories and B. K. Mueller (2000). "Ephrin-A5 induces collapse of growth cones by activating Rho and Rho kinase." J Cell Biol **149**(2): 263-70.

Wang, H. U., Z.-F. Chen and D. J. Anderson (1998). "Molecular Distinction and Angiogenic Interaction between Embryonic Arteries and Veins Revealed by ephrin-B2 and Its Receptor Eph-B4." Cell **93**: 741-753.

Wells, A., J. B. Welsh, C. S. Lazar, H. S. Wiley, G. N. Gill and M. G. Rosenfeld (1990). "Ligand-induced transformation by a noninternalizing epidermal growth factor receptor." Science **247**(4945): 962-4.

Wilkinson, D. G. (2000). "Eph receptors and ephrins: regulators of guidance and assembly." International Review of Cytology **196**: 177-244.

Wilkinson, D. G. (2000). "Topographic mapping: organising by repulsion and competition?" Curr Biol **10**(12): R447-51.

Wilkinson, D. G. (2001). "Multiple roles of EPH receptors and ephrins in neural development." Nat Rev Neurosci **2**(3): 155-64.

Winberg, M. L., L. Tamagnone, J. Bai, P. M. Comoglio, D. Montell and C. S. Goodman (2001). "The transmembrane protein Off-track associates with Plexins and functions downstream of Semaphorin signaling during axon guidance." Neuron **32**(1): 53-62.

Wong, K., X. R. Ren, Y. Z. Huang, Y. Xie, G. Liu, H. Saito, H. Tang, L. Wen, S. M. Brady-Kalnay, L. Mei, J. Y. Wu, W. C. Xiong and Y. Rao (2001). "Signal

transduction in neuronal migration: roles of GTPase activating proteins and the small GTPase Cdc42 in the Slit-Robo pathway." Cell **107**(2): 209-21.

Wyszynski, M., E. Kim, A. W. Dunah, M. Passafaro, J. G. Valtschanoff, C. Serra-Pages, M. Streuli, R. J. Weinberg and M. Sheng (2002). "Interaction between GRIP and liprin-alpha/SYD2 is required for AMPA receptor targeting." Neuron **34**(1): 39-52.

Xu, Q., G. Mellitzer, V. Robinson and D. G. Wilkinson (1999). "In vivo cell sorting in complementary segmental domains mediated by Eph receptors and ephrins." Nature **399**(6733): 267-71.

Yoshikawa, S., R. D. McKinnon, M. Kokel and J. B. Thomas (2003). "Wnt-mediated axon guidance via the Drosophila Derailed receptor." Nature **422**(6932): 583-8.

Yu, H. H., A. H. Zisch, V. C. Dodelet and E. B. Pasquale (2001). "Multiple signaling interactions of Abl and Arg kinases with the EphB2 receptor." Oncogene **20**(30): 3995-4006.

Yu, T. W. and C. I. Bargmann (2001). "Dynamic regulation of axon guidance." Nat Neurosci **4**(Suppl): 1169-76.

Zheng, J. Q. (2000). "Turning of nerve growth cones induced by localized increases in intracellular calcium ions." Nature **403**(6765): 89-93.

Zimmer, M., A. Palmer, J. Kohler and R. Klein (2003). "EphB-ephrinB bi-directional endocytosis terminates adhesion allowing contact mediated repulsion." Nat Cell Biol **5**(10): 869-878.

Zisch, A. H., M. S. Kalo, L. D. Chong and E. B. Pasquale (1998). "Complex formation between EphB2 and Src requires phosphorylation of tyrosine 611 in the EphB2 juxtamembrane region." Oncogene **16**(20): 2657-70.

Zou, J. X., B. Wang, M. S. Kalo, A. H. Zisch, E. B. Pasquale and E. Ruoslahti (1999). "An Eph receptor regulates integrin activity through R-Ras." Proc Natl Acad Sci U S A **96**(24): 13813-8.